ABSTRACT

Title of Thesis:	SIMULATIONS OF FIRE SMOKE MOVEMENT IN HIGH-RISE BHUILDINGS WITH FDS
	Hongda Xu, Master of Science, 2021
Thesis Directed By:	Professor Arnaud Trouvé Department of Fire Protection Engineering

The Fire Dynamics Simulator (FDS) developed by the National Institute of Standards and Technology (NIST) solves a form of the Navier-Stokes equations appropriate for low-speed (Ma < 0.3), thermally-driven flow with an emphasis on smoke and heat transport and has been shown to be capable of simulating the flow and temperature conditions in the vicinity of a fire [1]. In the present study, we evaluate the ability of FDS to simulate pressure dynamics in high-rise buildings, a pre-requisite to the correct simulation of smoke transport far from the fire.

The objective of this study is to test the accuracy of FDS for determining the conditions throughout the entire expanse of a 40-story high-rise building featuring an elevator shaft and four stairwells. The output from FDS is first compared to the results generated by a network model called COSMO. The comparison of the two outputs shows that correct results are predicted by FDS. Additionally, more realistic scenarios

are simulated with FDS and the results are compared with those of a network model called CONTAM and an in-house MATLAB program. The network model CONTAM and the MATLAB program do not represent the time-dependent thermal mixing process taking place inside the elevator shaft and the stairwells whereas FDS does. The comparison shows the importance of this thermal mixing process that impacts the pressure dynamics and smoke movement inside the building, with implications for the evacuation capability provided by the stairwells.

SIMULATIONS OF FIRE SMOKE MOVEMENT IN HIGH-RISE BHUILDINGS WITH FDS

by

Hongda Xu

Thesis submitted to the Faculty of the Graduate School of the
University of Maryland, College Park, in partial fulfillment
of the requirements for the degree of
Master of Science
2021

Advisory Committee:
Professor Arnaud Trouvé, Advisor
Professor James Milke, Committee Member
Professor Peter Sunderland, Committee Member

Acknowledgements

First of all, I would like to express my deepest gratitude to my advisor. Thank you, Dr. Arnaud Trouvé, for your patience, encouragement and support throughout the project. I learned a lot not only from your guidance and courses, but I was also impressed by your expertise, wisdom and serious attitude toward academic research. I also appreciate your understanding when I was planning to go back to my home country during the pandemic and the convenience you provided for me. More importantly, without your help, this work would not be close to what it is today.

I would also like to thank faculties, staffs and students in the FPE department at the University of Maryland. Thank you all for providing one of the world's most famous fire science study and research programs and helping me when I had difficulties. And a special gratitude is given to my advisory committee members. Thank you, Dr. Milke and Dr. Sunderland, for providing valuable comments during my presentation.

In addition, I would like to thank my friends and roommates. Thank you, Josh Shaner, Muhammad Jalani, Kenta Kurosawa, Hongen Zhou, Kevin Cho, Haipeng Zhang and Jingyi Wu for enriching my life during my graduate study in the U.S. Also, a special gratitude is given to my 'uncle'. Thank you, Qiang Qian, for taking care of me when I was in the U.S.

Last but not least, I would like to thank my parents. Thank you, my dad and mom, for always encouraging and supporting me. Without you, I would not be where I am today.

Thank you.

Table of Contents

Chapter 1: Introduction

1.1 Background

With the rapid development of urbanization and civil engineering technologies, huge numbers of people moved into metropolitan areas and more high-rise buildings are constructing in large cities. According to The Skyscraper Center of the Council on Tall Buildings and Urban Habitat (CTBUH) [13], there are 5,148 high-rise buildings (> 150 m) that have been constructed globally before 2020, and 685 under-construction high-rise buildings (> 150 m) will be completed all over the world in the next five years (2021 - 2026). Although the increasing quantity of high-rise buildings can meet the demands of urbanization, it increases the difficulty of fire protection and evacuation. When a fire is occurred in a high-rise building, the smoke generated by the fire can easily migrate inside the building and endangers people's life due to its toxicity and heat. Therefore, it is important to understand the mechanism of smoke movement inside these buildings and develop smoke control strategies to protect lives. To achieve this goal, some large-scale experiments have been conducted. However, for the purpose of being cost-efficient, many computer programs have been developed. And according to W.Z. Black, these programs can be classified into four broad categories: zone models, network models, differential models and CFD models[4].

Zone models, such as COMIS [5], typically divided fire room into two regions: a lower zone without smoke and an upper zone filled with hot smoke. They are mostly used to simulate the conditions within a fire room and its few adjacent compartments.

Network models, such as CONTAM[3] and AIRNET[6], assume that every enclosure within the building has a uniform set of properties, so that they are suitable to be used to determine conditions inside large buildings, but they are usually error-prone owing to the lack of a detailed heat transfer model.

Differential models, such as COSMO[4], are based on the network modeling/zone modeling approach and combine the advantages of these two methods, so they are popular to be used to predict and quantify the movement of smoke during a high-rise building fire in fire safety and HVAC communities.

CFD (computational fluid dynamics) models are based on the governing equations of fluid dynamics which utilizes numerical analysis methods and algorithms to solve problems involving fluid flows. They divide the domain of the problem into numerous cells and solve the equations for each cell, which could ensure more accurate solution if the size of cells is appropriately specified.

Fire Dynamics Simulator (FDS) [1], a CFD model of fire-driven fluid flow, will be used to simulate the fire smoke movement throughout the entire expanse of a high-rise building in this study.

1.2 Objectives

The computational complexity of solving a form of the Navier-Stokes equations appropriate for low-speed (Ma<0.3), thermally-driven flow with an emphasis on smoke and heat transport makes the application of FDS ideal for determining the properties in the vicinity of a fire [1], but some argue that it is impractical for FDS to predicting the conditions in every part of a high-rise building due to its high computational expense

with increased cells. However, with the continuously rapid advancement of High-Performance Computing (HPC) Cluster and Personal Computer (PC) nowadays, simulations with FDS can be ran quicker and quicker.

Therefore, the objective of this study is to test the accuracy of FDS for determining the conditions throughout the entire expanse of a 40-story high-rise building. The output from FDS is compared to the results generated by COSMO. The comparison of the two outputs shows that correct results were reported by FDS. Additionally, more realistic scenarios were simulated by using FDS and the results are compared with those of CONTAM and a MATLAB program to demonstrate the thermal mixing process in FDS and increase our basic understanding of smoke movement and management in high-rise buildings.

1.3 Pressure and Smoke Criteria

There are different ways to adjust the pressure and control fire smoke inside high-rise buildings, such as pressurization systems, zoned smoke control systems and combined systems. No matter what systems are installed in the buildings (or no such a system is used), safe evacuation normally requires that escape stairwell doors can be easily open at any time by occupants. If the pressure difference across the stairwell escape doors exceeds a certain value suggested in smoke control standards, it indicates that the evacuation of the occupants inside the buildings will be difficult.

NFPA 92 and Handbook of Smoke Control Engineering[10] both introduce the equation below showing the calculation of the maximum allowable pressure difference between the escape stairwell and the floor spaces. Depending on different properties of

escape doors and different total door-opening forces, the corresponding maximum pressure difference can be calculated. Typically, the total average door-opening force is around 133 N for human, so considering a 1.22 m wide and 2.13 m high escape door with 25 N door closer force and 7.62 cm length between the doorknob to the knob side of the door, the maximum pressure difference across the door is calculated as 78 Pa. In addition, the International Building Code (ICC 2018, Section 909.20.5) requires that each interior exit stairway should be pressurized no more than 87 Pa (if the building is equipped throughout with an automatic sprinkler system). Hence, from a conservative perspective, 78 Pa will be treated as a threshold value to determine whether evacuees will have a hard time opening the exit doors in this study.

$$\Delta P = \frac{2 \times (W - d) \times (F - F_{dc})}{W \times A} \tag{2.1}$$

where:

A – escape door area (m^2)

d – distance from doorknob to knob side of door (m)

F – total door-opening force (N)

F_{dc} – door closer force (N)

W – door with (m)

ΔP – maximum pressure difference (Pa)

Another important factor to ensure safe evacuation and the safety of occupants is that some spaces, such as stairwells and occupied spaces, inside the high-rise buildings need to be free of fire smoke. There are two ways to indicate the presence of the smoke

in FDS. One method is to use the visibility diagnostic function and another one is to use the temperature diagnostic function. Since it is difficult to have an accurate soot prediction of the design fire in FDS, monitoring visibility might not be a good approach to suggest where the hot smoke is. Hence, it is better to use a certain threshold temperature value to represent the indication of the hot smoke. According to some studies[15][16], the upper layer smoke temperature in an enclosure can range from 35 ℃ to 500 ℃ depending on different compartment configurations, fire sizes, ventilation conditions, boundary conditions and so on. For this study, the fire smoke will be defined as the region where the temperature takes values above a critical threshold of 40 degrees Celsius.

Therefore, in addition to test the accuracy of FDS for predicting the conditions inside the entire expanse of the high-rise building, the other two objectives of the simulations are: (1) evaluate whether hot air/fire smoke is spreading into the stairwells and will thereby endanger evacuees (by monitoring the mass flow rate from the fire floor to the stairwells; and by monitoring the temperature inside the stairwells); (2) evaluate whether the pressure difference between the stairwells and the different floor spaces is more than 78 Pa and will thereby make door opening difficult.

Chapter 2: Model Construction

2.1 Model Geometry

To perform a reasonable comparison, the conditions and configuration of the high-rise building in FDS are specified practically as same as in the COSMO program example demonstrated in Ref. [4]. The floor plan shown in Figure 2.1 depicts that the building has an open construction style with 2000 m^2 area on each floor, an eight-integrated elevator shaft in the center, and four stairwells located in each corner. Figure 2.2 provides a 3D outline of the 40-story building in Smokeview showing that the elevator shaft and the stairwells extend from the first floor to the top of the building. Note that the building is considered without pressurization systems for the stairwells and thus may not be compliant with codes and standards. The leaks and openings connecting the inside of the building to the atmosphere were specified uniformly in the surface of the building in the COSMO example. However, it is not necessary to specify the same leak distribution in FDS for the purpose of the simplification of the model construction and results analysis process. All leaks and openings were specified by using the HVAC network model in FDS. Air can enter the vertical shafts through these leaks and openings. In Addition, only one leakage path is specified between each individual space and all the leakage paths are located at the middle of each floor (The leakage path areas are calculated in Appendix D). This is to guarantee the same effect as uniform leak distribution has. The advantage of using the HVAC network model is that it can determine the mass flow rate through a leakage path based on the pressure difference on the two sides, especially when leaks are extremely small compared to the

size of computational cells and cannot be resolved by them. PyroSim [12], a graphical user interface for FDS that helps to quickly create and manage the details of complex models, is used to construct the configuration of the high-rise building. All the computational cells used in the following cases are 1 m^3 cubes and the computational domain for each case is uniformly divided to 41 meshes calculated via an HPC cluster.

2.2 Model Assumptions

The fire conditions in the COSMO program example are quantified by assuming that the pressure rise on the fire floor is 10 Pa above the ground-level atmospheric pressure and that the temperature of the combustion gases on the fire floor is 700 ℃. To achieve the same fire conditions in FDS, a 700 ℃ hot air supply with a constant mass flow rate is imposed on the first floor. The constant 10 Pa gauge pressure (defined as the absolute pressure with respect to the atmospheric pressure taken at the same elevation) on the first floor at 2 meters elevation was achieved through trial and error. Other major assumptions that are applied in this case are:

- The flow of air throughout the building occurs steadily.
- The thickness of all the floor slabs is assumed to be negligible (0 m) compared to the floor height (4 m), and they are adiabatic. In addition, there are no leaks or openings in the floor slabs. (Not that this follows the configuration in Ref. [4] but it may not be fully accurate and realistic.) However, the building roof (adiabatic) is assumed to be 1 m thick in order to specify the roof vents by the HVAC network model.
- The exterior surface of the building is adiabatic to avoid any flow that may exist

around the building owing to heat transfer.

- The interior wall surface of the building is at a fix temperature except that the walls on the first floor are all adiabatic for the purpose of a constant temperature and pressure condition. Note that the temperature of walls inside the stairwells and elevator shaft (40 ℃) is adopted from the input data in Ref. [4] for comparison but this value may not be realistic (22 ℃ would be more realistic).
- Eight elevator shafts are considered as a large integrated shaft without any obstructions.
- There are no stairs (obstructions) inside the stairwells. Note that the size of the stairwells (3 m by 3 m) is small compared with the typical stairwells size (3 m by 6 m).
- There is only one leakage path distributed in the walls of the elevator shaft and the four stairwells on each floor, respectively. In addition, the elevator shaft and the stairwells connect to the atmosphere only at the top of the building.
- The building has 40 identical floors. The floor plan is shown in Figure 2.1, and details regarding the elevator shaft and the stairwells are listed in Table 2.1.

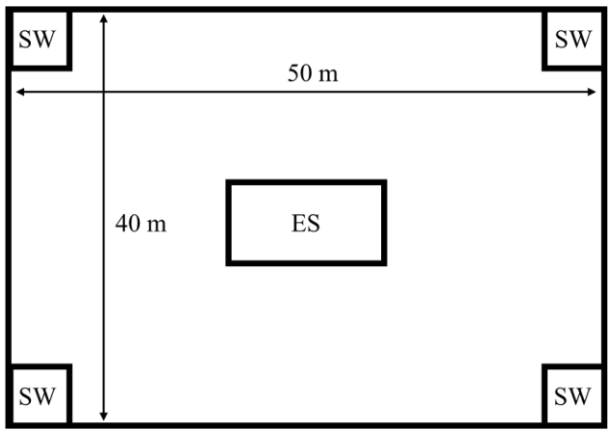

Figure 2.1: The floor plan of the high-rise building.

All the FDS inputs for the case that are used to compare with the COSMO example are listed in Table 2.1. All the values were selected to model a realistic high-rising building and a severe, ground-floor fire that could possibly exist in the real world. According to Table 2.1, the mass release rate per unit area for the hot air is only 0.0565 kg/(s·m2). This is to ensure the accuracy of the calculation, since FDS is only suitable for low-speed (Ma < 0.3) flow. Additionally, the atmospheric conditions and the constructions of the building, the elevator shaft, and the stairwells described in Table 2.1 are applied to every case in this paper. It is no doubt that changes in any of the parameters that have a major impact on the movement of air/smoke will lead to different results. Therefore, conclusions drawn from each case discussed below should only be attributed to the specific building configuration (including the elevator shaft and the stairwells), and the atmospheric conditions shown in Table 2.1 with their individual fire condition (e.g., hot air, fuel lean, fuel rich), boundary conditions (e.g. adiabatic, prescribed temperatures) and scenario (e.g., closed/open doors).

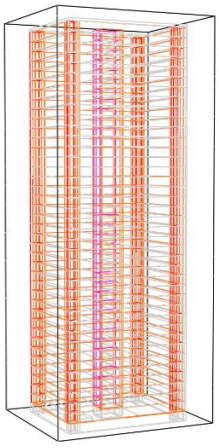

Figure 2.2: The outline of the high-rise building shown in Smokeview. The high-rise building has 40 floors with a lumped elevator shaft in the center and four stairwells in each corner.

Table 2.1: Input conditions to FDS for hot air case.

Input variable	Value
Atmospheric conditions	
Atmospheric temperature at grounded level	−17 °C (winter condition)
Atmospheric pressure at ground level	101.30 kPa
'Fire' conditions	
Mass flow rate per unit area of hot air supply	0.0565 kg/(s·m^2)
Surface area of the hot air supply	54 m^2
Temperature of hot air supply	700 °C
Initial temperature at fire floor	700 °C
Building construction	
Building height	160 m
Floor area in each floor	2000 m^2
Height of each floor	4 m (40 floors)
Area of leak openings in ext. surf. of building	0.252 m^2/floor
Initial temperature of entire building	22 °C
Surface temperature of floors	22 °C
Elevator shaft construction	
Number of elevator shafts	8
Number of cars in shafts	0
Surface temperature of elevator shafts	40 °C
Surface roughness of elevator surface	25 mm
Area of vent at top of elevator shafts	10.224 m^2
Area of leak openings in elevator shaft walls	0.2144 m^2/floor
Emissivity of elevator shaft surface	0.3
Interior length and width of the integrated shaft	8 m × 6 m
Stairwell construction	
Number of stairwells	4
Surface temperature of stairwells	40 °C
Surface roughness of stairwell surface	500 mm
Area of vent at top of stairwells	0.1 m^2
Area of leak openings in walls of each stairwell	0.0151 m^2/floor
Emissivity of stairwell shaft surface	0.3
Interior length and width of each stairwell	3 m × 3 m

2.3 Design Fires

Apart from the surrogate fire case described above, more realistic scenarios were also considered in this study. The design of fire is of great importance in designing realistic scenarios and it requires the understanding of fire growth and the reasonable selection of Heat Release Rate (HRR) values.

The curve of the time variations of HRR in fire growth stage can take many shapes, but t-square fire equation is commonly used to describes this relationship among fire protection engineers. This equation is shown below:

$$\dot{Q} = \alpha \times t^2 \tag{2.1}$$

where:

$\dot{Q}$ – heat release rate (kW)

α – fire growth coefficient (kW/s^2)

t – time from ignition (s)

The different fire growth coefficients are described in Table 2.2.

Table 2.2: Fire growth constants for T-Square fire

Fires	α (kW/s^2)
Slow	0.002931
Medium	0.01127
fast	0.04689
Ultra-Fast	0.1878

In FDS, the variable TAU_Q that is used to control the time for t-square fire to reach the fully developed stage can be calculated by the equation below:

$$t_g = \sqrt{\frac{\dot{Q}_{max}}{\alpha}} \tag{2.2}$$

where:

t_g – time for t-square fire to reach the maximum heat release rate (kW)

$\dot{Q}_{max}$ – maximum heat release rate of design fire

There are totally seven simulations that were conducted in this study and they are listed in Table 2.3. FDS cases 1 to 5 has a simulation time of 3600 s and FDS cases 6 and 7 has a simulation time of 600 s.

Table 2.3: Summary of scenarios that were specified in different cases.

Cases	Fire Conditions	Fire Location	Doors	Boundary Conditions
1	No fire/hot air supply	1st floor	All close	Fix temperature (Table 2.1)
2	Hot air supply	1st floor	All close	Fix temperature (Table 2.1)
3	10 MW t-square fire	1st floor	All close	All adiabatic
4	2.5 MW t-square fire	1st floor	All close	All adiabatic
5	2.5 MW t-square fire	35th floor	All close	All adiabatic
6	2.5 MW t-square fire (60 s delay)	1st floor	All close	All adiabatic
7	2.5 MW t-square fire (60 s delay)	1st floor	Only the stairwell doors to the fire floor are open	All adiabatic

Chapter 3: Results

The results and graphs that appear in this paper were generated by FDS for a 40-story building with 2000 m^2 area on each floor that has a large eight-integrated elevator shaft and four stairwells during winter weather conditions. In addition to test the accuracy of FDS for predicting the conditions inside the entire expanse of the high-rise building, the other two objectives of the simulations are: (1) evaluate whether hot air/fire smoke is spreading into the stairwells and thereby endanger evacuees (by monitoring the mass flow rate from the fire floor to the stairwells; and by monitoring the temperature inside the stairwells); (2) evaluate whether the pressure difference between the stairwells and the different floor spaces is more than 78 Pa and will thereby make door opening difficult.

3.1 Case 1: No Fire/Hot Air

Stack effect is the movement of air through leaks and openings into and out of buildings (or structures) due to air buoyancy resulting from the temperature difference between inside air and outside air. The greater the difference of air temperature, the greater the difference of air density, and thus the greater the buoyancy force leading to a greater stack effect. During winter season, the warmer indoor air rises up through stairwells, elevator shafts, leaks and openings inside the building and escapes in the upper part of the building. This rising warm air reduces the pressure in the lower floor spaces, thus drawing cold air from atmosphere into the building through leaks and openings. During summer season, the stack flow is reversed, but usually weaker owing to lower temperature differences [11].

A terminology called neutral pressure plane (NPP) is directly related to the stack effect. It is defined as the elevation of a horizontal plane where there is no pressure difference between the inside and the outside, and thus the magnitude of mass flow rates would be zero in leakage paths at its location. Note that, in this study, the NPP for the floors is in terms of the pressure difference between the floors and the atmosphere, but the NPPs for the elevator shaft and the stairwells are in terms of the pressure difference between a given shaft and the floors (instead of being in terms of the pressure difference between a given shaft and the atmosphere).

This section is to test whether FDS can simulate the stack effect for the high-rising building with the conditions shown in Table 2.1 but without the 'fire' conditions. A representative sample of time evolutions of pressure and temperature inside the building is plotted in Figure 3.1. It takes about 3000 s for the quasi-steady state to be established in the entire building. (It is not true steady state, because the temperature inside the building is still slowly changing after 3000 s because of cold inflow at the base of the building. However, it is slow enough so that it can be treated as a quasi-constant numerical value. The more evident temperature change on the ground floor is due to the greater mass flow rate through leaks illustrated in Figure 3.3.) All the results analyzed here are taken at a time of 3600 s.

According to the gauge pressure and the absolute pressure distributions inside the building shown in Figure 3.4 and 3.5, it is apparent that the gauge pressure inside the floors is negative in the lower part of the building and positive in the upper part of the building. This leads to the air infiltration at the bottom of the building and air exfiltration at the top of the building which is consistent with what is shown in Figure

3.2 and Figure 3.3. Moreover, the pressure inside the floors is greater than the pressures within both shafts in lower part of the building, but less than the pressures within both shafts in the upper part of the building. Hence, it encourages air to spread into both shafts in the lower part of the building and be forced back into the floors in the upper part of the building as shown in Figure 3.2 and Figure 3.3. Also, the gauge pressures at the topmost of the elevator shaft and the stairwells exceed zero, so it is logical to predict that air will escape the building through the top vents in both shafts, and this conclusion is confirmed after examining the pressure on the two sides of these top vents. In addition, Figure 3.7 demonstrates that the maximum pressure difference between the escape stairwells and the floors is 91 Pa and the pressure difference across the exit stairwell doors exceeds 78 Pa above 38th floor, so it would be difficult for the occupants on the topmost two floors to open the fire escape doors. Hence, some pressure control systems are suggested to be implemented in the building even if under the normal condition (no fire).

Moreover, Figure 3.7 shows the temperature distribution inside the high-rise building. Due to the adiabatic boundary condition and stronger stack flow on the first floor, the temperature inside the first floor space has a more dramatic decline and hence the stairwells and the elevator shaft also have a lower temperature. The temperature inside the stairwells in the upper part of the building reaches 37 degree Celsius, because of the 40 degree Celsius boundary condition and heat transfer between the gases and the walls. However, even though the elevator shaft has a same boundary condition as the stairwells does, the elevator shaft has a lower temperature in the upper part of the building. It is because that there is more cold air entering into the elevator shaft than

into the stairwells from the lower floors as shown in Figure 3.3. Additionally, owing to the warm air inside the stairwells pushed into the upper floors, the temperature inside the upper floors becomes higher than the initial condition (22 degree Celsius).

Taken together, it is reasonable to conclude that FDS is able to model the stack effect in the high-rise building. Consequently, the success of simulating the stack effect for this high-rise building in FDS provides the basis for the smoke movement modeling and further validations are discussed in the following section.

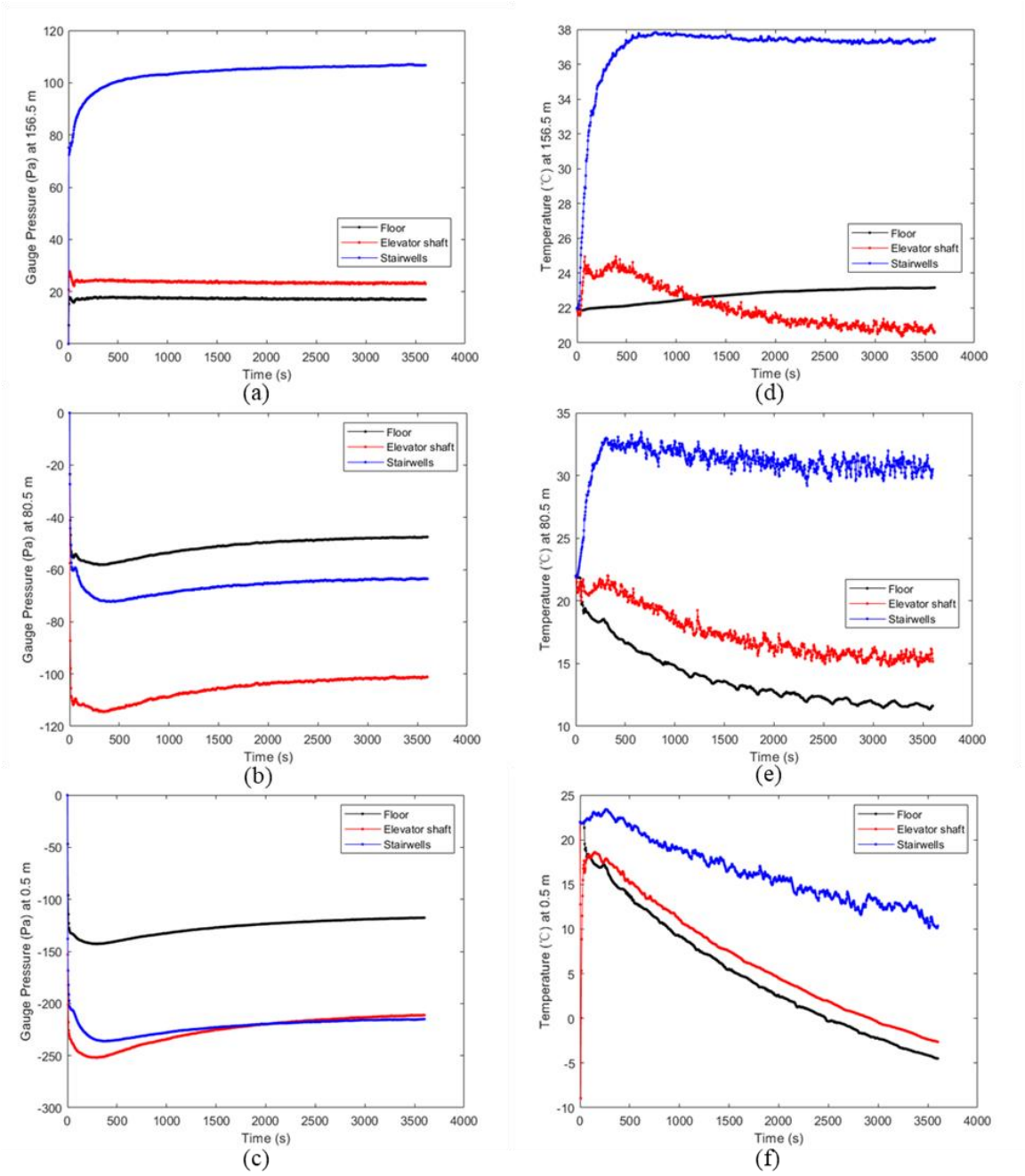

Figure 3.1: Time variations of the gauge pressure and temperature within the floors, the elevator shaft, and the stairwells at the heights of: (c)-(f) 0.5 m (1st floor); (b)-(e) 80.5 m (21st floor); and (a)-(d) 156.5m (40th floor) for the case without hot air/fire.

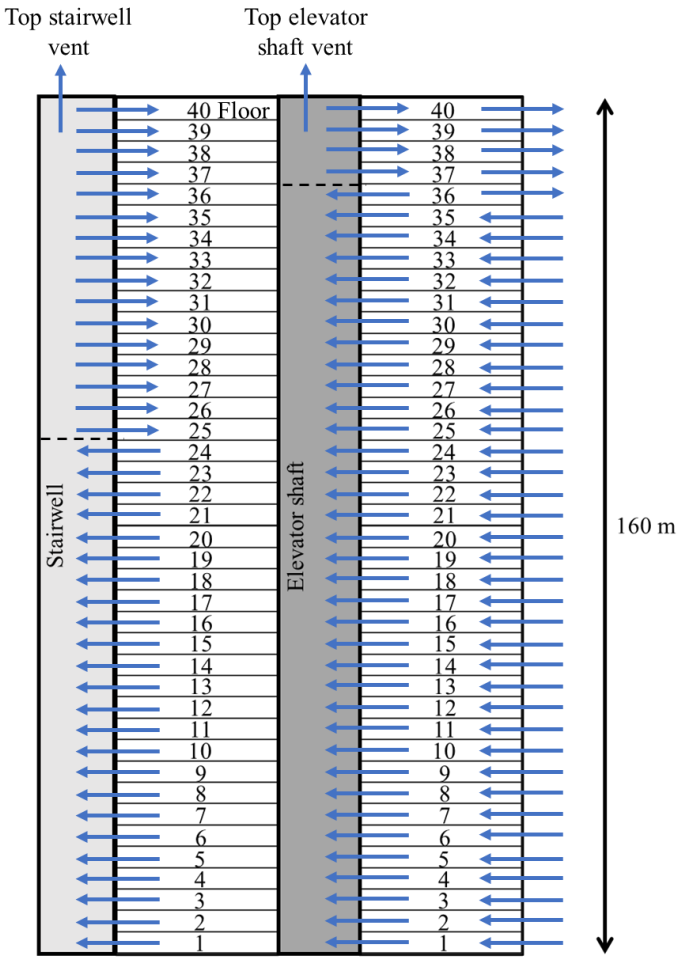

Figure 3.2: The directions of flow across the entire 40-story building for the case without hot air/fire. The drawing shows the flow paths through the roof vents at the top of the stairwells and the top of the elevator shaft, and through the leak passages between each floor space and the exterior, the stairwells and the elevator shaft. The blue single headed arrows indicate the flow direction through the corresponding vent or leak passage and the direction is determined by examining the pressure on the two sides of each leaks and vents. The dotted lines indicate the locations of NPPs for the elevator shaft and the stairwells. Note that, for simplicity, only one stairwell is represented (all four stairwells are identical and play the same role in the flow pattern).

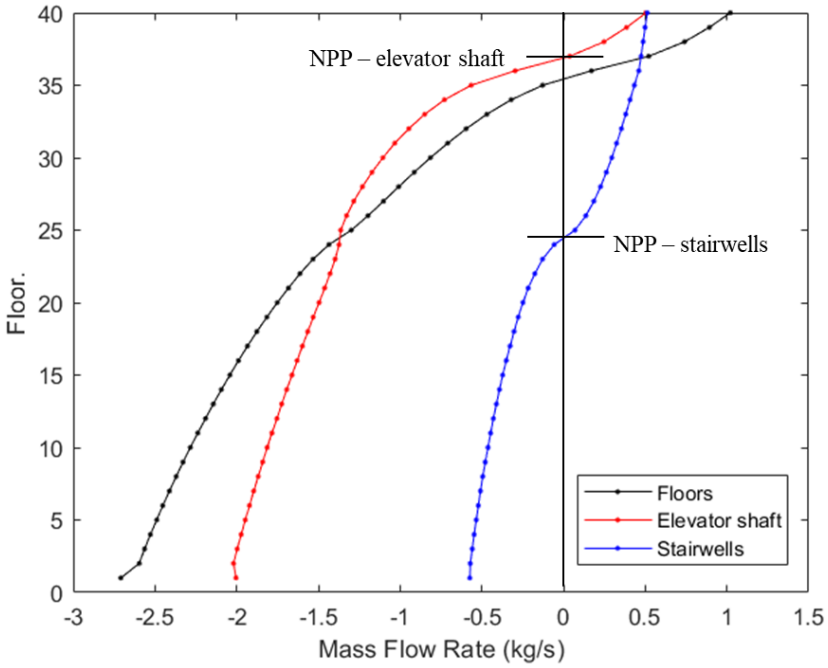

Figure 3.3: Elevation versus mass flow rate for each floor for the case without hot air/fire. Note that: (1) the black curve indicates the mass flow rates between the floors and the outside; (2) the red curve represents the mass flow rates between the floors and the elevator shaft; (3) the blue curve represents the mass flow rates between the floors and the four stairwells; (4) Negative values are inflow; positive values are outflow.

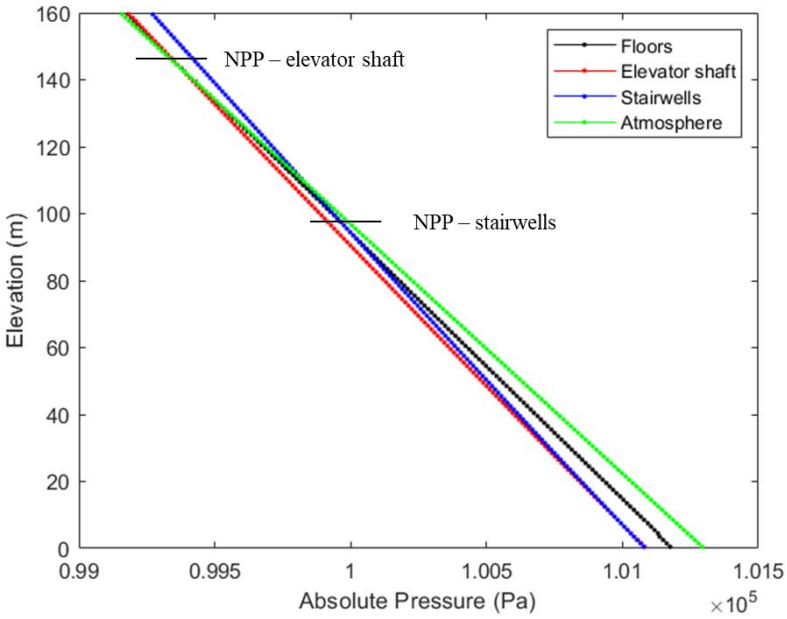

Figure 3.4: Elevation versus absolute pressure inside the high-rise building for the case without hot air/fire.

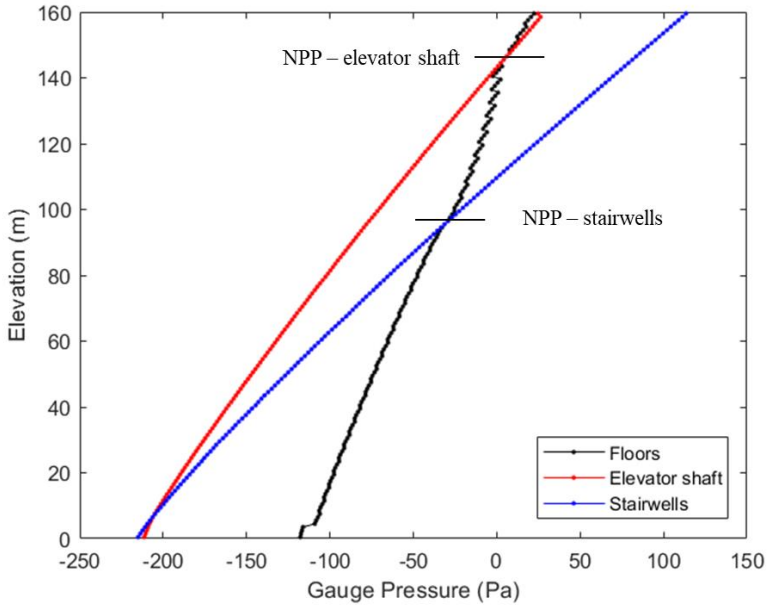

Figure 3.5: Elevation versus gauge pressure (defined as the absolute pressure with respect to the atmospheric pressure taken at the same elevation) inside the high-rise building for the case without hot air/fire.

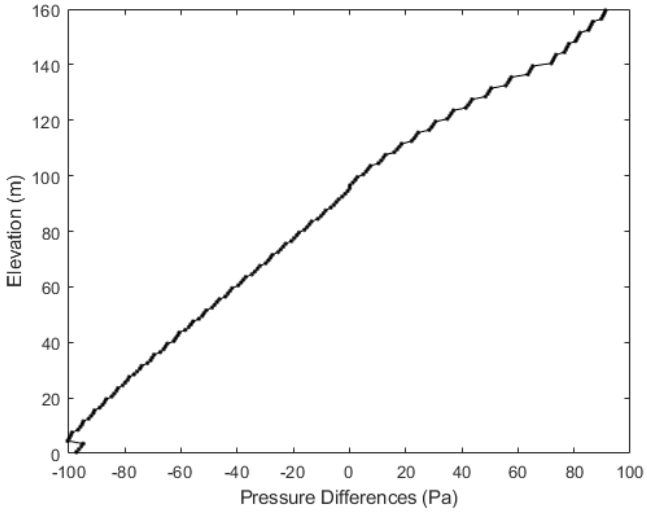

Figure 3.6: Elevation versus pressure differences between the stairwells and the floors for the case without hot air/fire. (Pressure differences = the pressure inside the stairwells – the pressure inside the floors.)

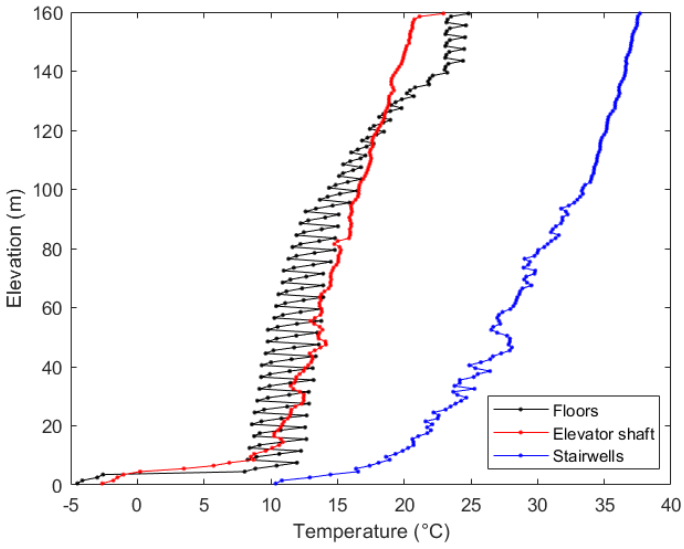

Figure 3.7: Elevation versus temperature inside the high-rise building for the case without hot air/fire.

3.2 Case 2: Hot Air Supply Case (Surrogate Fire Case)

The gauge pressure and temperature as a function of time within the floors, the elevator shaft, and the stairwells at the heights of 0.5 m (1st floor), 80.5 m (21st floor), 156.5m (40th floor) for the conditions given in Table 2.1 are illustrated in Figure 3.8. According to Figure 3.8-(f), the temperature inside the first-floor space reached the true steady state after 1000 s. However, it is apparent that the temperature inside the other floors is still subjected to slow changes after 1000 s due to the gases with different temperatures (compared to the floors' current temperatures) being drawn into these floors. Additionally, the change in the temperature has an influence on the pressure. Therefore, the gauge pressure at every part of building reached a quasi-steady state instead of a true steady state resulting in that the condition inside the entire building is also a quasi-steady state after 1000 s. Nevertheless, the quasi-steady state is a situation that is changing slowly enough so that it can be considered to be constant. Hence, the state of the mass flow rates through leaks between each individual space can be considered to be steady after 1000 s based on Eq. (3.1), because the loss coefficient (K) and the area of leak openings (A) are constant; and due to the relatively slow changes of the temperature, the density of gases (ρ) and the pressure difference between the two sides (ΔP) are also nearly constant. The FDS results that are plotted in this section are chosen at 3600 s of the simulation time.

$$\dot{m} = \rho \cdot A \cdot \sqrt{\frac{2 \cdot \Delta P}{K \cdot \rho}} \tag{3.1}$$

The mass flow directions through the roof vents at the top of the stairwells and the top of the elevator shaft, and through the leak passages between each floor space and

the outside, the stairwells, and the elevator shaft are drawn in Figure 3.9 by comparing the absolute pressure on the two sides of leaks and vents provided by FDS. It can be seen that the hot air generated on the ground floor enters the stairwells and the elevator shaft and all the way leaves the building though the top vents, and thereby the fire escape stairwells are potentially unsafe for occupants to evacuate. According to the red arrows, the floors above the 24th floor are contaminated by the hot air, thus leading to the fact that occupants need to evacuate out of these floors due to the polluted environment. Furthermore, the floors above the 36th floor is contaminated more seriously, because not only does hot air from the stairwells but also from the elevator shaft travel into these floor spaces, and no fresh air is drawn into these floor spaces through the floor leaks from the exterior. However, the floors below the 25th floor (and above the ground floor) are free of the heated air in accordance with the blue arrows. In this regard, these floor spaces are expected to be safe, unless the structure of the building is damaged by the fire. (Commonly, the structure of the second floor can be damaged by a real large fire happening on the ground floor, because the floor slab made usually by concrete for high-rise buildings can quickly absorb heat from the fire and then fail to work properly. Consequently, it is also important for the occupants on the second floor to evacuate.) (Moreover, as discussed above, the temperature inside most floors is still changing after 1000 s. Due to the fact that only the cold air from the atmosphere is drawn into the floors below the 25th floor (and above the ground floor), it is reasonable to predict that the temperature inside these floors will eventually reach – 17 ℃ which is identical with the temperature of the atmosphere, if the boundary condition inside the floors is adiabatic.)

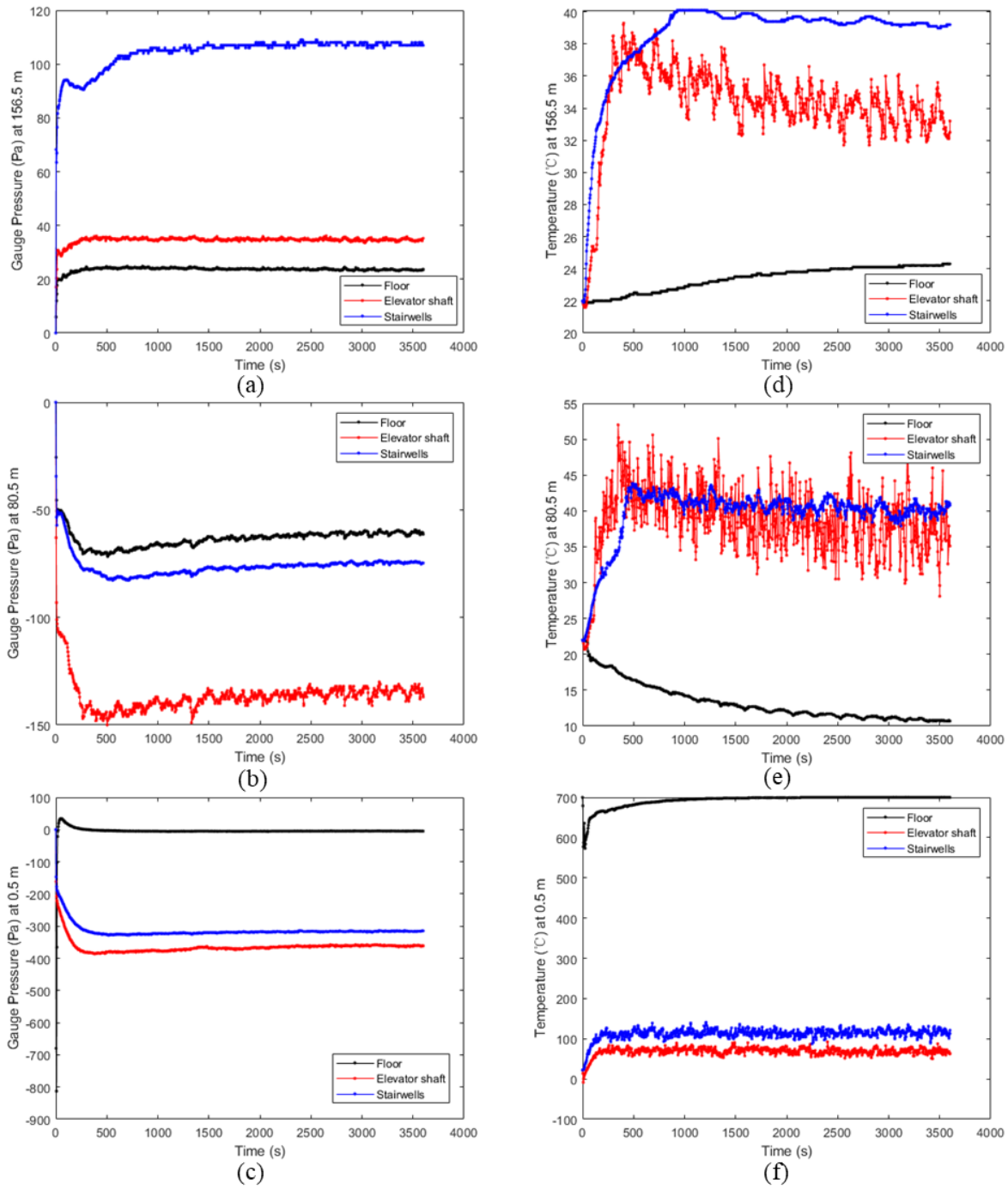

Figure 3.8: Time variations of the gauge pressure and temperature within the floors, the elevator shaft, and the stairwells at the heights of: (c)-(f) 0.5 m (1st floor); (b)-(e) 80.5 m (21st floor); and (a)-(d) 156.5m (40th floor) for the hot air supply case.

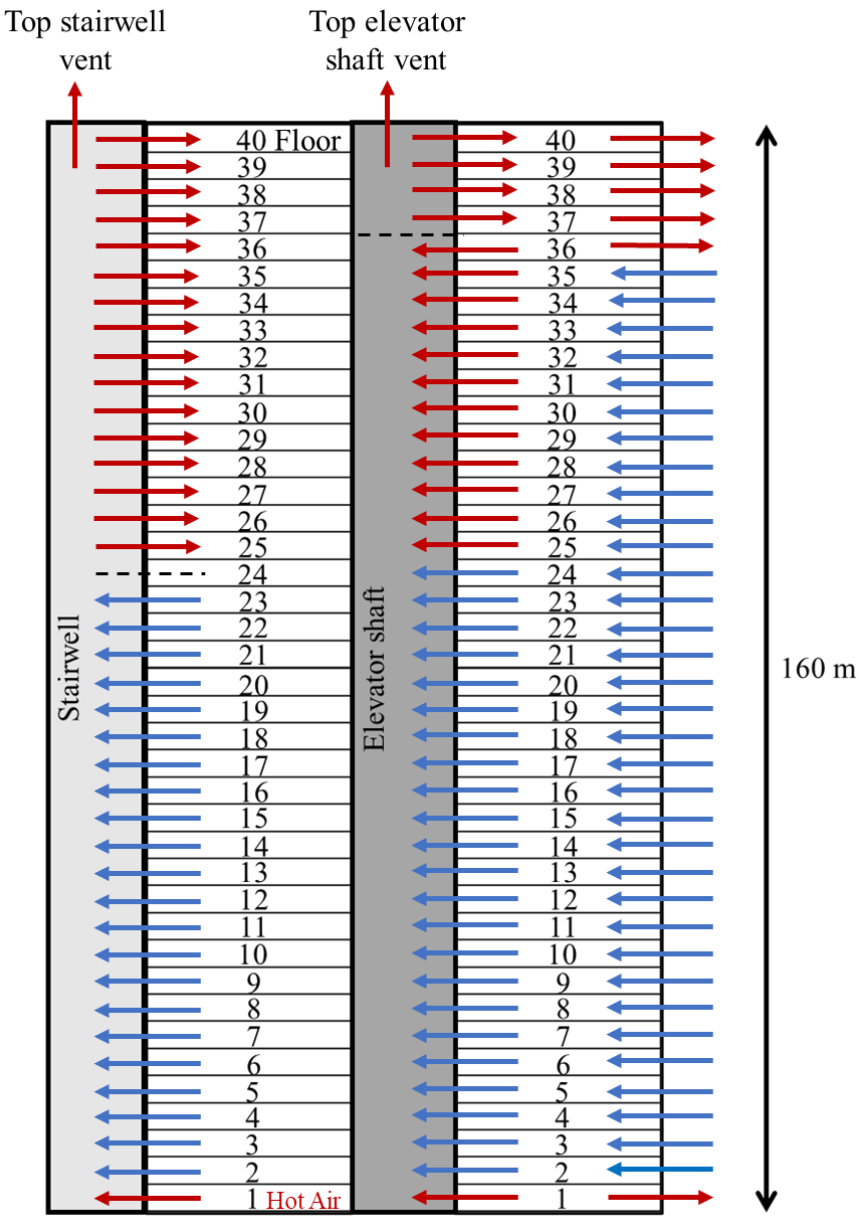

Figure 3.9: The directions of flow across the entire 40-story building for the hot air supply case. The blue arrows represent the directions of flows that are not contaminated by 700 ℃ hot air. The red arrows represent the directions of flows that are influenced by the 700 ℃ hot air. The dotted lines indicate the locations of NPPs for the elevator shaft and the stairwells. Only one stairwell is represented (all four stairwells are identical and play the same role in the flow pattern).

The examination of the mass flow rate variation in and out of both shafts and the floors versus elevation shown in Figure 3.10 reveals that the mass flow rates in the elevator shaft are far greater than the mass flow rates in the stairwells. Thus, it is logical to conclude that the elevator shaft carries more hot gases than the stairwells. The elevation of the neutral pressure plane is apparent in this figure where the curves for the elevator shaft and stairwells pass through the zero-mass flow rate axis. Based on this figure, it is evident that the conservation of mass is satisfied at every floor of the building. For instance, below the NPP for the stairwells, the rate at which gases are transferred from the outside to each floor is equal to the rate at which gases are transferred into the elevator shaft and into the stairwells from each floor; and above the NPP for the elevator shaft, the rate at which gases are transferred into each floor from the elevator shaft and from the stairwells is equal to the rate at which gases are transferred from each floor to the atmosphere.

Figures 3.12 to 3.14 compare the results provided by FDS and COSMO showing that the magnitudes of the variations in mass flow rates obtained with FDS are found to be slightly smaller than those obtained with COSMO. (Note that we did not run COSMO but used the data from Ref. [4].) This could result from the minor differences in the loss coefficient (K) used in the two models. In the COSMO program, it is called the discharge coefficient (C_d), and the relationship between the loss coefficient and the discharge coefficient is:

$$C_d = \frac{1}{\sqrt{K}}$$

The correlation between the pressure difference (ΔP) and the loss coefficient is:

$$\Delta P = \frac{1}{2} K \rho v^2$$

And the relationship between the pressure difference (ΔP) and the discharge coefficient is:

$$\Delta P = \frac{\rho v^2}{2 C_d^2}$$

where v is the velocity of flow in the leakage path, ρ is the density of the flow in the leakage path.

In the FDS simulation, *K* is specified as equal to 2.778 corresponding to that C_d is equal to 0.6. However, C_d is not indicated explicitly in the COSMO example. Therefore, this could explain the discrepancies observed in Figures 3.12 to 3.14. Also, it would be reasonable to suggest that C_d is greater than 0.6 in the COSMO example, if ΔP and ρ are consistent in both models, since the greater the C_d, the greater the v that will thereby lead to a larger value of mass flow rate for COSMO example as shown in Figures 3.12 to 3.14.

Another possible reason that may explain the smaller numerical values for the mass flow rates in the FDS simulation could be due to differences in the specified leakage areas between the two models according to Eq. (3.1), because the cross-section area of leaks is dependent on the wall area of the elevator shaft and the stairwells, and there is no information regarding the exact dimensions of the elevator shaft and the stairwells in the COSMO example. Finally, the discrepancies could be attributed to the difference in the absolute pressure obtained by two models that will be discussed in the following paragraphs regarding the pressure comparison.

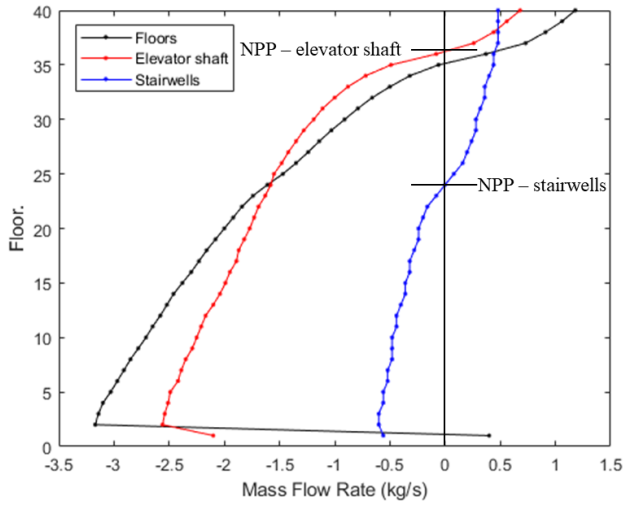

Figure 3.10: Elevation versus mass flow rate for each floor for the hot air supply case. Note that: (1) the black curve indicates the mass flow rates between the floors and the outside; (2) the red curve represents the mass flow rates between the floors and the elevator shaft; (3) the blue curve represents the mass flow rates between the floors and the stairwells. Negative values are inflow; positive values are outflow.

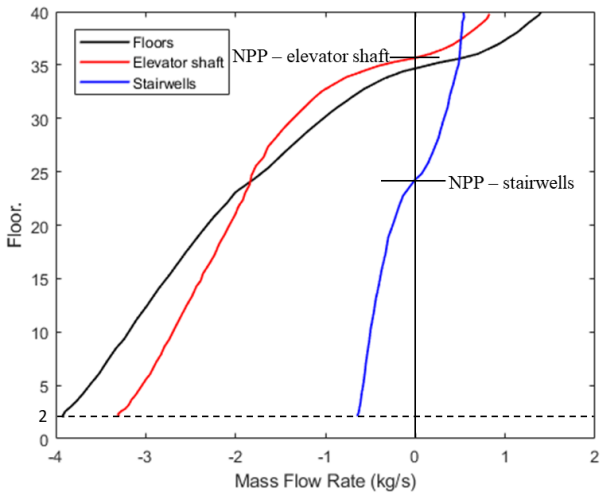

Figure 3.11: Elevation versus mass flow rate for each floor for the COSMO example [4]. Note that the data in Ref. [4] is only available above the second floor. See the caption of Fig. 3.9.

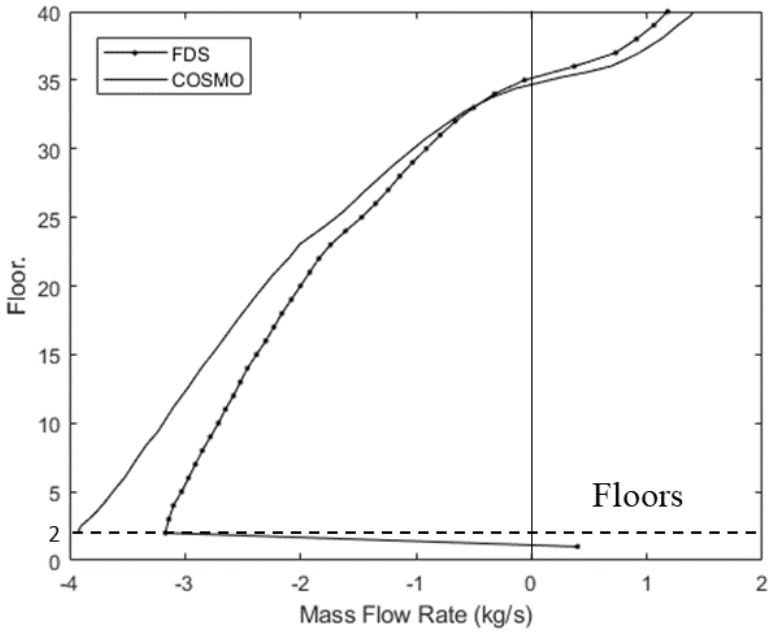

Figure 3.12: Comparison of results obtained with FDS and COSMO – mass flow rate between the floors and the exterior.

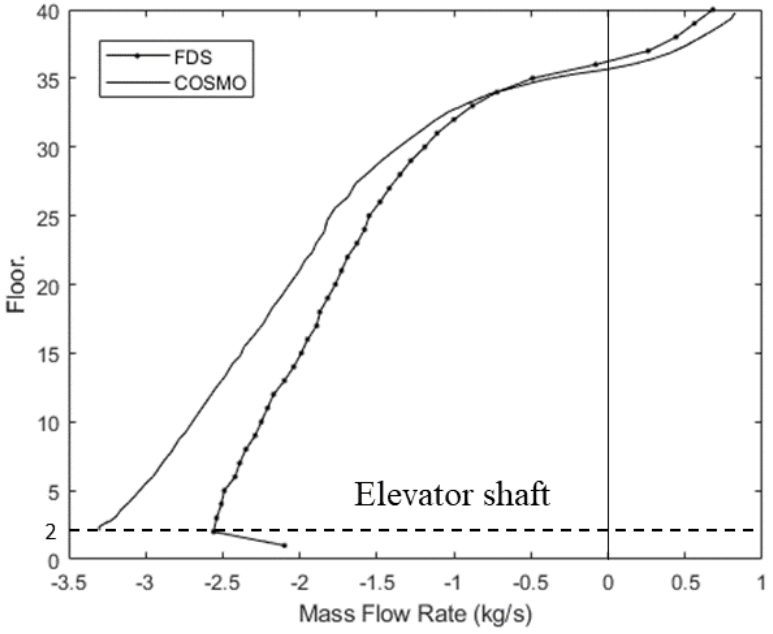

Figure 3.13: Comparison of results obtained with FDS and COSMO – mass flow rate between the floors and the elevator shaft.

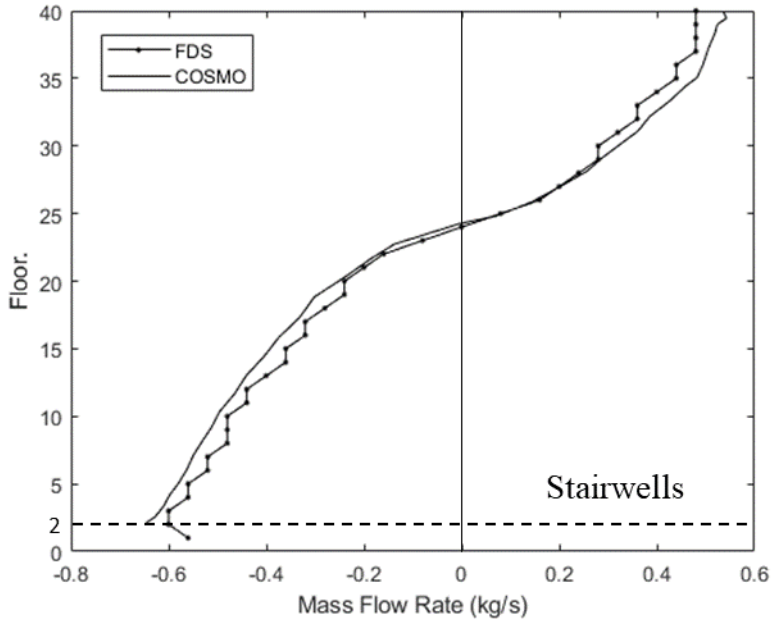

Figure 3.14: Comparison of results obtained with FDS and COSMO – mass flow rate between the floors and the stairwells.

Figure 3.15 compares the total vertical mass flow rates of the gases throughout the elevator shaft and the stairwells. It is obvious that the total vertical mass flow rate is much more in the elevator shaft than in the stairwells. Additionally, the amount of air that is carried to the upper part of the building (Note that the upper part of the building here means the part that is above their respective NPPs) is approximately seven times greater in the elevator shaft than in the stairwells which is similar to the outputs of the COSMO case shown in Figure 3.16. Thus, the elevator shaft providing the preferred path for the gases is the major "polluter" for the upper floors. The FDS predictions for the vertical mass flow rates inside both shafts are slightly smaller than those obtained in the COSMO example. This is consistent with the results presented in Figures 3.12 to 3.14 where lower numerical values of mass flow rate are obtained by FDS. The

elevation of the NPPs for each shaft is located where the respective curves reach the maximum value and the flow between the shafts and the floors reverses direction. Furthermore, COSMO predicts the locations of the NPPs to be at 35th floor and 24th floor for the elevator shaft and the stairwells, respectively. And the NPP for the stairwells in FDS is located at the 24th floor which is the same as in COSMO. However, the locations of the NPP for the elevator shaft calculated in FDS and COSMO are not exactly the same. In the FDS simulation, the NPP for the elevator shaft is located between the 36th floor and the 37th floor which is a floor higher than that in the COSMO example. This could be attributed to the fact that the lower total vertical mass flow rate in elevator shaft calculated by FDS diminishes the accumulation process in the upper part of the elevator shaft so that the pressure in the elevator shaft is only higher than the pressure inside the topmost four floors (37th to 40th floor).

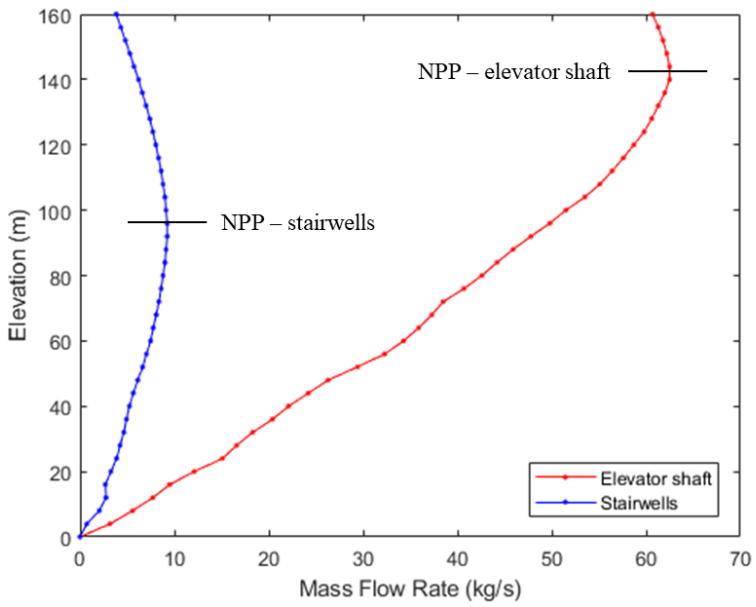

Figure 3.15: Elevation versus vertical mass flow rate inside the elevator shaft and stairwells for the hot air supply case.

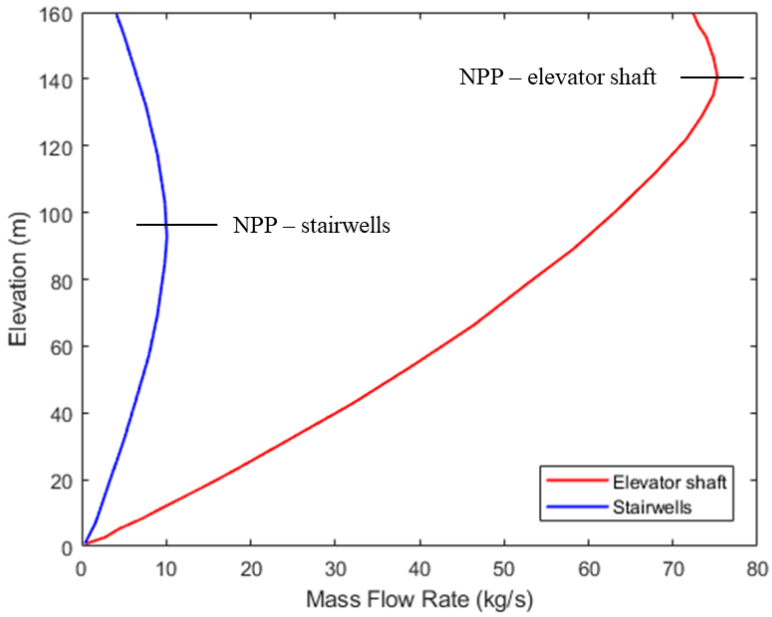

Figure 3.16: Elevation versus vertical mass flow rate inside the elevator shaft and stairwells for the COSMO example [4].

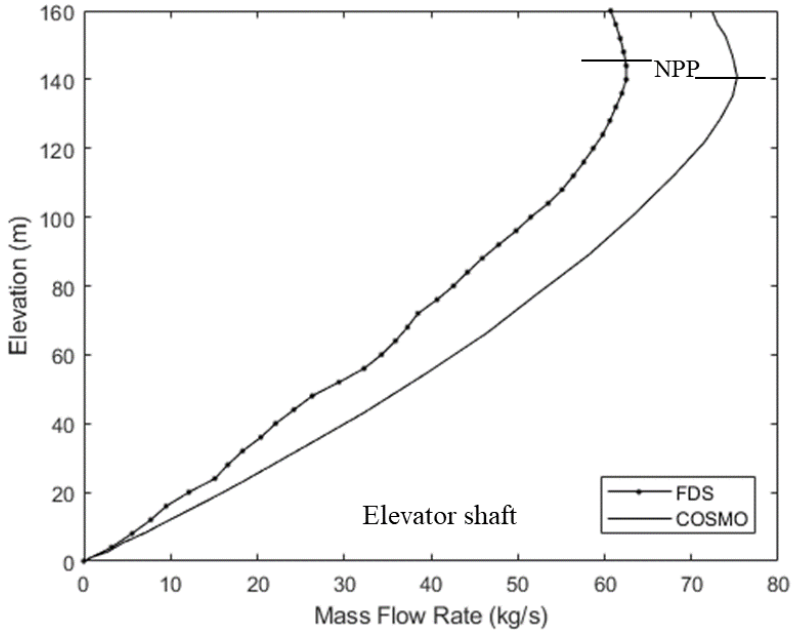

Figure 3.17: Comparison of results obtained with FDS and COSMO – elevation versus vertical mass flow rate inside the elevator shaft.

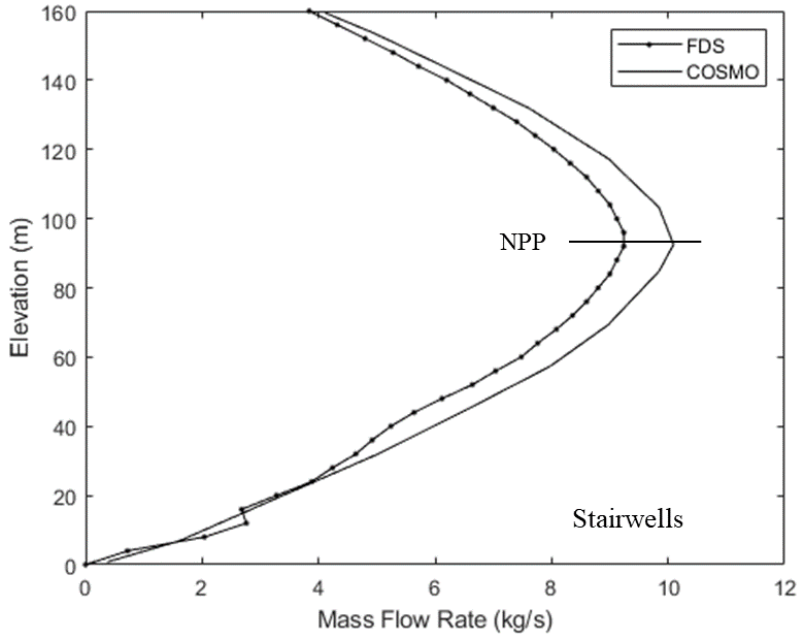

Figure 3.18: Comparison of results obtained with FDS and COSMO – elevation versus vertical mass flow rate inside the stairwells.

The distributions of the absolute pressure, gauge pressure inside the floors, the elevator shaft and the stairwells, and the pressure differences across the escape stairwells for the hot air supply case are plotted in Figures 3.19, 3.25 and 3.26. According to Figure 3.25 and Figure 3.26, the maximum pressure difference between the stairwells and the floors above the neutral pressure plane for the stairwells is about 92 Pa. And the over-pressure across the fire escape doors exceeds 78 Pa above the 38th floor. In addition, the open direction of fire escape doors is normally designed toward fire escape stairwells, thus resulting in the fact that it would be difficult for the occupants at the topmost two floors (39th floor and 40th floor) to open the fire escape doors and evacuate. Moreover, the pressure within the floors is lower than the pressure

inside the elevator shaft above the NPP for the elevator shaft. Therefore, the hot air is forced into the upper floor spaces from the elevator shaft. Below their respective NPPs, the absolute pressure in the floors is much higher than in both shafts because of the strong stack effect augmented by the ground-floor fire. Consequently, both shafts are filled with hot air from the fire floor and the lower floors will not be contaminated by hot air from the two vertical shafts.

According to Figure 3.19 and Figure 3.20, the trends of the absolute pressure distribution presented here looks nearly the same as those shown in the COSMO example. And the comparisons of the absolute pressure distribution are plotted in Figures 3.21 to 3.24. Based on these figures, it is apparent that the atmospheric pressures obtained with FDS and COSMO are the same. However, the absolute pressure reported by FDS for the floors, the elevator shaft and the stairwells are less than those obtained by COSMO. This could be explained by the temperature disparities reported by the two models, since the temperature plays a significant role in impacting the pressure inside building and more detail information will be discussed in the next few paragraphs regarding the temperature comparison. Moreover, in the COSMO case, the pressure differences between the fire floor and the stairwells and the elevator shaft are around 400 Pa and 600 Pa, respectively. However, in the FDS simulation, the pressure differences between the fire floor and the stairwells and the elevator shaft are only around 310 Pa and 360 Pa, respectively. Additionally, the pressure differences across the stairwell doors and the elevator doors are always less in the FDS case than in the COSMO case throughout the entire height of the building (except the pressure difference cross the stairwell doors at its NPP location due to the same NPPs for

stairwells in both cases). Hence, according to Eq. (3.1), this explains the lower values of the mass flow rate provided by FDS.

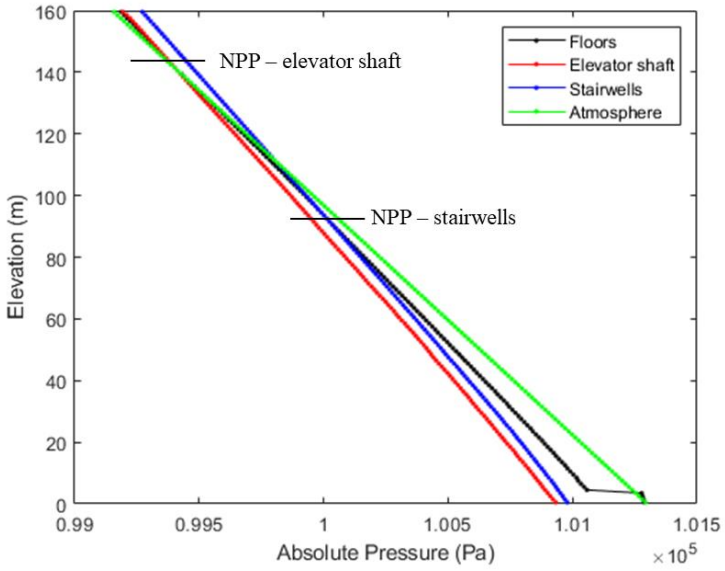

Figure 3.19: Elevation versus absolute pressure inside the high-rise building for the hot air supply case.

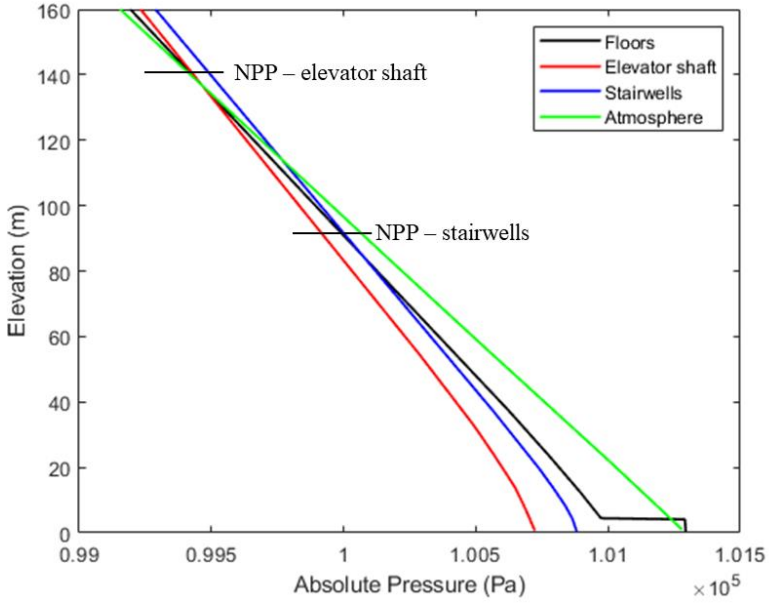

Figure 3.20: Elevation versus absolute pressure for the COSMO example [4].

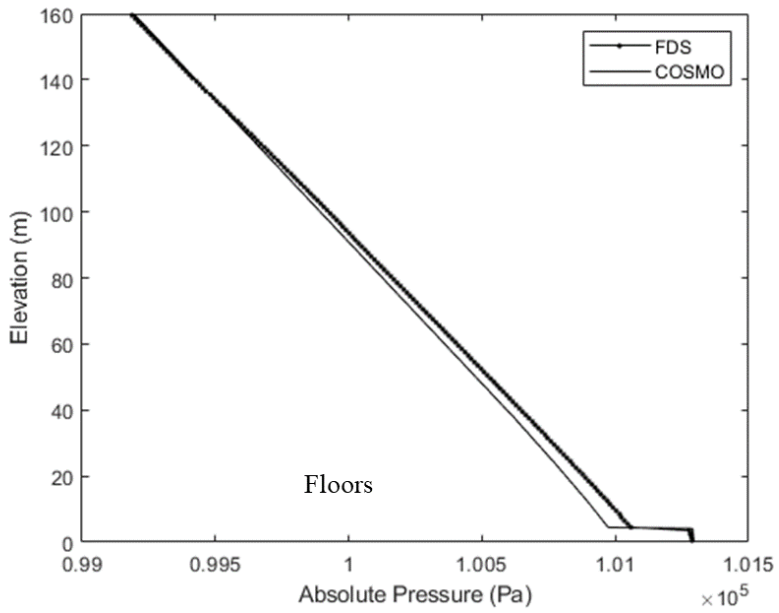

Figure 3.21: Comparison of results obtained with FDS and COSMO – absolute pressure distribution inside the floors.

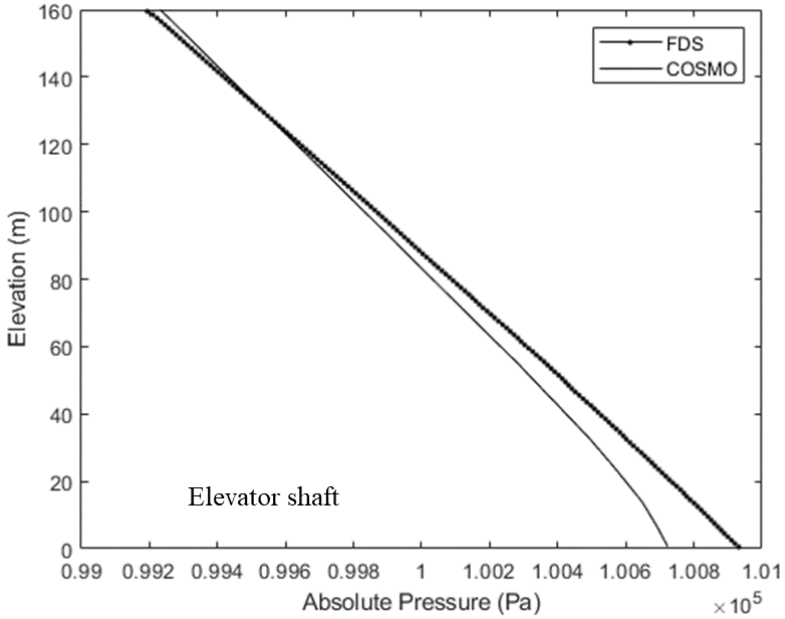

Figure 3.22: Comparison of results obtained with FDS and COSMO – absolute pressure distribution inside the elevator shaft.

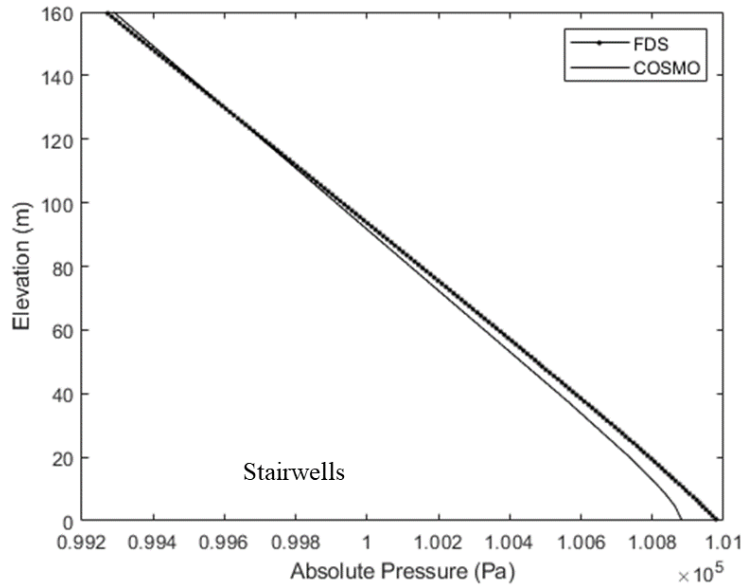

Figure 3.23: Comparison of results obtained with FDS and COSMO – absolute pressure distribution inside the stairwells.

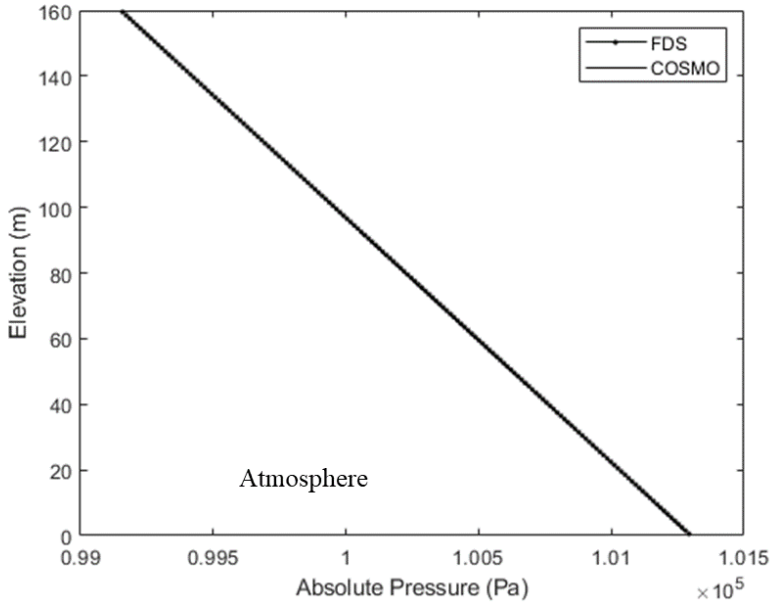

Figure 3.24: Comparison of results obtained with FDS and COSMO – atmospheric pressure distribution.

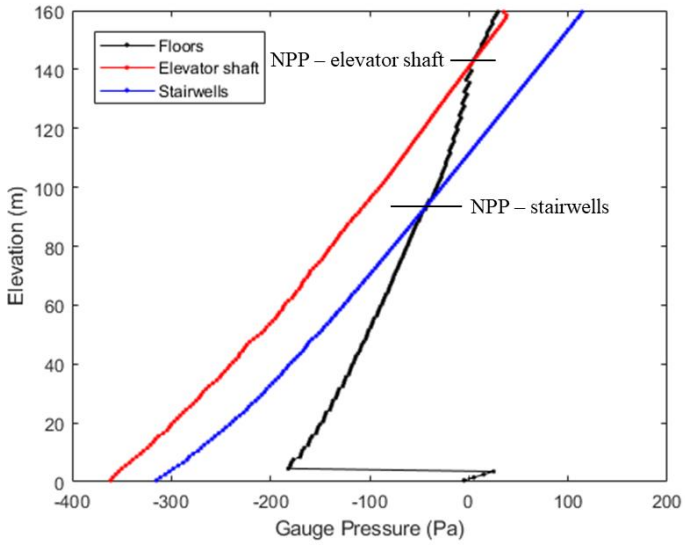

Figure 3.25: Elevation versus gauge pressure (defined as the absolute pressure with respect to the atmospheric pressure taken at the same elevation) inside the high-rise building for the hot air supply case.

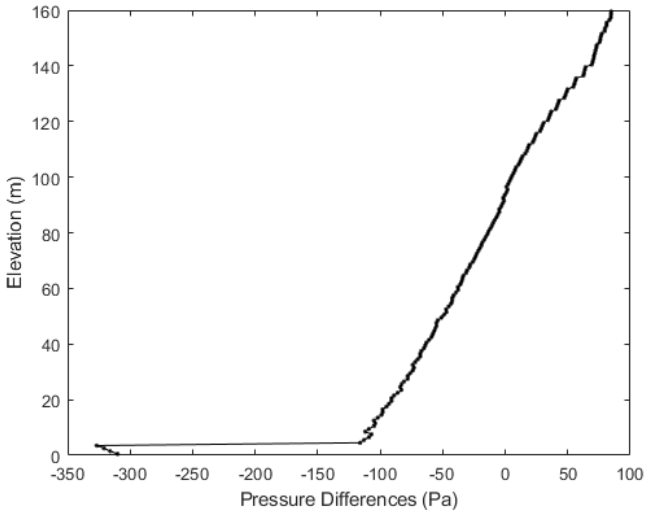

Figure 3.26: Elevation versus pressure differences between the stairwells and the floors for the hot air supply case. (Pressure differences = the pressure inside the stairwells – the pressure inside the floors.)

Figure 3.27 shows the distributions of temperature within the floors, the elevator shaft, and the stairwells. The temperature variations inside the floors drop rapidly from the ground floor temperature as cold air enters the floors from the atmosphere. Above the NPP for the floors, the temperature inside floors are increased as hot air is drawn from the elevator shaft and the stairwells and escapes to the outside atmosphere through the floor leaks. In addition, the temperature of gases in the elevator shaft and the stairwells gradually decreases from the lower floors to the upper floors, because the higher pressure within the floor spaces below NPP for the stairwells results in cold air spreading into the shafts. Moreover, when the hot air reaches about the sixth floor, the temperature inside the four egress stairwells decreases to a point which is less than 80 ℃ meaning that it will not cause hyperthermia in a short amount of time (10 minutes) [14]. However, the temperature throughout the entire height of the stairwells is always greater than 40 ℃, so the smoke fills in the stairwells meaning that evacuees are potentially hurt by the toxicity of the fire smoke. In addition, the increased temperature inside the elevator shaft and the stairwells enhances the air buoyancy force, and thereby strengthens the stack effect inside the building. Therefore, greater mass flow rates between each space are observed in the hot air case (Figure 3.10) than in the case without fire (Figure 3.3).

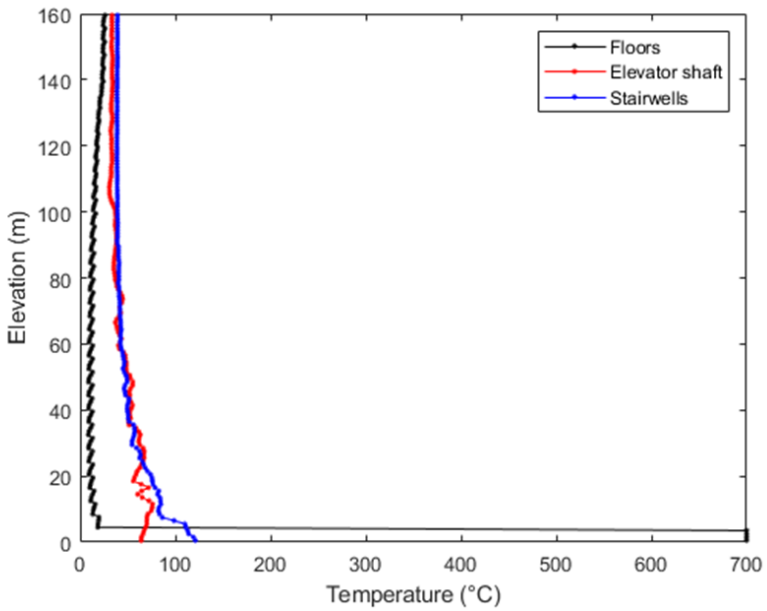

Figure 3.27: Elevation versus temperature inside the high-rise building for the hot air supply case.

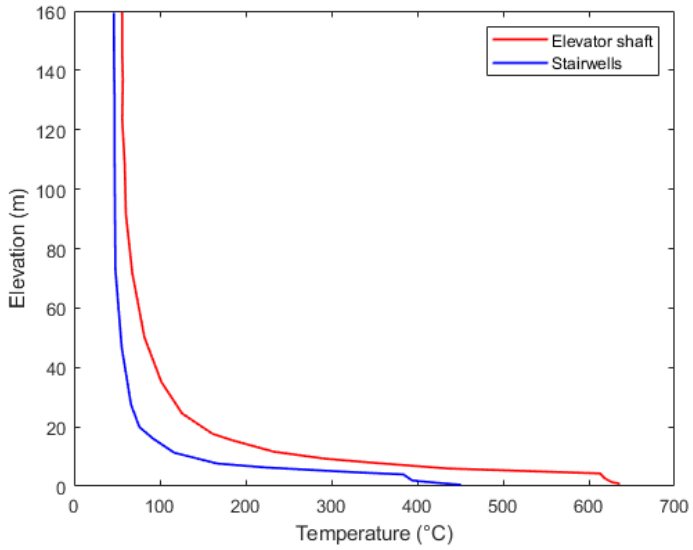

Figure 3.28: Elevation versus temperature for the COSMO example [4]. Note that the distribution of temperature inside the floor space is not provided in Ref. [4].

According to Figures 3.29 to 3.30, the trends of the temperature for the stairwells and the elevator shaft illustrated here are practically identical as the profiles for the COSMO case, but there is significant difference in the magnitude of the temperatures obtained with two models. This could be attributed to three reasons. First, the assumptions and the radiation heat transfer models that applied in the two models are different. (For instance, the COSMO model assumes that the flow of smoke in all vertical shafts within the building is one-dimensional and varies only with vertical height, whereas FDS which is based on CFD calculates the flow in a three-dimension way. In addition, the temperature change of gases through openings is assumed to be negligible in the COMSO simulation, but the HVAC network model in FDS solves the equation for the conservation of energy. Also, the radiation heat transfer models are different in FDS and COSMO. The absorption coefficient of combustion gas can be specified in the COSMO simulation, but the absorption of the hot air cannot be specified in FDS.) Second, the boundary conditions that are specified in the two models are different. All the interior surfaces of the building in the COSMO model are isothermal whereas only the interior surfaces of the walls are isothermal in the FDS model. (The floors and ceilings are treated as adiabatic, so it is reasonable to suggest that the output of the temperature inside the lower floor spaces is lower in FDS resulting in the fact that the temperatures inside both vertical shafts are also lower compared with the COSMO example. Note that: (1) this adiabatic boundary condition is specified for the purpose of avoiding any errors that would exist at the interfaces of meshes during the FDS simulation; (2) the boundary conditions inside both shafts are nearly the same for the FDS case and the COSMO example, because there are not any floors and

ceilings inside them except for the building ground floor and the building top ceiling.) Finally, the different constructions of the two models, such as the areas of the elevator shaft and the stairwells, the distribution of the leaks and the locations of the diagnosis's devices could potentially impact the calculation for temperature. Therefore, taken together, it is observed that the temperature drops more dramatically from the fire floor to the elevator shaft and stairwells in the FDS simulation (more energy loss) and the temperatures for the stairwells and the elevator shaft reported by FDS are always less than those reported by COSMO throughout entire height of the building. Furthermore, these lower temperature values could lead to less pressures in the elevator shaft and the stairwells and to a weaker stack effect compared to the COSMO example as we discussed above.

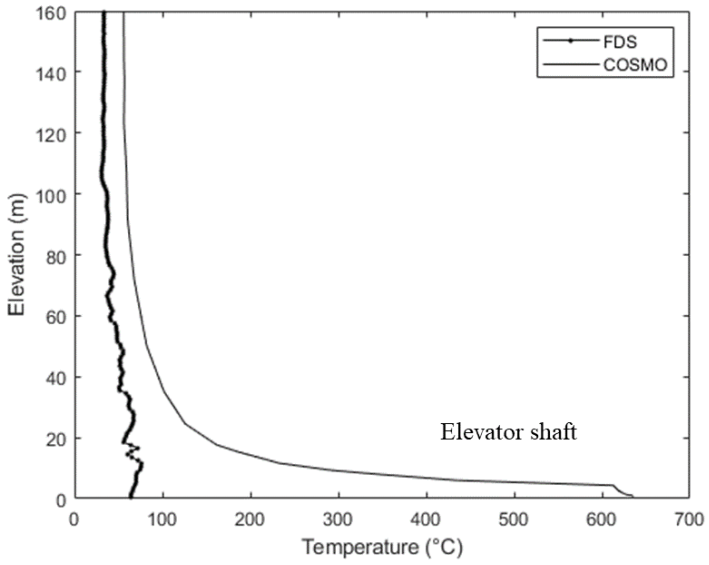

Figure 3.29: Comparison of results obtained with FDS and COSMO – temperature distribution within the elevator shaft.

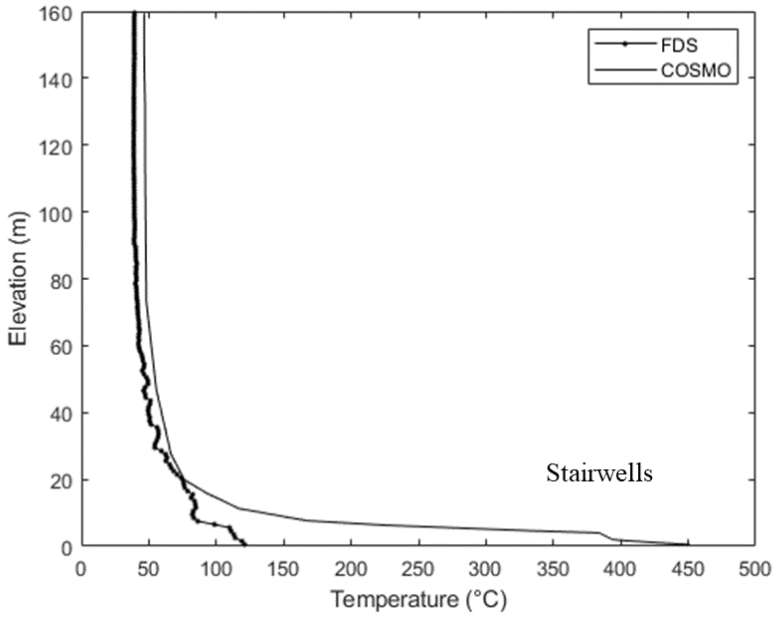

Figure 3.30: Comparison of results obtained with FDS and COSMO – temperature distribution within the stairwells.

In conclusion, the outputs provided by FDS and COSMO are qualitatively the same suggesting that the hot air/fire smoke spreads to the elevator shaft, the stairwells, and the upper floor spaces from the ground floor. Additionally, the discrepancies between results obtained with the FDS and COSMO models remain small and can be explained by the differences in the modeling assumptions between the two programs and slight differences between the model geometries and boundary conditions.

Chapter 4: Fire Cases

4.1 Case 3: 10 MW Design Fire

We now turn to the simulation of more realistic fire conditions. According to the conservation of energy, a propane fire with an HRR of 3.4 MW would be expected to create the same condition as the surrogate fire conditions described above, as long as the configuration of the high-rise building and the atmospheric conditions are kept unchanged (and the oxygen inside the fire floor is infinite). The hand calculations are as follows:

The first-floor area without the elevator shaft and the stairwells is chosen as the control volume. For the hot air case, according to conservation of mass, at steady state, the total amount of air that is imposed into the first-floor space per unit time is equal to the total amount of air that leaves the first-floor space per unit time:

$$\dot{m}_{out} = \dot{m}_{in} = \dot{m}_{hot\ air} = 0.0565 \times 54 = 3.051\ kg/s$$

According to the conservation of energy, at steady state, the rate of the total amount of energy that is added into the control volume by the hot air is equal to the rate of the total amount of energy that is reduced by outflow:

$$\dot{m}_{out} \times c_{out} \times T_{out} = \dot{m}_{in} \times c_{in} \times T_{in} = \dot{m}_{hot\ air} \times c_{hot\ air} \times T_{hot\ air}$$
$$= 3.051 \times 1.1417 \times (700 + 273) = 3389.28\ kW \approx 3.4\ MW$$

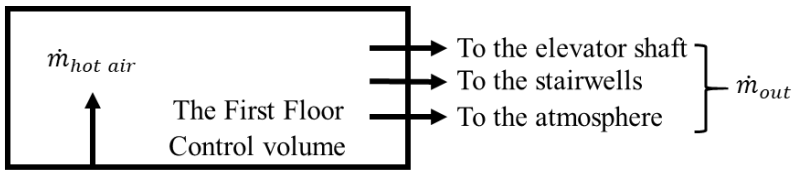

Figure 4.1: Mass flow directions for the first-floor control volume at steady state for the hot air case.

Assume that there is only outflow through leakage paths in the control volume under the design fire condition, so based on the conservation of the energy:

$$\dot{Q} = \dot{m}_{out} \times c_{out} \times T_{out} \approx 3.4\ MW$$

Therefore, a design fire with a HRR of 3.4 MW would create similar conditions inside the fire floor. However, considering the depletion of the oxygen, when the condition inside the control volume becomes steady, there would be cold fresh air entering into the control volume. Therefore, in the real simulations, this fire will not produce similar conditions inside the building and thereby a fire with higher HRR value is required to keep the similar conditions inside the fire floor. (This calculation is to give a sense of the energy released by the hot air supply and the corresponding fire size to readers.)

By assuming that the first floor is a shopping center and according to Ref.[17], an ultra-fast t-square 10 MW fire is going to be specified inside the fire floor, and the fuel selected here is propane (chemical formula: C_3H_8). According to Eq. (2.2), the time to reach 10 MW can be calculated:

$$t_g = \sqrt{\frac{10000\ kW}{0.1878}} \approx 231\ s$$

So, TAU_Q is specified as equal to 231 in the FDS codes.

Now, let us estimate when the oxygen inside the control volume will be completely consumed:

Assume that the oxygen mass loss to the stairwells, the elevator shaft and the outside is neglectable and that under-ventilation condition would not occur prior to the oxygen level going to 0, the time required to consume the initial amount of oxygen contained inside the first-floor control volume can be calculated:

The total volume of the control volume is:

$$V_{CV} = \big(40 \times 50 - (4 \times 4 \times 4 + 10 \times 8)\big) \times 4 = 7424\ m^2$$

Assume ideal gas conditions, the total amount of oxygen inside the control volume is:

$$n_{O_2,total} = 7424\ m^2 \times 0.21 \div 22.4\ L/mol = 69600\ mol$$

From 0 s to 231 s, the total energy released by the design fire is:

$$Q = \int_0^{231} 10000 \times \frac{t^2}{231^2}\, dt = 770000\ kJ$$

And during this time, the amount of oxygen that is be consumed is:

$$n_{con,0-231} = 770000kJ \div 13.1\ kJ/g \div 32\ g/mol = 1836\ mol$$

After 231 s, the oxygen that is left in the control volume is:

$$n_{left,231} = 69600\ mol - 1836\ mol = 67764\ mol$$

The simplified combustion equation (ignore the soot) for propane is:

$$C_3H_8 + 5O_2 \rightarrow 3CO_2 + 4H_2O$$

FDS reports that the mass flow rate of the fuel is 220 g/s, so 5 mol/s of propane is consumed corresponding to the fact that 25 mol/s of oxygen will be consumed. Hence, the time for consuming the rest of the oxygen after 231 s is:

$$t = 67764\ mol \div 25\ mol/s = 2710\ s$$

Therefore, the total time required for consuming the oxygen is:

$$t_{total} = 231\ s + 2710\ s = 2942\ s$$

So, after 2942 s, there will be fresh air entering into the fire floor.

The development of the heat release of the design fire is shown in Figure 4.2. The fully developed state is reached at 231 seconds as specified, but the HRR declines evidently after around 700 seconds due to the depletion of the oxygen and the design fire becomes under-ventilated followed by a phase in which the HRR reaches back to around 10 MW due to the flames migrating to oxygen-rich locations (see below). At 3600 s of the simulation time, based on the results provided by FDS, the global equivalence ratio of the design fire is:

$$\Phi = \frac{(A/F)_{stoic}}{(A/F)} \approx \frac{\left(\frac{4.76 \times 5 \times 28.88}{44}\right)}{\left(\frac{2.4}{0.22}\right)} \approx 1.4$$

So, the design fire is under the fuel rich/under-ventilation condition at 3600 s. Furthermore, it is noticed that in Smokeview the flame leaves the specified burner surface, migrates to the fire floor leak towards the outside, and intrudes into the elevator shaft when the design fire becomes under-ventilated for the purpose of having more oxygen.

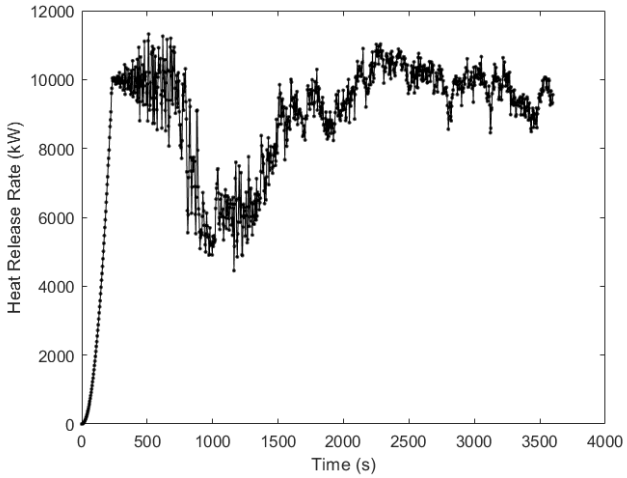

Figure 4.2: The time variations of the heat release rate of the ultra-fast t-square 10 MW fire.

For this fuel rich case, the time evolutions of the gauge pressure and temperature within the floors, the elevator shaft, and the stairwells at the heights of 0.5 m (1st floor), 80.5 m (21st floor), and 156.5m (40th floor) are shown in Figure 4.3. According to Figure 4.3-(c), the pressure inside the fire floor reaches a peak value at around 245 s of the simulation time which is after a few seconds when the HRR reaches the maximum value. The decline of the pressure is owing to the fact that the oxygen inside the fire floor is not enough for supporting the design fire and the HRR is thereby decreased. Hence, the huge amount of outflow from fire floor to the outside along with the decreased HRR drops the pressure inside the fire floor, and the cold fresh air is then drawn into fire floor until the inside gauge pressure becomes negative. Additionally, from these graphs, the quasi-steady state of the entire building is approximately achieved after 2000 s. Considering the different phenomena at different stage of the design fire, the graphs that are demonstrated below in this section are from the FDS results at 245 s and 3600 s.

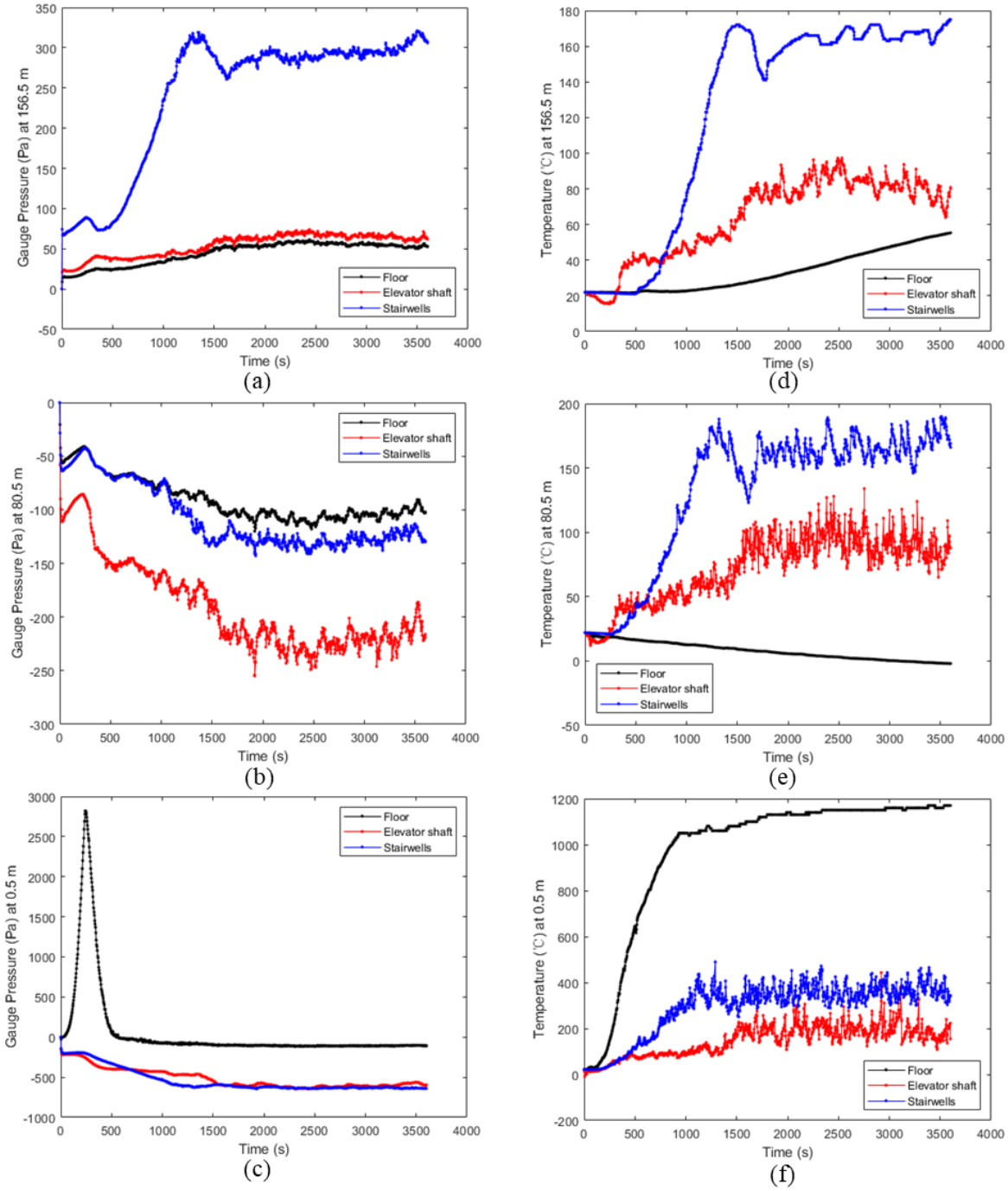

Figure 4.3: Time variations of the gauge pressure and temperature within the floors, the elevator shaft, and the stairwells at the heights of: (c)-(f) 0.5 m (1st floor); (b)-(e) 80.5 m (21st floor); and (a)-(d) 156.5m (40th floor) for the fuel rich case.

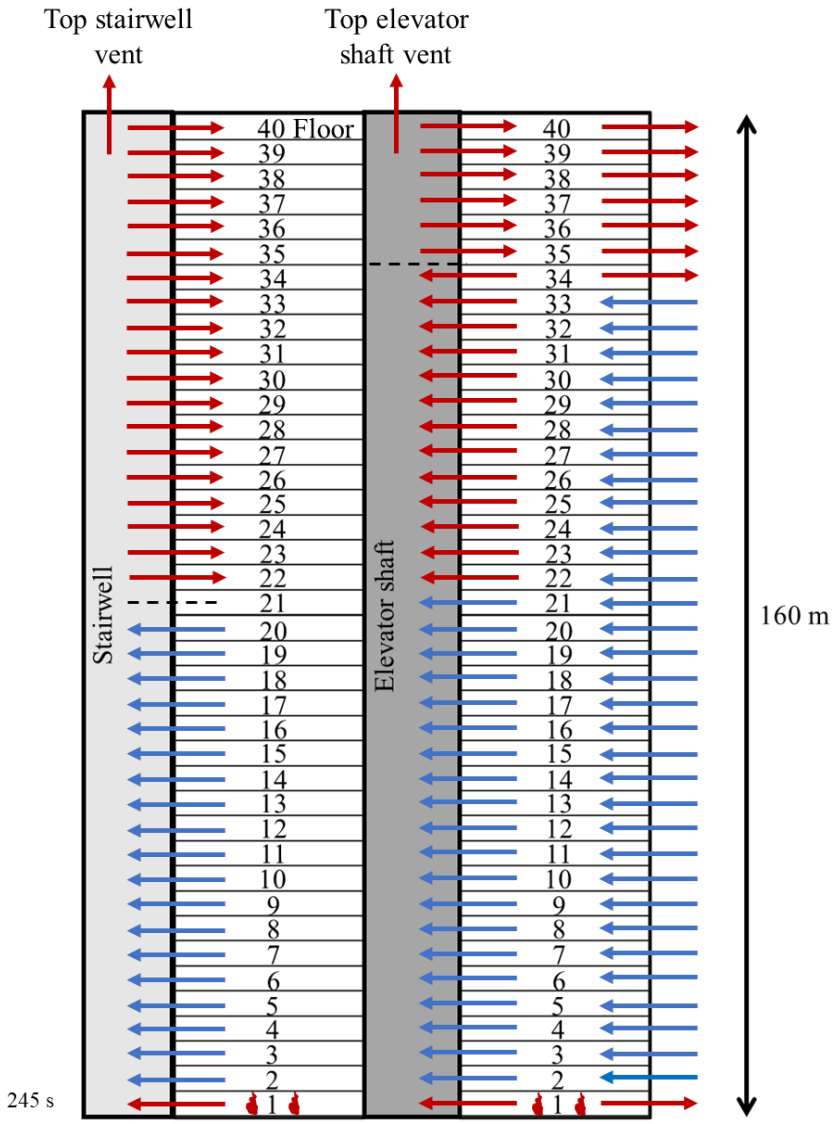

Figure 4.4: The directions of flow across the entire 40-story building for the fuel rich case at 245 s. Note that: (1) the blue arrows represent the directions of flows that are not contaminated by the hot smoke; (2) the red arrows represent the directions of flows that are influenced by the hot smoke; (3) the dotted lines indicate the locations of NPPs for the elevator shaft and the stairwells; (4) for simplicity, only one stairwell is represented (all four stairwells are identical and play the same role in the flow pattern).

Figure 4.4 shows the flow patterns across the building leaks and vents at 245 s. According to the red arrows, the fire smoke generated inside the first floor enters the stairwells, the elevator shaft and the outside, and migrates into upper floors that are above the NPP of the stairwells. The blue arrows demonstrate that only fresh cold air is drawn into the floor spaces between the fire floor and the 21st floor. Hence, the flow directions illustrated here at 245 s are similar to the those in the hot air case at 3600 s. The difference is that the NPPs for the stairwells and the elevator shaft lowers to 21st floor and the position between the 34th floor and 35th floor, respectively. This could be attributed to the fact that more flows were pushed into both two shafts due to the greater pressure differences between the floors and the stairwells and the elevator shaft. According to Figures 4.6 to 4.8, the over-pressure across the escape stairwells doors is 3020 Pa and that across the elevator doors is 3080 Pa. These are extremely large pressure differences, thus causing a greater mass flow rate depicted in Figure 4.5 at first floor. In addition, due to the high pressure inside the fire floor at 245 s which is about 2820 Pa greater than the atmospheric pressure, approximately 10.5 kg/s flows are pushed into the outside. This is about 27 times greater than the outflow from the fire floor in the hot air case at 3600 s. However, the pressure differences between the floors and the stairwells and the elevator shaft do not surpass the 78 Pa throughout the entire height of the building. Consequently, the evacuees would not have difficulty in opening the fire escape doors and escape at this moment. Finally, the temperature distributions inside the high-rise at 245 s are demonstrated in Figure 4.9. The temperature inside the first floor at the location near the leaks towards the stairwells is around 200 ℃. The temperature inside the stairwells is always less than 40 ℃ above

the 3rd floor meaning that only small amount of the fire smoke is transported in the stairwells and thus the evacuees would not be seriously affected at this time. Additionally, the more evident decline in the temperature in the upper part of the elevator shaft may be attributed to the combined effect that more cold air being drawn into elevator shaft compared to the inflow of hot smoke and large amounts of gases escaping through the top elevator vent.

In a word, the conditions inside the building are still acceptable at 245 s and the interesting part is the very high pressure inside the fire floor developing a greater mass flow rate between each space on the first floor.

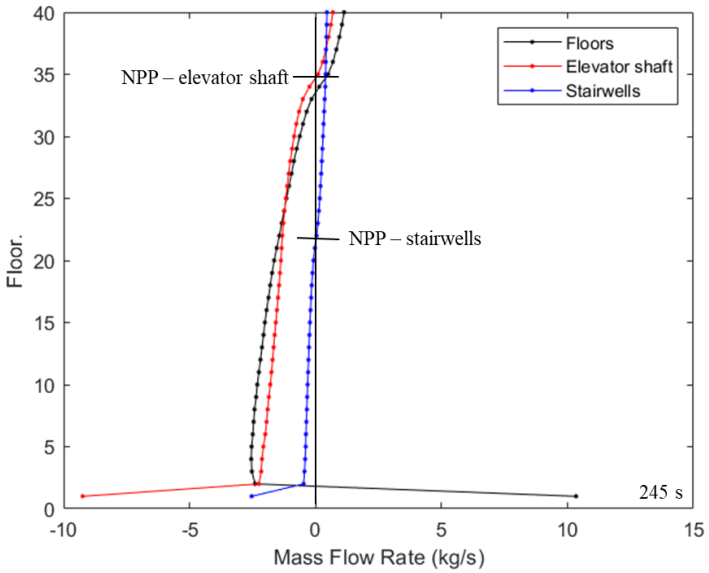

Figure 4.5: Elevation versus mass flow rate for each floor for the fuel rich case at 245 s. Note that: (1) the black curve indicates the mass flow rates only between the floors and the outside; (2) the red curve represents the mass flow rates only between the floors and the elevator shaft; (3) the blue curve represents the mass flow rates only between the floors and the stairwells. Negative values are inflow; positive values are outflow.

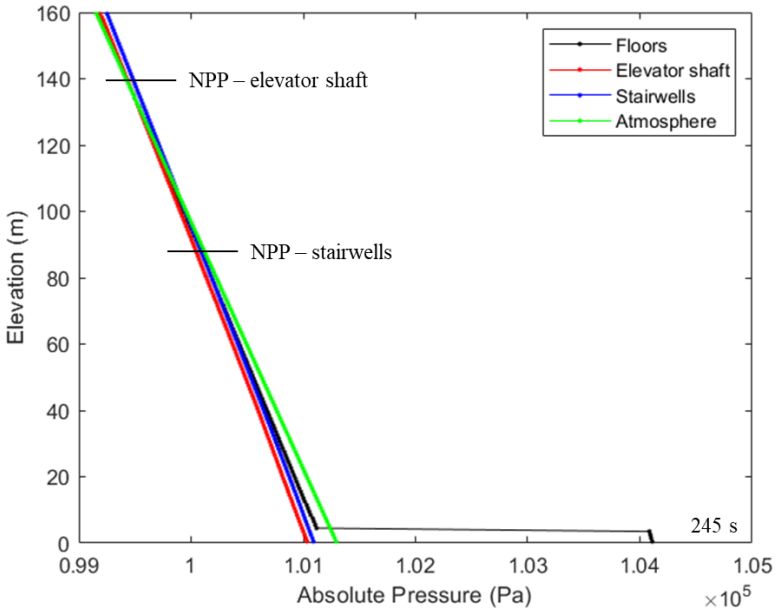

Figure 4.6: Elevation versus absolute pressure inside the high-rise building for the fuel rich case at 245 s.

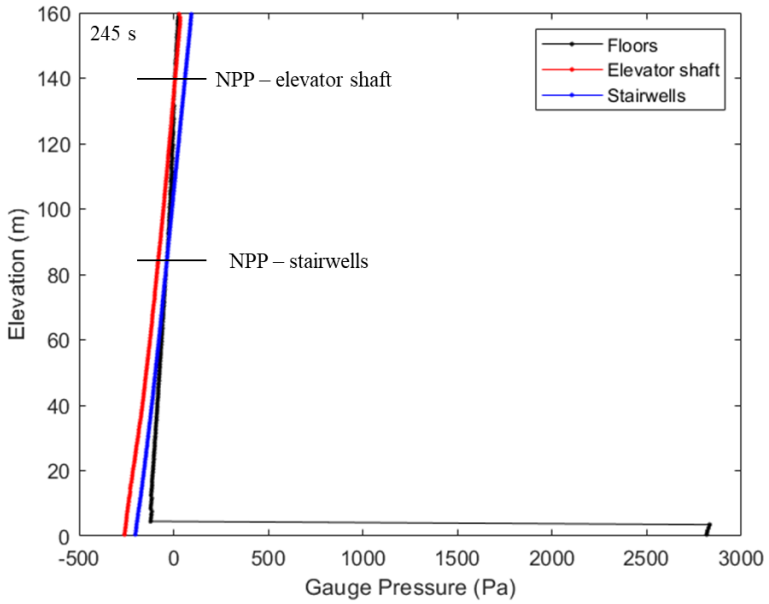

Figure 4.7: Elevation versus gauge pressure inside the high-rise building for the fuel rich case at 245 s.

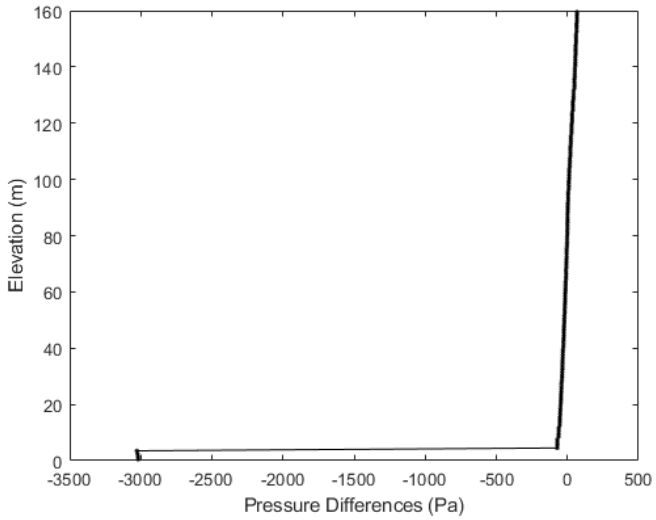

Figure 4.8: Elevation versus pressure differences between the stairwells and the floors for the fuel rich case at 245 s. (Pressure difference = the pressure inside the stairwells – the pressure inside the floors.)

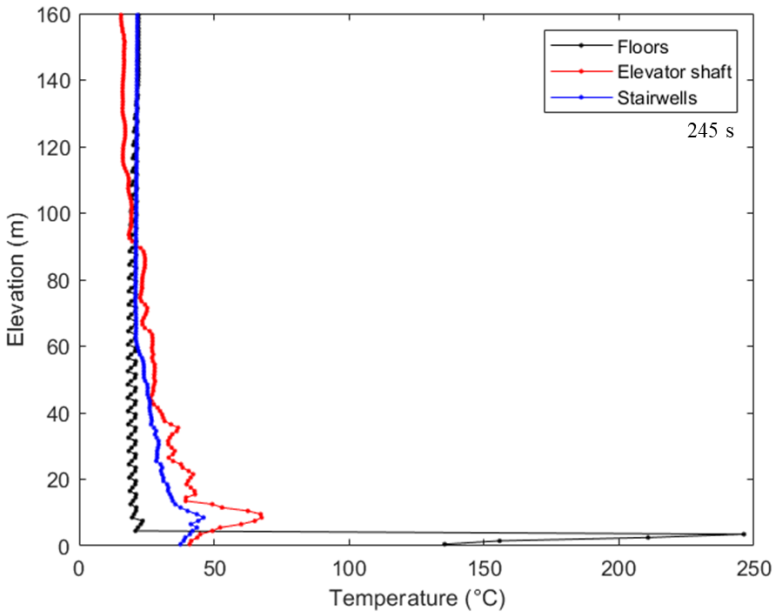

Figure 4.9: Elevation versus temperature inside the high-rise building for the fuel rich case at 245 s.

By comparing the absolute pressure on the two sides of every leakage path, the mass flow directions between each individual space at 3600 s are shown in Figure 4.10. The red arrows illustrate that the fire smoke is spreading into not only the elevator shaft but also the stairwells which means that these fire escape stairwells would be unsafe for occupants to evacuate. Also, the red arrows show that hot smoke is forced into the floors above the 23rd floor from the stairwells and into the floors above the 35th floor from the elevator shaft resulting in a polluted environment in these areas. Hence, occupants inside these floor spaces need to evacuate and some smoke control strategies must be applied to the building in order to ensure safe egress. According to the blue arrows, only cold air from the atmosphere is drawn into the floor space between the fire floor and the 24th floor so that occupants are safe and will not be influenced by hot smoke (as long as the structure is not damaged by the fire and the fire is extinguished before it spreads into upper floors). These arrows also suggest that the fire smoke does not escape to the outside atmosphere through the first-floor leaks but only through the upper-floor leaks and roof vents. This is because, according to Figures 4.12 to 4.14, the gauge pressure inside the fire floor is negative resulting from the depletion of the oxygen and the fact that the fire needs the support of oxygen from the atmosphere.

Figure 4.11 provides the mass flow rate in and out of both shafts and the floors at 3600 s. It shows that the NPP for the elevator shaft is the same as that found in the hot-air-supply case. The NPP for the stairwells lowers slightly to the location between the 23rd floor and the 24th floor for the fuel rich case at 3600 s. Furthermore, based on the mass flow rate presented in Figure 4.11, it is apparent that the amount of fire smoke is

greater in the elevator shaft than in the stairwells due to the greater mass flow rate of air from the floors to the elevator shaft. However, compared to the hot-air-supply case, all the mass flow rates are higher in this case. This could be explained by the fact that, even if the gauge pressure inside the fire floor is negative, the greater pressure differences between the fire floor and the stairwells (530 Pa) and the elevator shaft (490 Pa) leads to a stronger stack effect in the building.

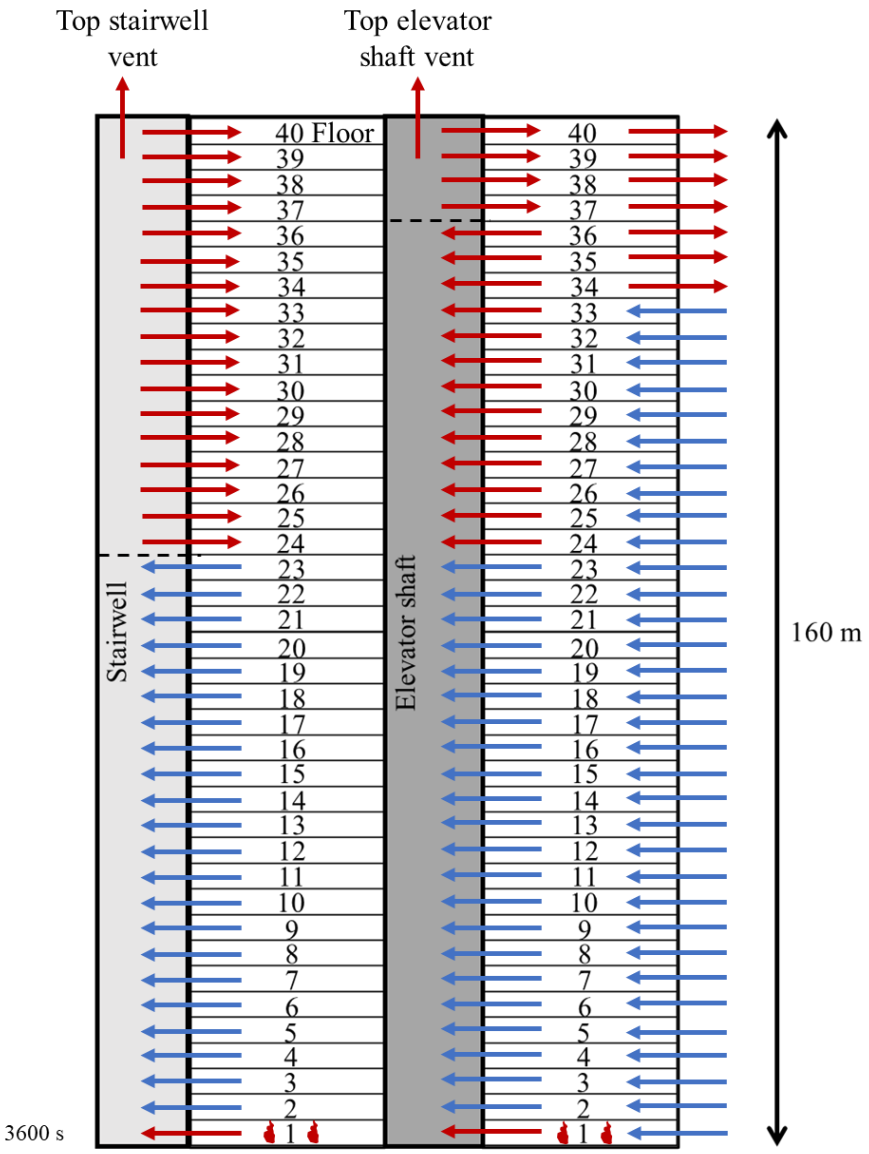

Figure 4.10: The directions of flow across the entire 40-story building for the fuel rich case at 3600 s. Note that: (1) the blue arrows represent the directions of flows that are not contaminated by the hot smoke; (2) the red arrows represent the directions of flows that are influenced by the hot smoke; (3) the dotted lines indicate the locations of NPPs for the elevator shaft and the stairwells; (4) for simplicity, only one stairwell is represented (all four stairwells are identical and play the same role in the flow pattern).

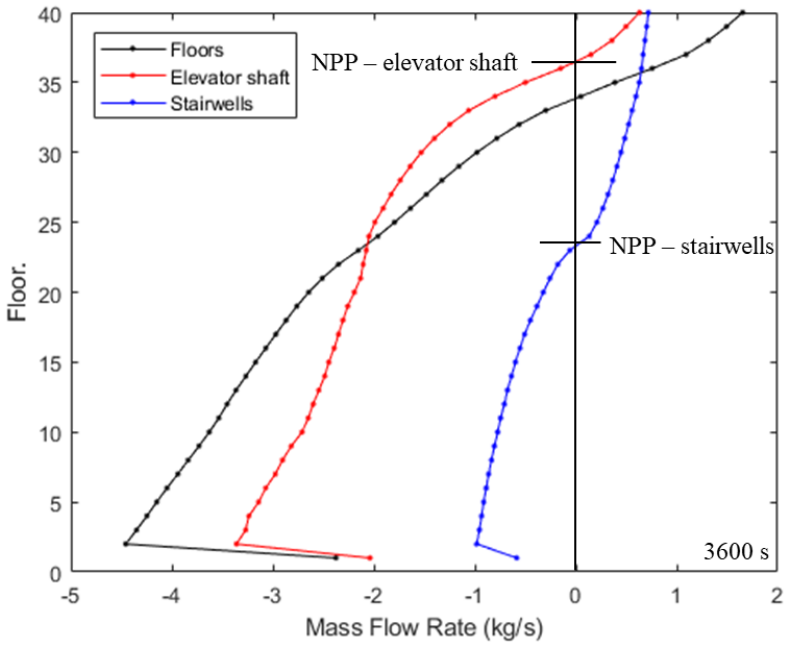

Figure 4.11: Elevation versus mass flow rate for each floor for the fuel rich case at 3600 s. See the caption of Fig. 4.5.

As shown in Figures 4.12 and 4.13, the absolute and gauge pressure curves for this case at 3600 s are similar to those obtained in the hot-air-supply case. However,

the gauge pressure at the fire floor illustrated in Figure 4.13 is negative, and the curves in Figure 4.12 show that the pressure inside the fire floor is lower than the atmospheric pressure. This is the reason why fresh cold air is drawn from the atmosphere to feed the design fire and no smoke escapes through the fire floor leakage path. Therefore, this result is not identical to the surrogate fire case that creates a positive 10 Pa gauge pressure on the ground floor. According to Figure 4.14, above the 28th floor, the pressure difference across the fire escape door exceeds 78 Pa and the maximum pressure difference is more than 250 Pa on the topmost floor which means that occupants would have extreme difficulty in opening the fire egress doors and evacuate if no smoke control plans are used for the building.

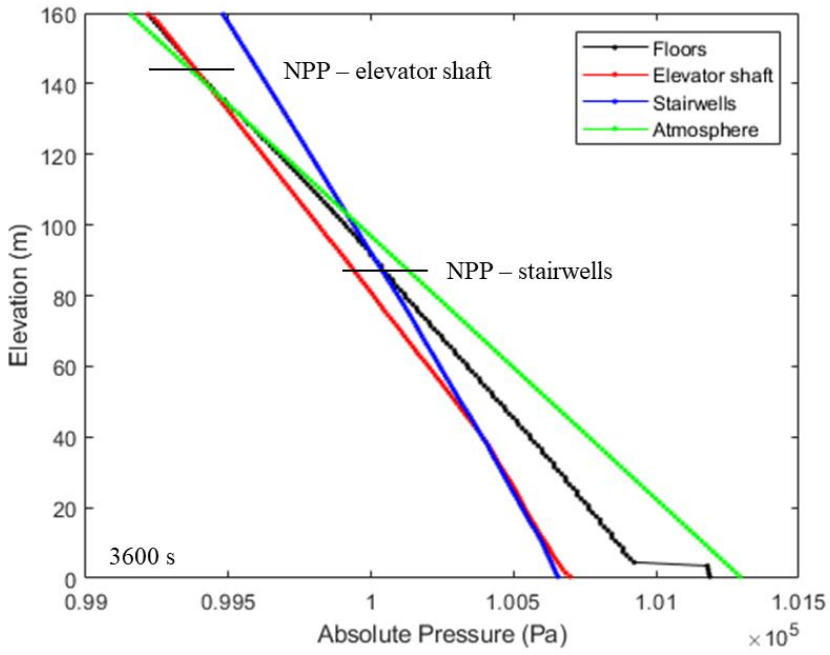

Figure 4.12: Elevation versus absolute pressure inside the high-rise building for the fuel rich case at 3600 s.

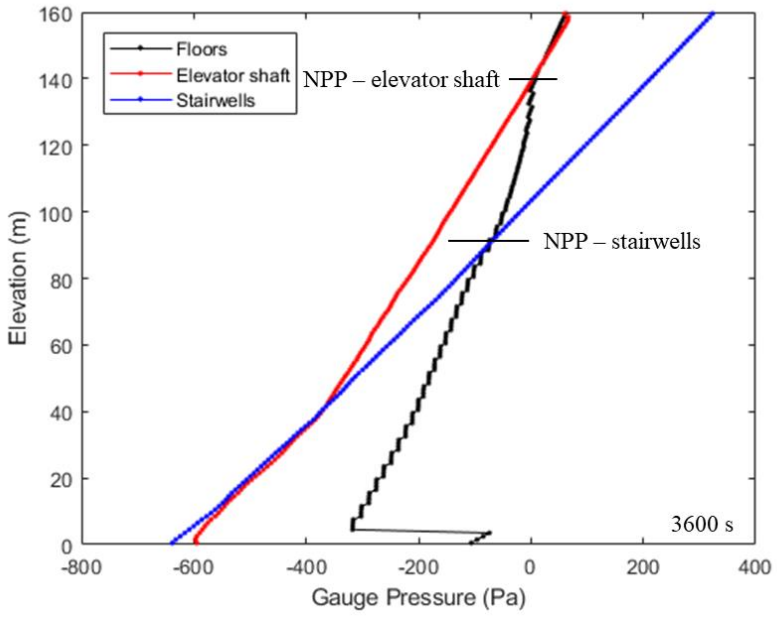

Figure 4.13: Elevation versus gauge pressure inside the high-rise building for the fuel rich case at 3600 s.

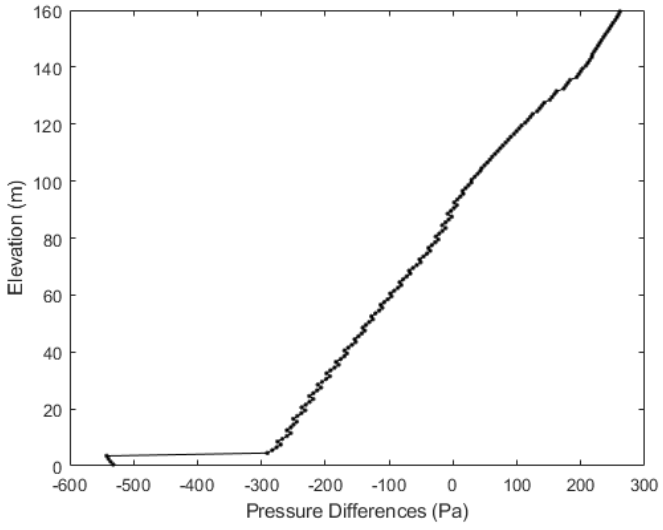

Figure 4.14: Elevation versus pressure differences between the stairwells and the floors for the fuel rich case at 3600 s. (Pressure difference = the pressure inside the stairwells – the pressure inside the floors.)

Figure 4.15 shows the temperature distribution for this case. (Note that the location of the temperature device has an influence on the temperature output in FDS due to the fact that the temperature inside a fire room is not uniformly distributed. The temperature devices of the floors are located near to the floor leaks towards the stairwells for the purpose of monitoring the temperature of gases in and out the floors from the stairwells.) The temperature of gases inside the floors decreases from the ground floor as height increases, but it increases as height increases above the neutral pressure plane for the stairwells due to hot smoke drawn into these upper floors. Additionally, the temperatures of gases in both shafts at the top of the building are still featuring high values (above 40 ℃) indicating that smoke is present in both shafts, so it would potentially lead to incapacitation if the exposure time is long. Finally, the shapes of the temperature curves are nearly the same as those of the surrogate fire case.

To sum up, at 3600 s, this design fire case results in more serious conditions within the building compared those obtained with the hot-air-supply case. The major difference between the two cases discussed above is that fresh cold air enters the fire floor to support the combustion of propane due to the negative gauge pressure in the case at 3600 s, whereas the hot air is pushed out of the ground floor due to the positive gauge pressure in the hot-air-supply case.

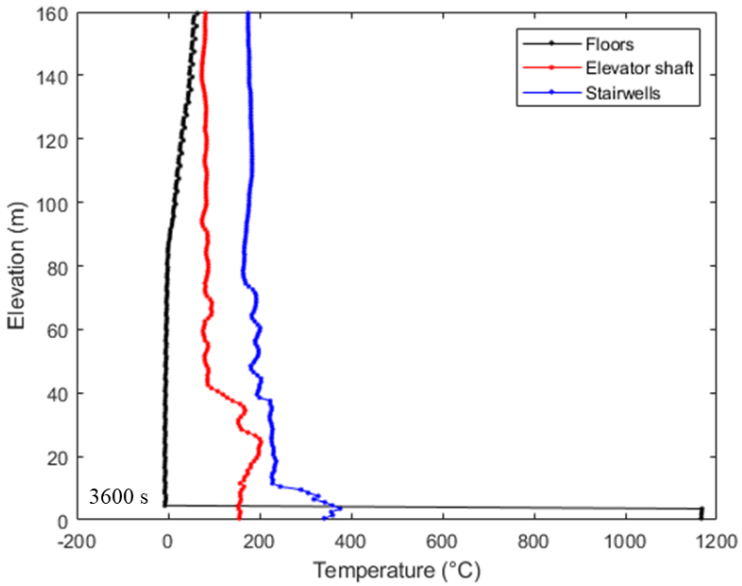

Figure 4.15: Elevation versus temperature inside the high-rise building for the fuel rich case at 3600 s.

4.2 Case 4: 2.5 MW Design Fire

As the discussion above, it turns out that the 10 MW design fire finally becomes a fuel rich/under-ventilated fire. Now, a 2.5 MW ultra-fast t-square design fire is going to be specified inside the first floor for the purpose of simulating a fuel lean/over-ventilated condition.

According to Eq. (2.2), the time to reach 2.5 MW can be calculated:

$$t_g = \sqrt{\frac{2500\ kW}{0.1878}} \approx 115\ s$$

So, TAU_Q is specified as equal to 115 in the FDS codes.

According to the FDS outputs, the global equivalence ratio of this case at 3600 s is:

$$\Phi = \frac{(A/F)_{stoic}}{(A/F)} \approx \frac{\left(\frac{4.76 \times 5 \times 28.88}{44}\right)}{\left(\frac{2.1}{0.055}\right)} \approx 0.4$$

So, the fuel lean condition is created in this case.

The development of the heat release rate for this case is shown in Figure 4.16. The fire reaches the fully developed stage at 115 s which is the same as the value specified in the FDS codes. Additionally, the HRR is always around 2.5 MW which means that the fire is over-ventilated condition. Also, from the Smokeview animation of this case, the flame does not migrate to other locations from the burner surface during the entire simulation time.

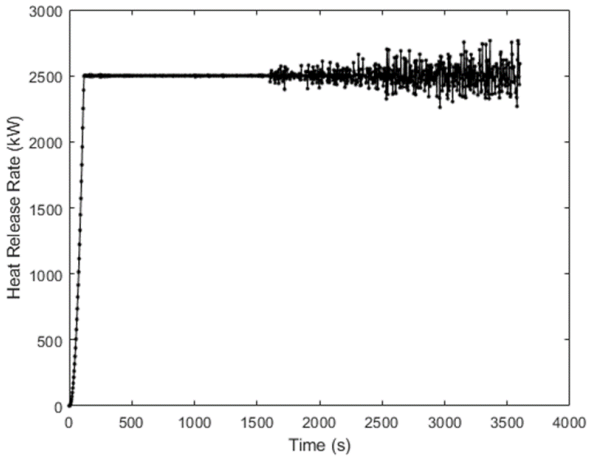

Figure 4.16: The time variations of the heat release rate of the ultra-fast t-square 2.5 MW fire.

The time variations of the gauge pressure and the temperature inside three representative floors are demonstrated in Figure 4.17. The quasi-steady state is reached approximately after 2000 s. The pressure inside the fire floor reaches the peak value at 130 s which is a few seconds after the fire reaches the fully developed stage. The discussion in this section will include the results provided by FDS at 130 s and 3600 s due to the two different conditions.

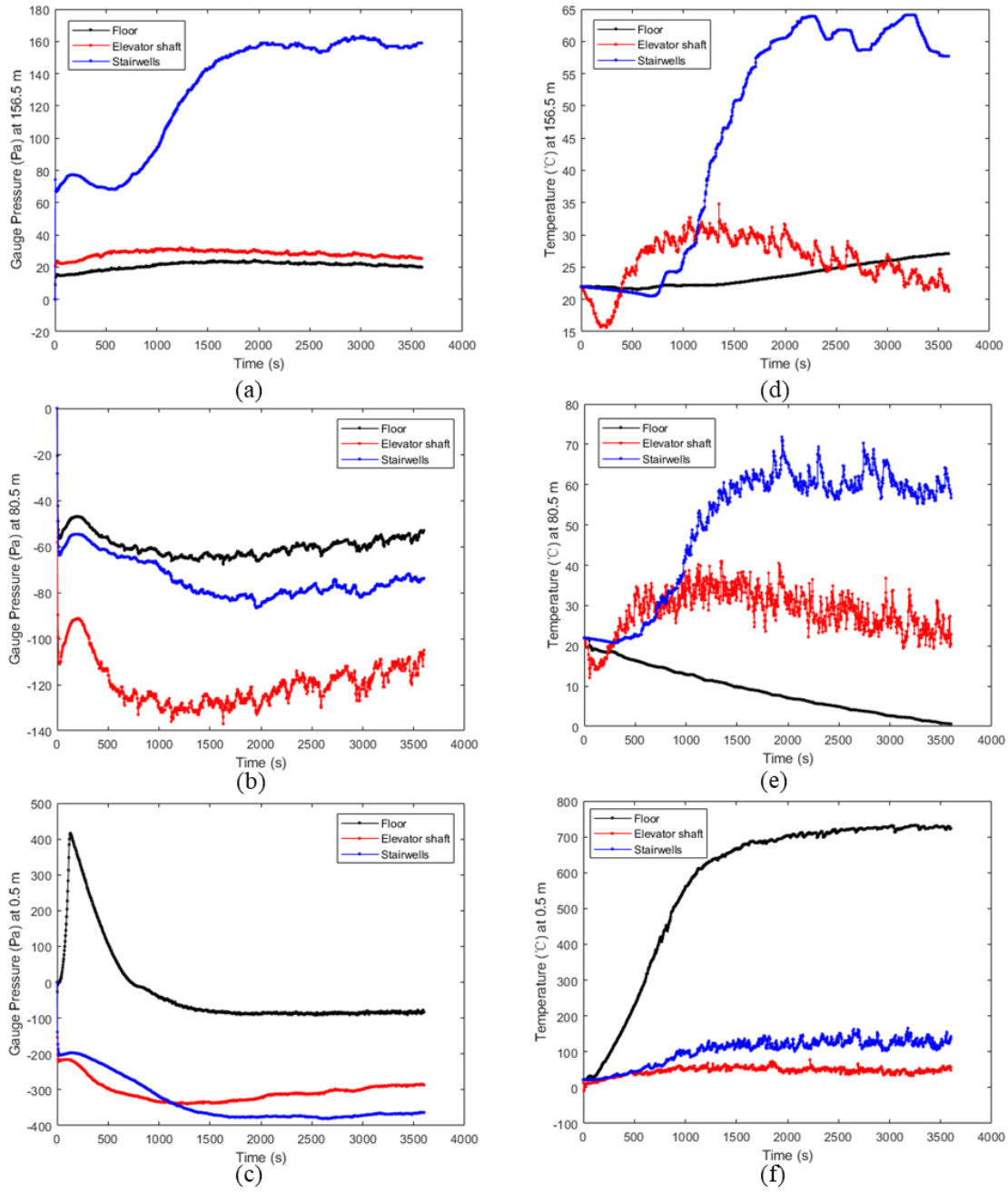

Figure 4.17: Time variations of the gauge pressure and temperature within the floors, the elevator shaft, and the stairwells at the heights of: (c)-(f) 0.5 m (1st floor); (b)-(e) 80.5 m (21st floor); and (a)-(d) 156.5m (40th floor) for the fuel lean case.

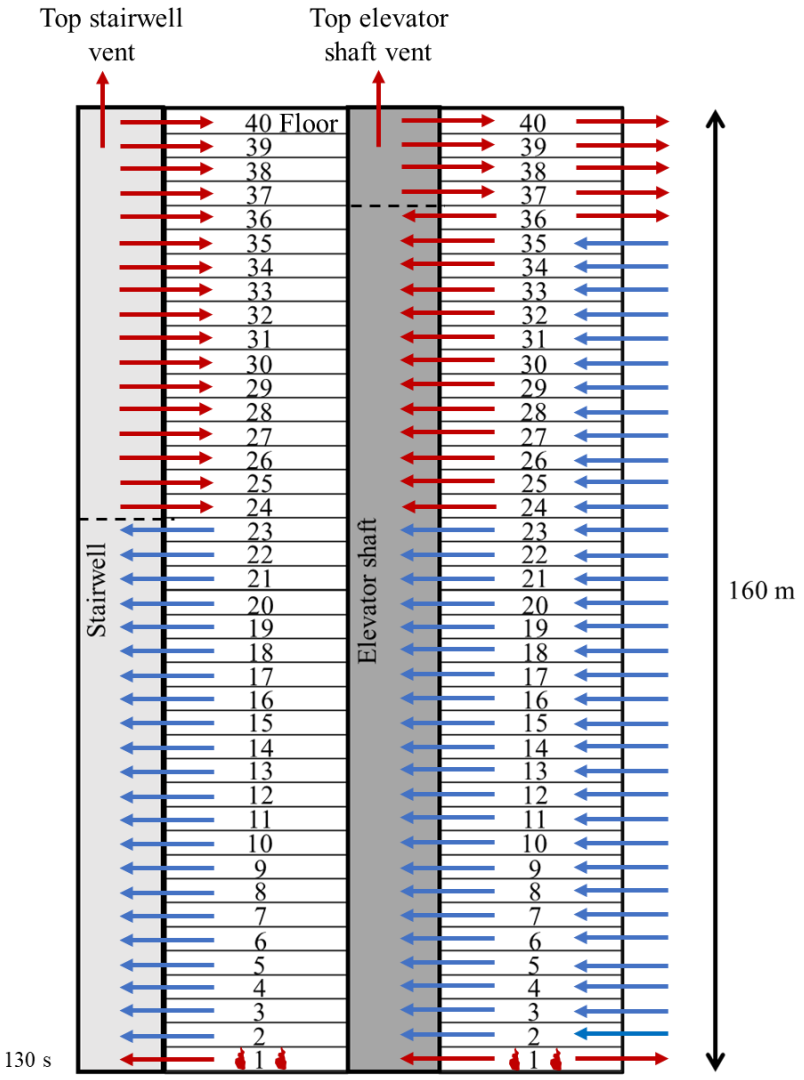

Figure 4.18: The directions of flow across the entire 40-story building for the fuel lean case at 130 s. Note that: (1) the blue arrows represent the directions of flows that are not contaminated by the hot smoke; (2) the red arrows represent the directions of flows that are influenced by the hot smoke; (3) the dotted lines indicate the locations of NPPs for the elevator shaft and the stairwells; (4) for simplicity, only one stairwell is represented (all four stairwells are identical and play the same role in the flow pattern).

At 130 s, according to Figures 4.18 to 4.23, the results here are similar to the results obtained by the 10 MW fire case at 245 s and the main differences are the magnitudes of the mass floor rate, the pressure and the temperature.

Figure 4.18 shows that the fire smoke generated inside the first floor migrates directly to the exterior through the fire floor leakage path, spreads into the two shafts through their respective leaks, then enters the upper floors and leaves the building thought the top vents and the upper floor leaks. Moreover, this figure illustrates that the NPP for the stairwells is located between the 23rd floor and 24th floor and the NPP for the elevator shaft is located between the 36th floor and 37th floor.

Based on Figure 4.19, the mass flow rate though the fire floor leak is about 4.6 kg/s and this is approximately 11 times greater than the outflow through the fire floor leak for the hot air case at 3600 s and approximately 2 times less than the outflow through the fire floor leak for the 10 MW design fire case at 245 s.

Figures 4.20 to 4.22 show that the over-pressure inside the first floor is around 620 Pa for the stairwells and 640 Pa for the elevator shaft. Additionally, the maximum over-pressure across the stairwell escape doors is only 61 Pa which means that at this stage occupants can open the stairwell escape door and evacuate.

Figure 4.23 demonstrates that the temperature inside the entire stairwells is below 40 ℃, so even though the flow patterns indicates that the fire smoke enters into the stairwells, this temperature suggests a small amount of fire smoke that would not affect the evacuees at this moment.

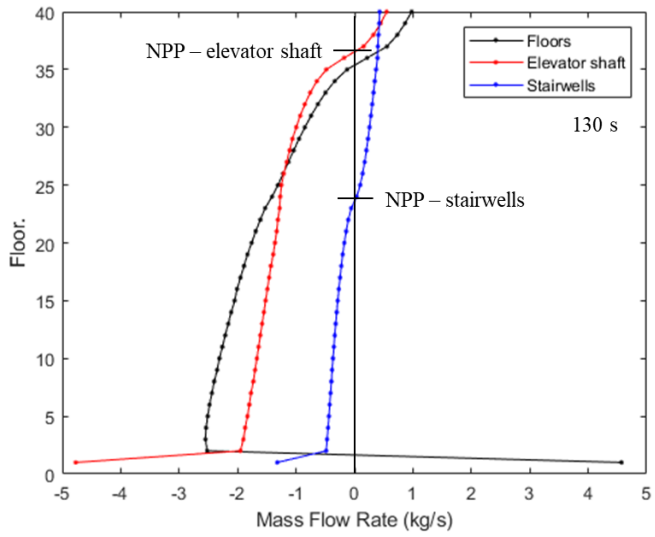

Figure 4.19: Elevation versus mass flow rate for each floor for the fuel lean case at 130 s. See the caption of Fig. 4.5.

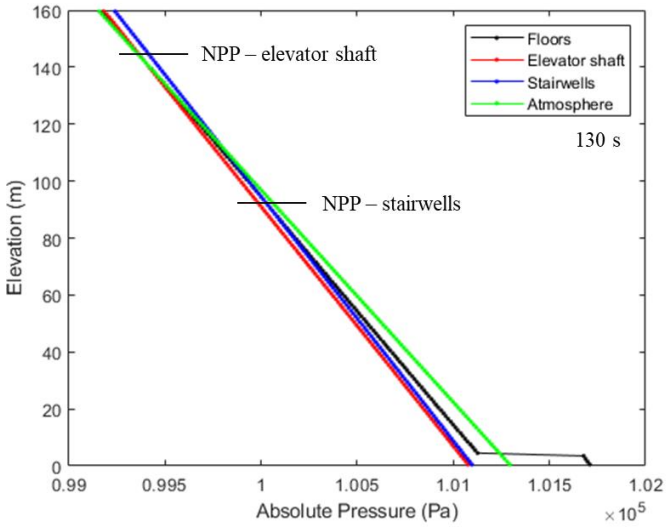

Figure 4.20: Elevation versus absolute pressure inside the high-rise building for the fuel lean case at 130 s.

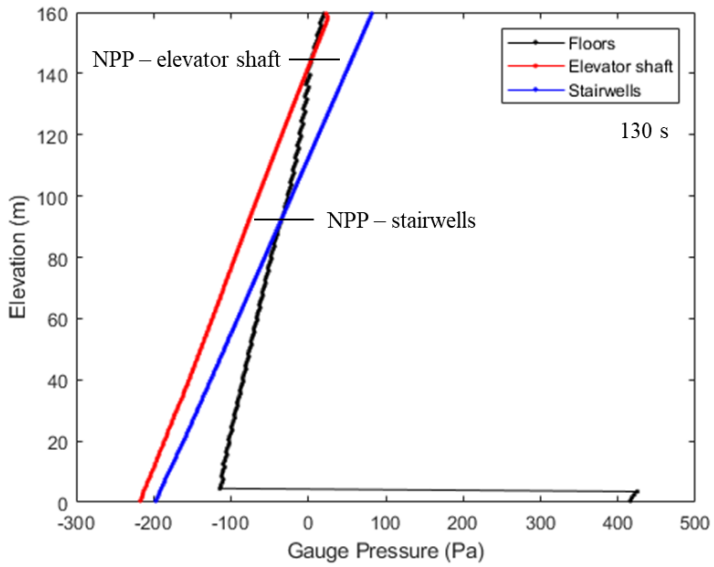

Figure 4.21: Elevation versus gauge pressure inside the high-rise building for the fuel lean case at 130 s.

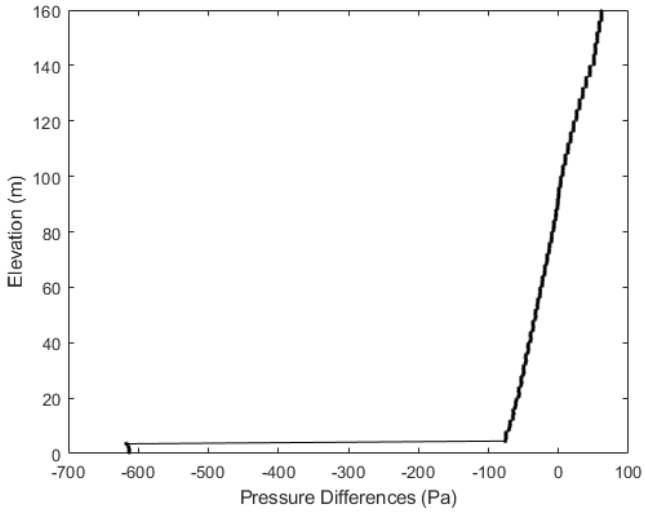

Figure 4.22: Elevation versus pressure differences between the stairwells and the floors for the fuel lean case at 130 s. (Pressure difference = the pressure inside the stairwells – the pressure inside the floors.)

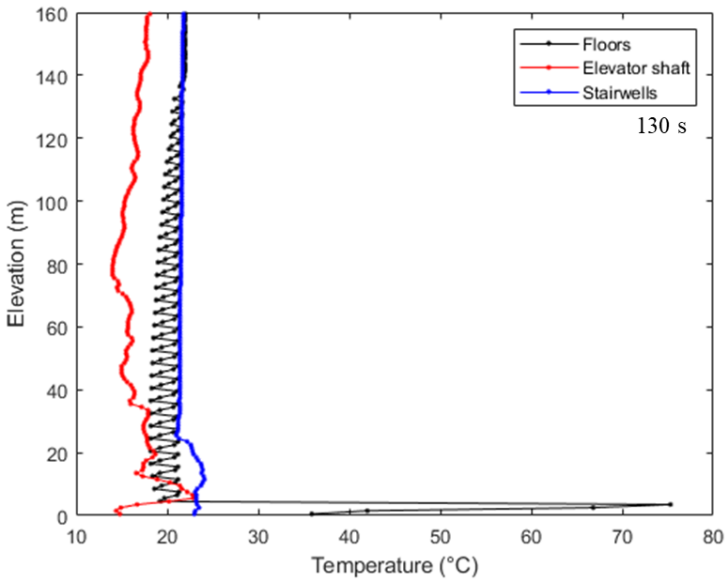

Figure 4.23: Elevation versus temperature inside the high-rise building for the fuel lean case at 130 s.

At 3600 s, Figure 4.24 depicts that the fire smoke follows same paths as previous cases and contaminates both vertical shafts and the upper floors. And similar to the 10 MW design fire case at 3600 s, the smoke does not escape the fire floor to the outside directly through the fire floor leak due to the demand for oxygen. Furthermore, compared with this case at 130 s, the NPPs for stairwells and the elevator shaft do not change.

Owing to the lower pressure differences between the floors and the stairwells and the elevator shaft shown in Figures 4.26 to 4.28 (compared with 10MW design fire case at 3600 s), the results in Figure 4.25 suggests that the mass flow rate between these areas are lower. Additionally, the maximum pressure difference across the stairwell doors is 142 Pa and the stairwell over-pressure exceeds 78 Pa above 32nd floor. Thus, it is difficult for occupants inside the upper floors to evacuate.

The trends of the temperature distribution inside the building shown in Figure 4.29 are similar to those of the previous cases. The figure illustrates that the temperature maintains a high value (above 40 ℃) throughout the entire height of stairwells which means that the stairwells are filled with fire smoke and thereby will potentially hurt occupants.

In conclusion, compared to the10 MW design fire case, there are not many differences in terms of the flow patterns, the main differences are the magnitudes of the mass flow rate, the pressure, and the temperature. In addition, it is observed that the larger the fire size, the greater the values for the mass flow rate, the pressure and the temperature and thus the stronger the stack effect.

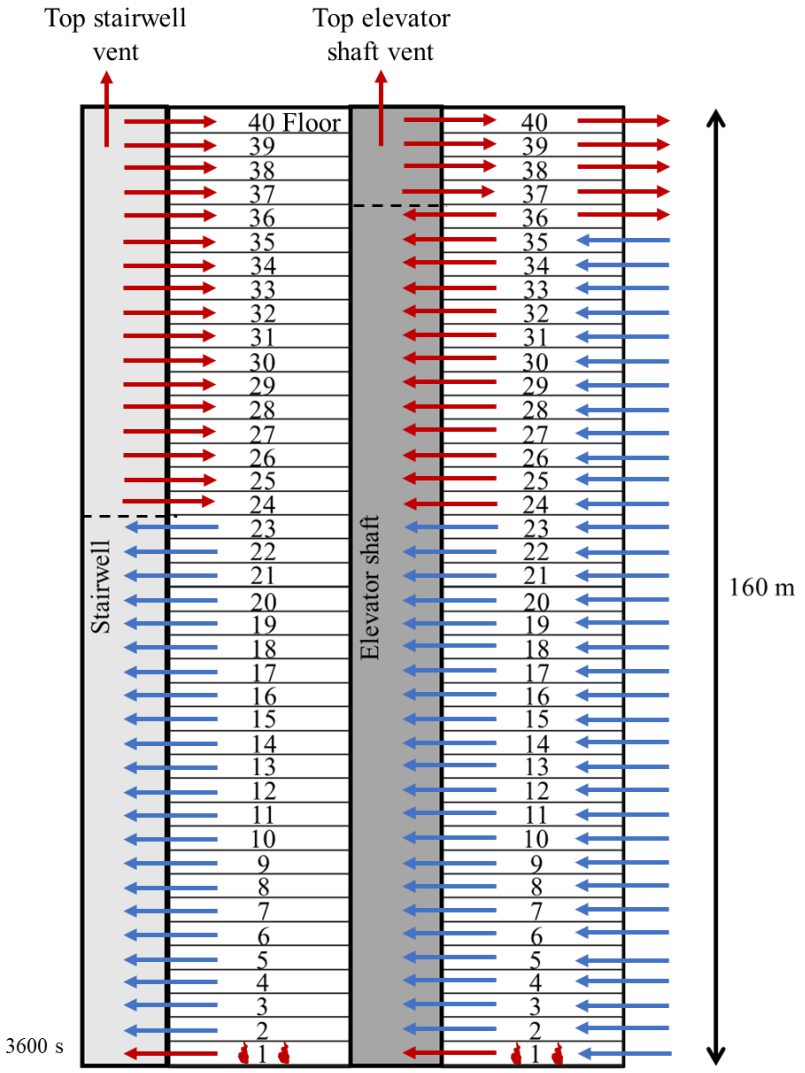

Figure 4.24: The directions of flow across the entire 40-story building for the fuel lean case at 3600 s. Note that: (1) the blue arrows represent the directions of flows that are not contaminated by the hot smoke; (2) the red arrows represent the directions of flows that are influenced by the hot smoke; (3) the dotted lines indicate the locations of NPPs for the elevator shaft and the stairwells; (4) for simplicity, only one stairwell is represented (all four stairwells are identical and play the same role in the flow pattern).

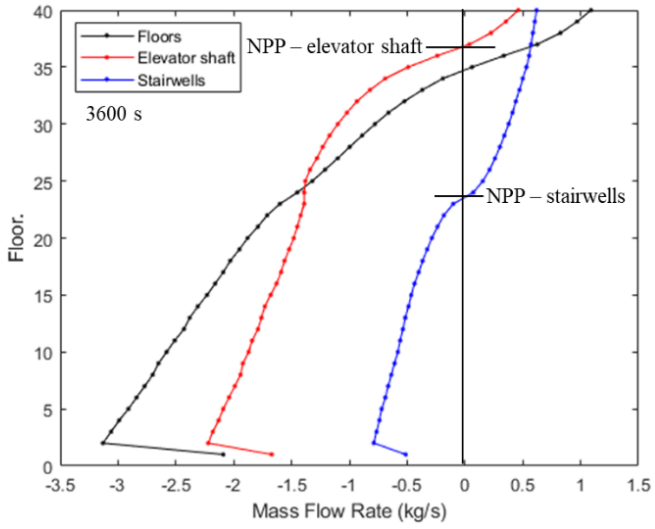

Figure 4.25: Elevation versus mass flow rate for each floor for the fuel lean case at 3600 s. See the caption of Fig. 4.5.

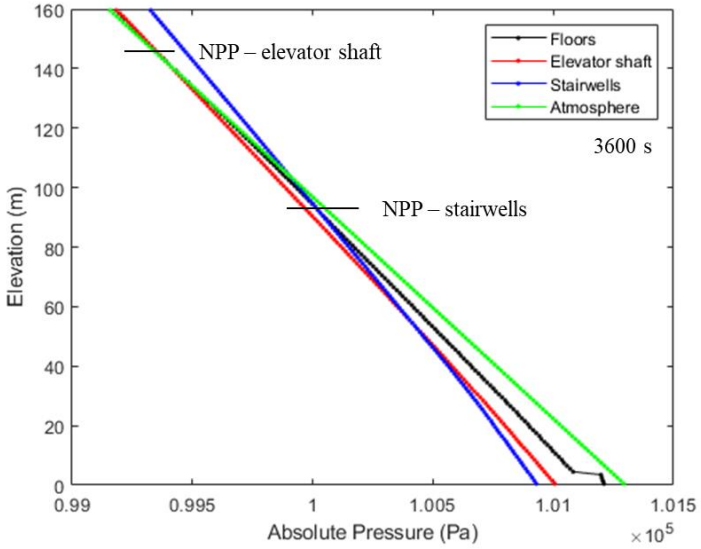

Figure 4.26: Elevation versus absolute pressure inside the high-rise building for the fuel lean case at 3600 s.

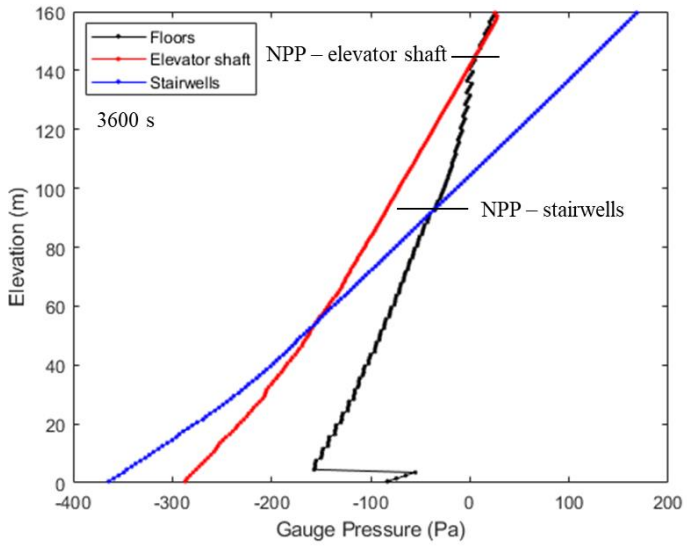

Figure 4.27: Elevation versus gauge pressure inside the high-rise building for the fuel lean case at 3600 s.

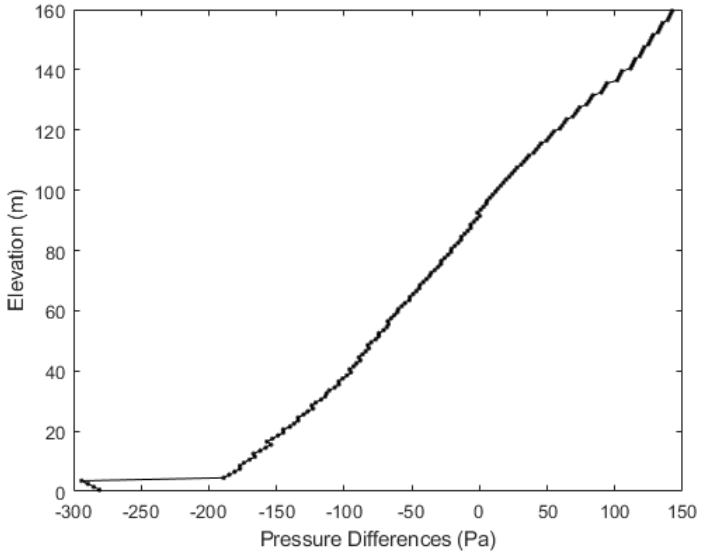

Figure 4.28: Elevation versus pressure differences between the stairwells and the floors for the fuel lean case at 3600 s. (Pressure difference = the pressure inside the stairwells – the pressure inside the floors.)

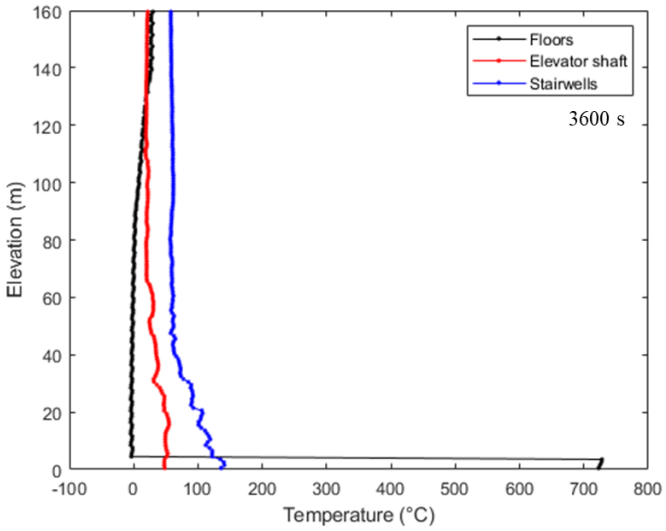

Figure 4.29: Elevation versus temperature inside the high-rise building for the fuel lean case at 3600 s.

4.3 Case 5: Design Fire at the Height of NPP

Now, we are going to elevate the design fire to a high elevation that is near the height of the NPP for the floors in order to see some different phenomena. The NPP for the floors is located between 35th and 36th floor, so the design fire is specified on the 35th floor for this case and the fire size is 2.5 MW.

The developments of the heat release rate inside the four stairwells, the elevator shaft and the fire floor are illustrated in Figure 4.30. The HRR inside the stairwells keeps zero throughout the entire simulation time. The HRR inside the elevator shaft increases after about 2700 s which indicates that the flame intrudes into the elevator shaft. And this is consistent with what is shown in Smokeview. The summation of the HRR in these spaces is equal to the total HRR calculated by FDS (this can be found in *hrr.csv* file) that is shown in Figure 4.31. Therefore, according to this figure, it is concluded that there is unburnt fuel inside the fire floor which means that the condition inside the fire floor turns to be fuel rich/under-ventilated after around 2600 s. And the globe equivalence ratio for this case at 3600 s is:

$$\Phi = \frac{(A/F)_{stoic}}{(A/F)} \approx \frac{\left(\frac{4.76 \times 5 \times 28.88}{44}\right)}{\left(\frac{0.2}{0.055}\right)} \approx 4.3$$

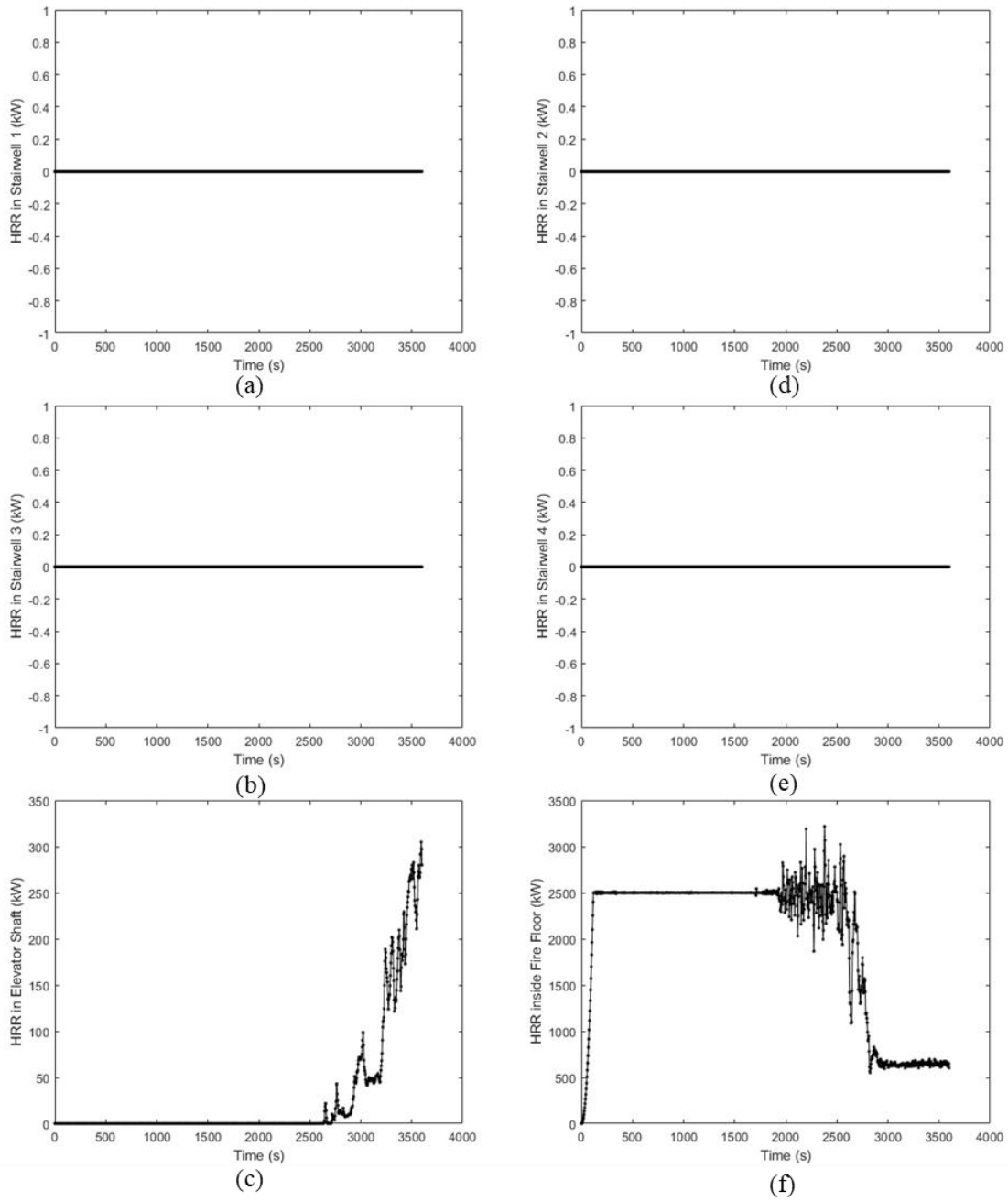

Figure 4.30: The time variations of the heat release rate inside: (a)-(d)-(b)-(e) the four stairwells; (c) the elevator shaft; and (f) the floor space for Case 5.

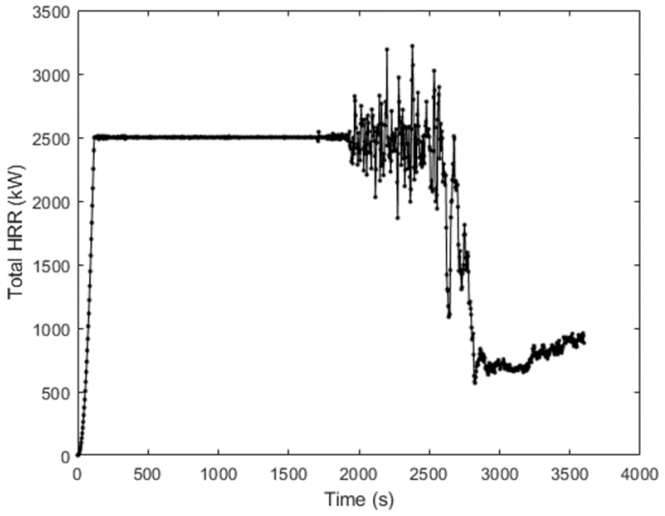

Figure 4.31: The time variations of the total heat release rate for Case 5.

The time variations of the gauge pressure and the temperature inside the floors, the stairwells, and the elevator shaft on the 1st floor, 35th floor and 40th floor are shown in Figure 4.32. The gauge pressure and the temperature on the first floor are still evidently changing at 3600 s, since the cold fresh air is continuously drawn into the first floor. Additionally, because of the adiabatic boundary condition, it is reasonable to predict that the temperature inside the lower floor space will eventually reach – 17 ℃ which is as same as the atmospheric temperature. On the fire floor, the gauge pressure reaches its peak value at approximately 126 s. Due to the fact that the fire size decreases after reaching its fully developed stage, the gauge pressure and the temperature inside the stairwells on topmost floor initially increases and then declines. Also, the condition inside the whole building does not become steady at 3600 s. Considering the different phenomena, the outputs that is discussed in the following paragraphs are chosen at 126 s and 3600 s.

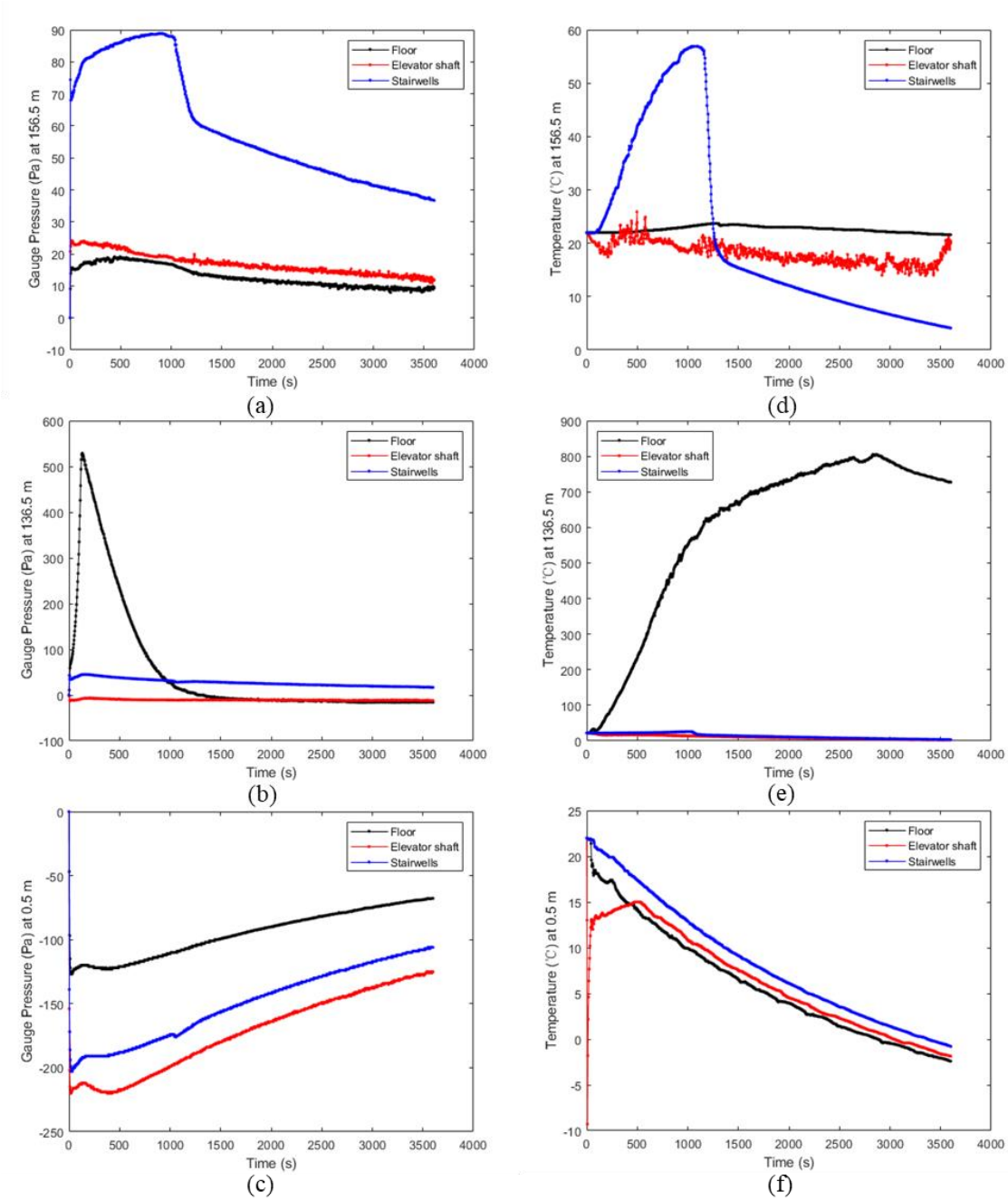

Figure 4.32: Time variations of the gauge pressure and temperature within the floors, the elevator shaft, and the stairwells at the heights of: (c)-(f) 0.5 m (1st floor); (b)-(e) 136.5 m (35th floor); and (a)-(d) 156.5m (40th floor) for Case 5.

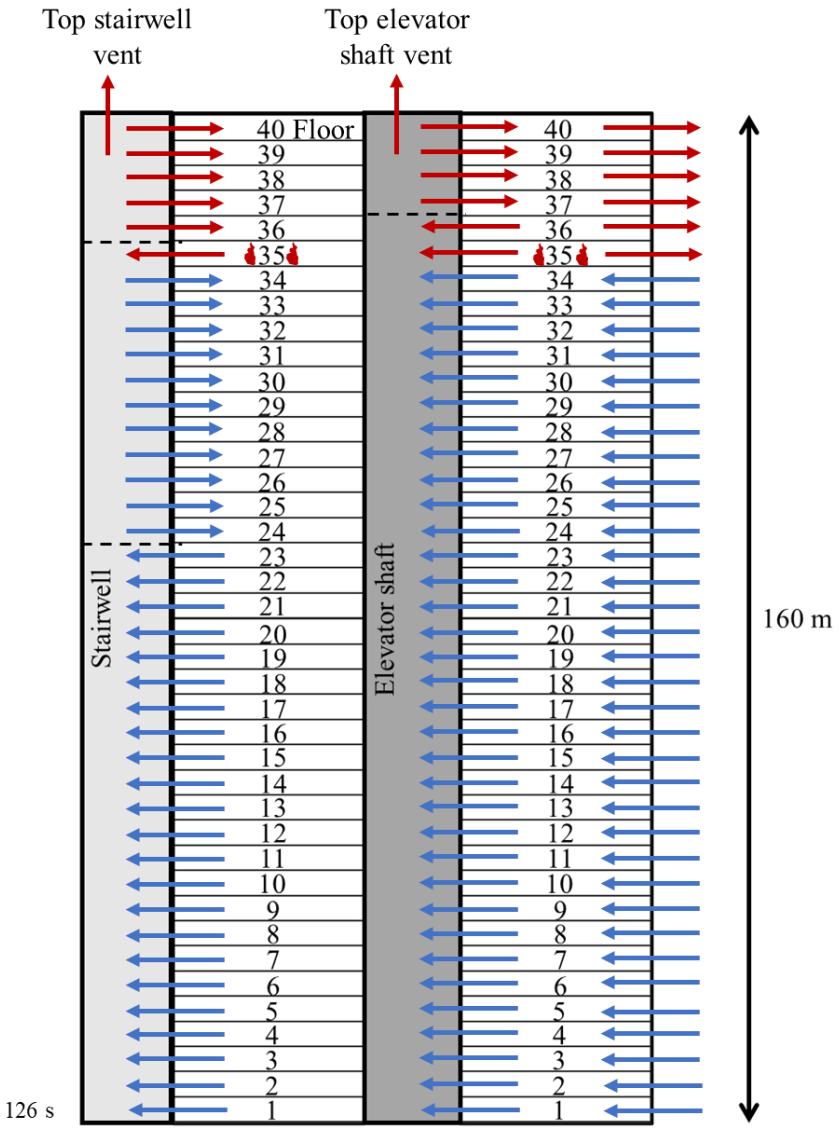

Figure 4.33: The directions of flow across the entire 40-story building for Case 5 at 126 s. Note that: (1) the blue arrows represent the directions of flows that are not contaminated by the hot smoke; (2) the red arrows represent the directions of flows that are influenced by the hot smoke; (3) the dotted lines indicate the locations of NPPs for the elevator shaft and the stairwells; (4) for simplicity, only one stairwell is represented (all four stairwells are identical and play the same role in the flow pattern).

According to Figure 4.33, the lower part of the building is free of smoke whereas the floors above the 35th floor are all contaminated by the fire smoke at this moment. Inside the stairwells, there are two neutral pressure planes. The NPP located between the 23rd floor and the 24th floor is due to the natural stack effect and the additional NPP located between the 35th floor and the 36th floor is caused by the design fire that creates outflows towards stairwells from the fire floor. The NPP for the elevator is located between the 36th floor and 37th floor.

The mass flow rate towards the outside is around 5.1 kg/s based on Figure 4.34 due to the high gauge pressure inside the fire floor (about 520 Pa) shown in Figures 4.35 to 4.36. Additionally, Figure 4.37 shows that the pressure difference across the stairwell doors and the elevator doors are around 490 Pa and 520 Pa. So, the fire floor conditions are very similar to those of Case 4. Additionally, the maximum over-pressure inside the stairwells is only 63 Pa which means that the evacuees do not have difficulty in opening the stairwell escape door and evacuating.

The temperature distributions inside the building are shown in Figure 4.38. The low temperature throughout the entire height of the elevator shaft and the stairwells results from the more atmospheric cold air than the hot fire smoke spreading into both shafts. Therefore, the density of the smoke inside the escape stairwells is too low so that it could be neglected. Consequently, occupants are able to safely evacuate at this stage.

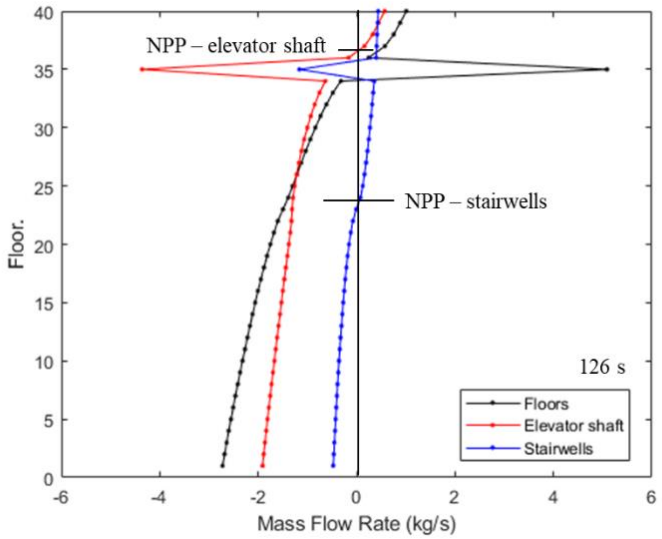

Figure 4.34: Elevation versus mass flow rate for each floor for Case 5 at 126 s. See the caption of Fig. 4.5.

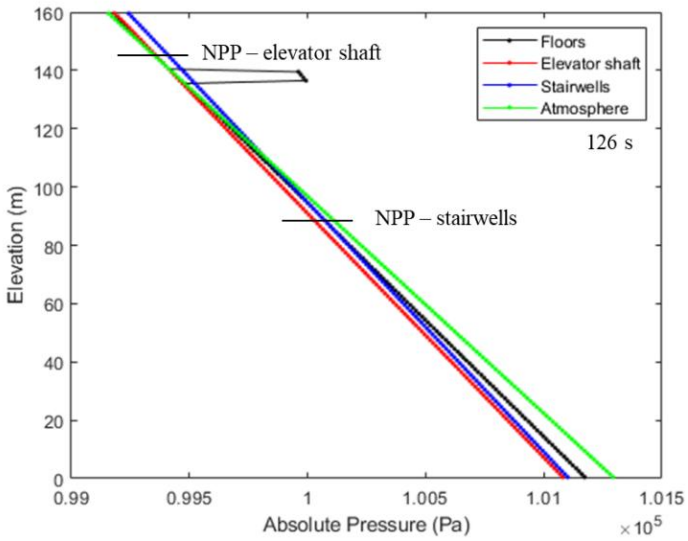

Figure 4.35: Elevation versus absolute pressure inside the high-rise building for Case 5 at 126 s.

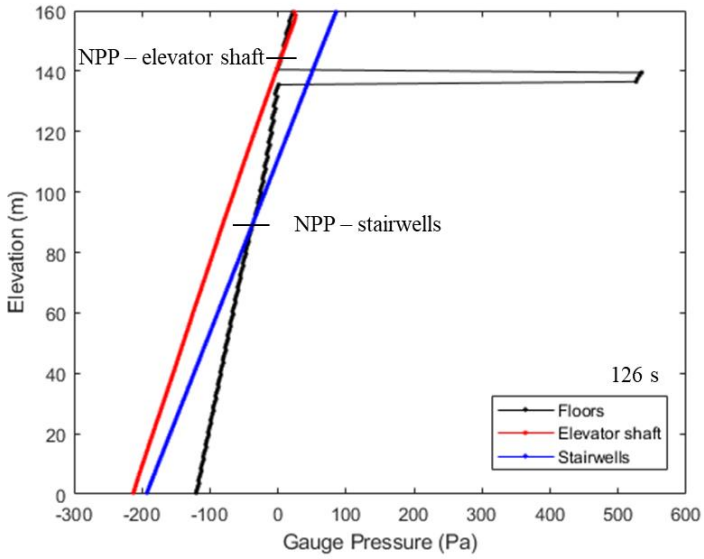

Figure 4.36: Elevation versus gauge pressure inside the high-rise building for Case 5 at 126 s.

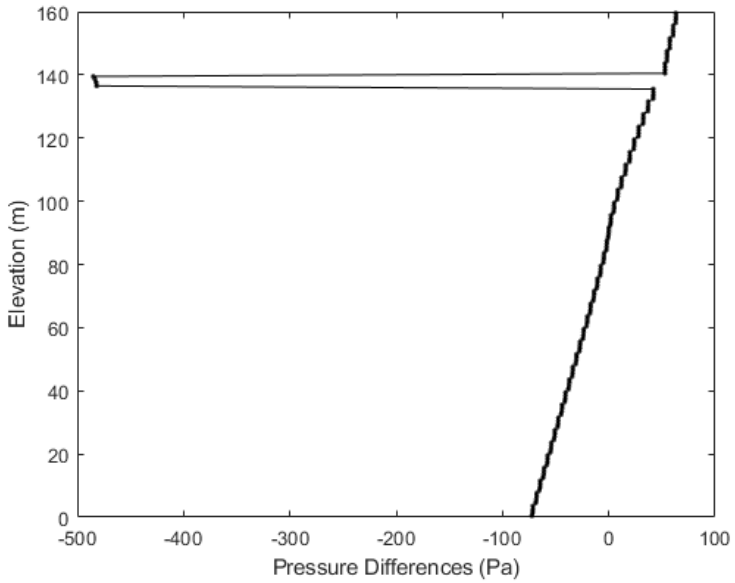

Figure 4.37: Elevation versus pressure differences between the stairwells and the floors for Case 5 at 126 s. (Pressure difference = the pressure inside the stairwells – the pressure inside the floors.)

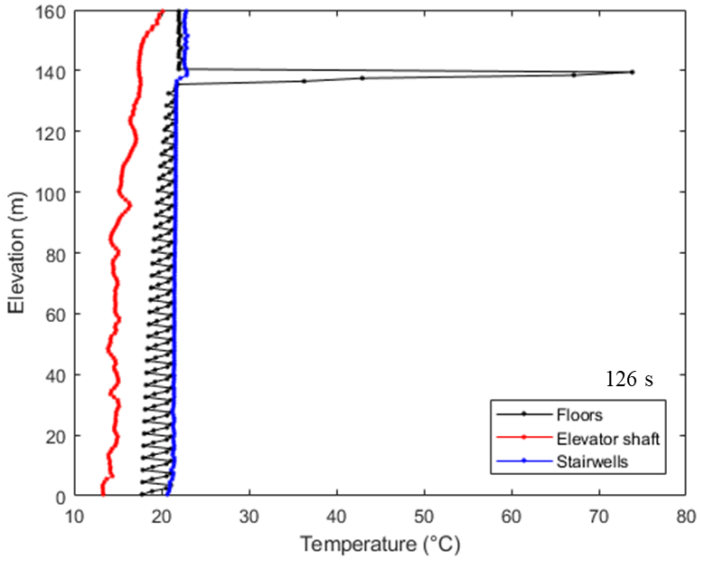

Figure 4.38: Elevation versus temperature inside the high-rise building for Case 5 at 126 s.

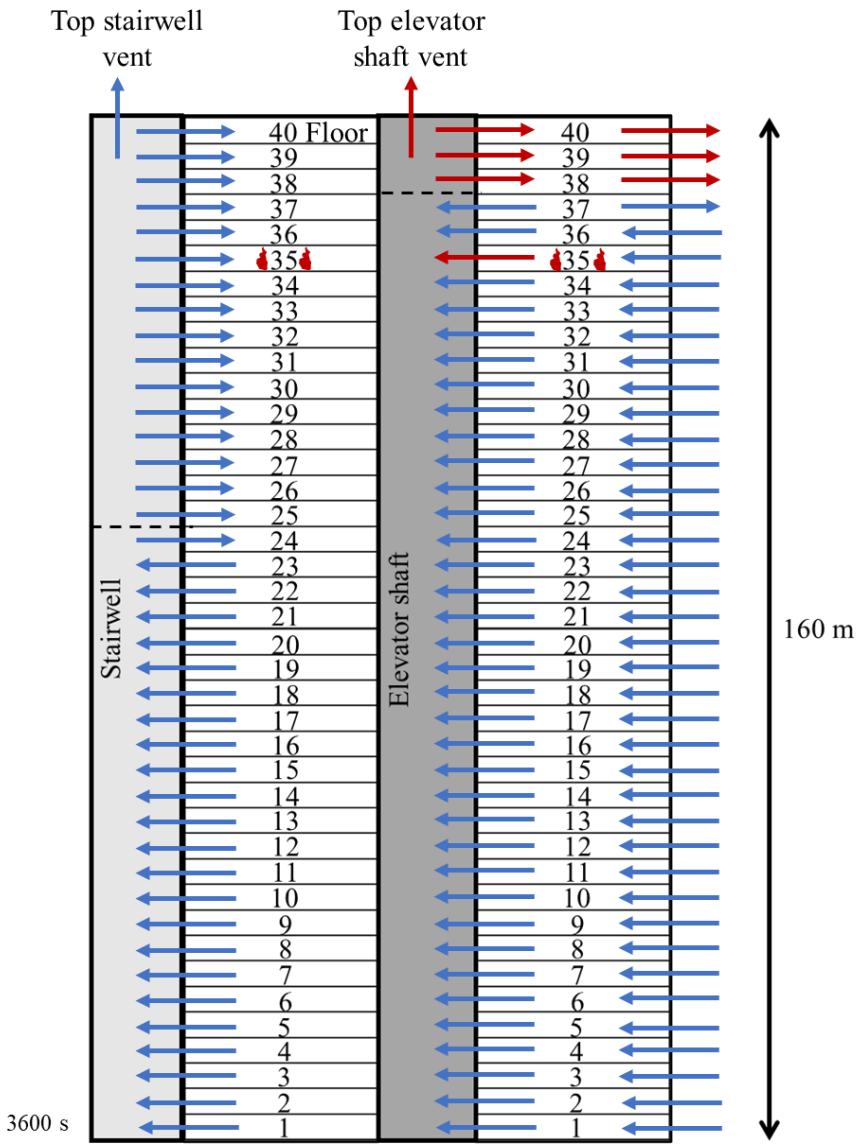

Figure 4.39: The directions of flow across the entire 40-story building for Case 5 at 3600 s. Note that: (1) the blue arrows represent the directions of flows that are not contaminated by the hot smoke; (2) the red arrows represent the directions of flows that are influenced by the hot smoke; (3) the dotted lines indicate the locations of NPPs for the elevator shaft and the stairwells; (4) for simplicity, only one stairwell is represented (all four stairwells are identical and play the same role in the flow pattern).

Figure 4.34 shows that the stairwells is free of fire smoke. This is because that, according to Figure 4.28-(b), when there is unburnt fuel inside the fire floor, the pressure inside the stairwells is lower than the pressure inside the fire floor. Hence, fire smoke does not enter the stairwells and the existed fire smoke escapes though the stairwell top vents to the atmosphere leading to the fact that the stairwells is safe at this moment. Moreover, the flame migrates into the elevator shaft, but both HRRs inside the elevator shaft and the fire floor are low. The fire with this low HRR is not able to increase the pressure at the height between the 36th floor and 37th floor (leading to a weaker stack effect between the fire floor and the topmost floor). So, the NPP for the elevator shaft is elevated to the position between the 37th floor and the 38th floor.

The mass flow rates between each space in Figure 4.35 looks similar to those of the case without fire/hot air at 3600 s. The difference is that the mass flow rates between each space on the fire floor is dramatically decreased for this case due to the fact that the design fire create a higher pressure resulting in that the pressure difference between each space is lower as shown in Figures 4.36 and 4.37. Additionally, these two figures indicate that the maximum over-pressure inside the stairwells at this moment is only 25 Pa. Consequently, opening the stairwell escape door is not difficult for occupants at this time. Furthermore, the temperature distributions in Figure 4.38 show that the temperature inside the stairwells is very low throughout the entire height of the building due to the lack of fire smoke.

To sum up, the conditions at 130 s and 3600 s are both tenable. (According to Figures 4.28-(a) and 4.28-(d), the temperature is above 40 ℃ and the over-pressure is above 78 Pa inside the stairwells from about 500 s to 1000 s.) And the design fire

located near the NPP for the floors does not create severe conditions compared with the design fire located on the first floor.

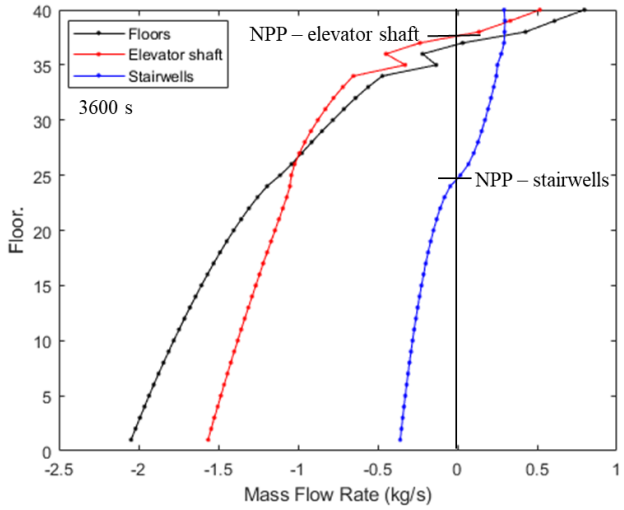

Figure 4.40: Elevation versus mass flow rate for each floor for Case 5 at 3600 s. See the caption of Fig. 4.5.

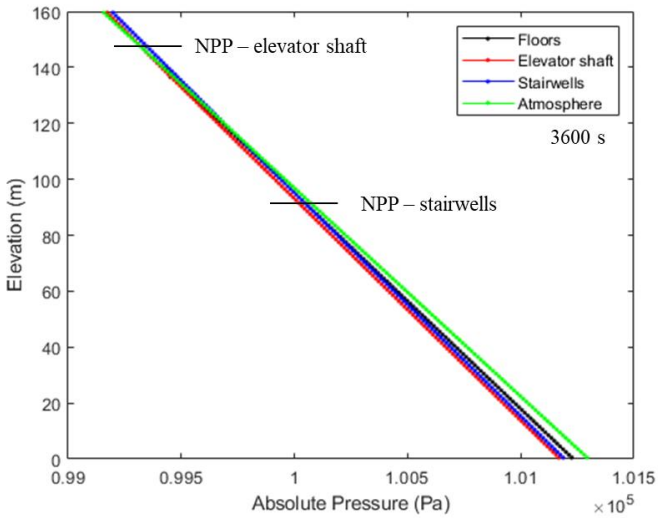

Figure 4.41: Elevation versus absolute pressure inside the high-rise building for Case 5 at 3600 s.

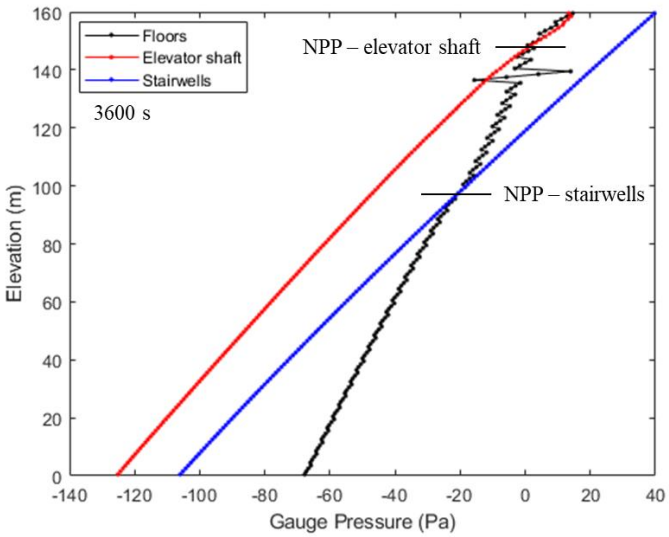

Figure 4.42: Elevation versus gauge pressure inside the high-rise building for Case 5 at 3600 s.

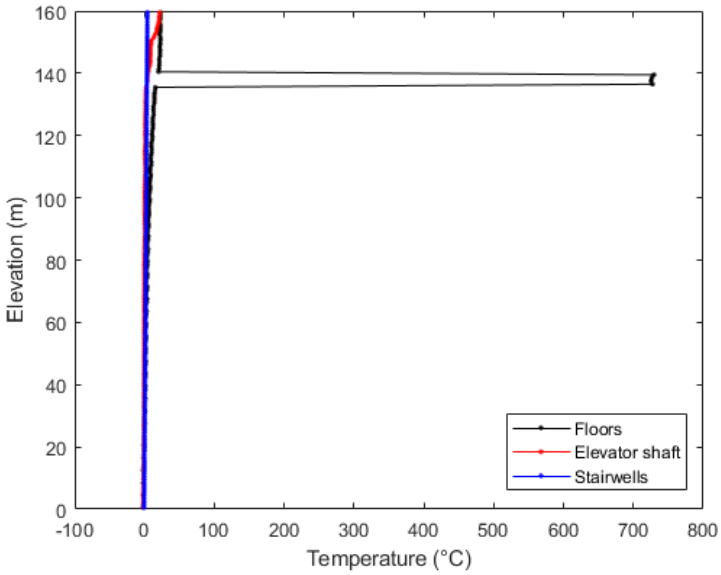

Figure 4.43: Elevation versus pressure differences between the stairwells and the floors for Case 5 at 3600 s. (Pressure difference = the pressure inside the stairwells – the pressure inside the floors.)

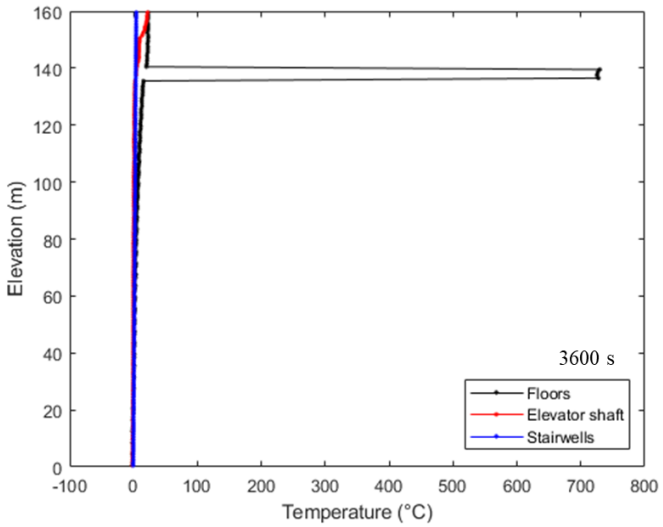

Figure 4.44: Elevation versus temperature inside the high-rise building for Case 5 at 3600 s.

Chapter 5: Fire Cases with Open Doors: Thermal Mixing

This chapter aims to explore more realistic scenarios (open doors), study the thermal mixing in FDS and compare the results with CONTAM and a MATLAB program for the same scenarios. The MATLAB code is an in-house solver based on the classical flow-pressure coupling, Bernoulli expressions for flow velocity, and a steady state assumption, and developed during this project for additional insights and understanding. Note that since the FDS model ignores the effects of the stairs and the landing platforms (no stairwells and obstruction) inside the stairwells, they are also ignored in the MATLAB code for the comparison. Additionally, in CONTAM, the "shaft airflow model" is used for specifying not only the elevator shaft but also the stairwells for the comparison with FDS, and the "orifice equation" with a pressure exponent equal to 0.5 is used for specifying all the leakages and openings.

5.1 Cases 6: Closed doors

This first section provides results for the comparison with the following simulation. For this case, the 2.5 MW ultra-fast t-square fire is specified to start at the 60 seconds and no doors are open during the simulation. The configuration of the building is not changed, and all the surfaces of the building are adiabatic. The configurations and conditions of the model in CONTAM and MATLAB are the same as that in FDS. The total simulation time is 600 s for this case, and it takes less than 90 minutes to complete by Deepthought2 (an HPC cluster provided by UMD).

The heat released rate for this case is shown in Figure 5.1. The fire starts at 60 s and reaches the maximum HRR at 175 s which takes 115 s as specified (see case 2). Also, the fire is over-ventilated throughout the simulation time.

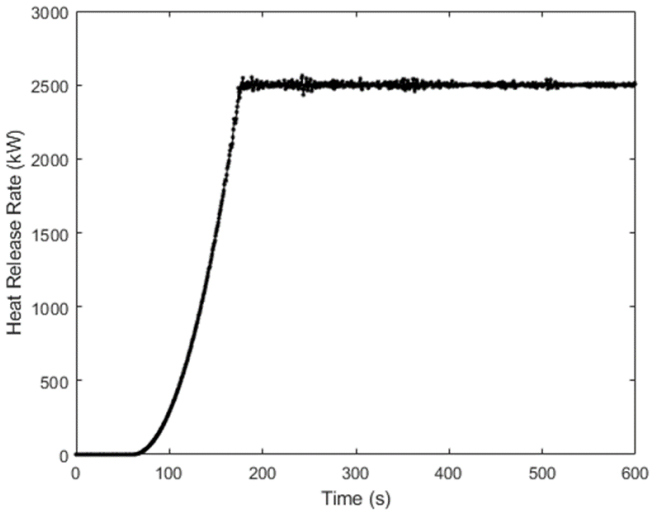

Figure 5.1: The time variations of the heat release rate for case 6.

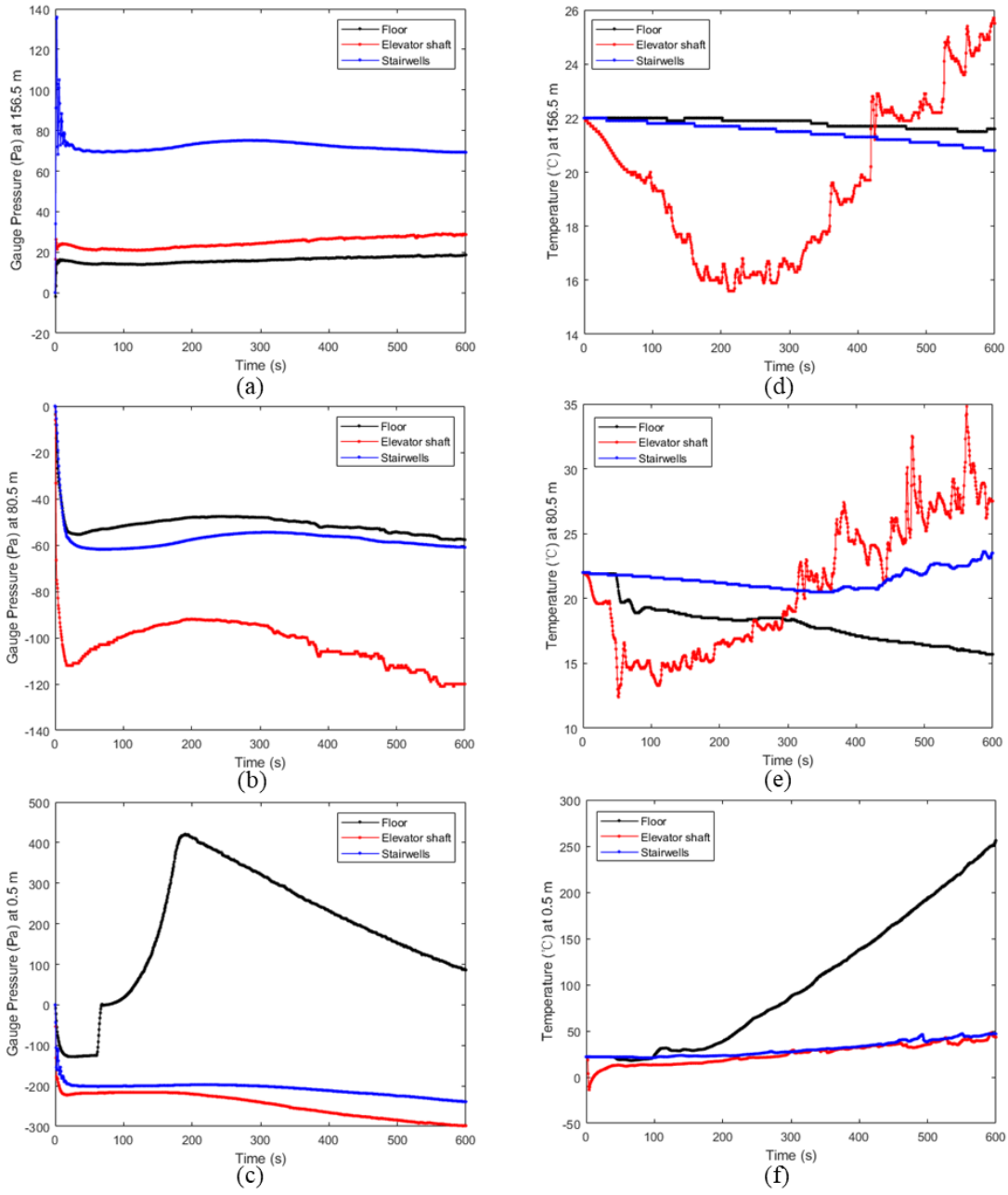

Figure 5.2: Time variations of the gauge pressure and temperature within the floors, the elevator shaft, and the stairwells at the heights of: (c)-(f) 0.5 m (1st floor); (b)-(e) 80.5 m (21st floor); and (a)-(d) 156.5m (40th floor) for case 6.

Examinations of the time variations of the gauge pressure and temperature within the floors, the elevator shaft, and the stairwells on three representative floors are illustrated in Figure 5.3. The pressure inside the fire floor is increased after that the fire starts and reaches the peak value at 180 s which is a few second after the fire is fully developed. The temperature inside the three spaces on the first floor has an evident increment at the end of the simulation. The results from 55 s to 600 s are included in the discussion for this section.

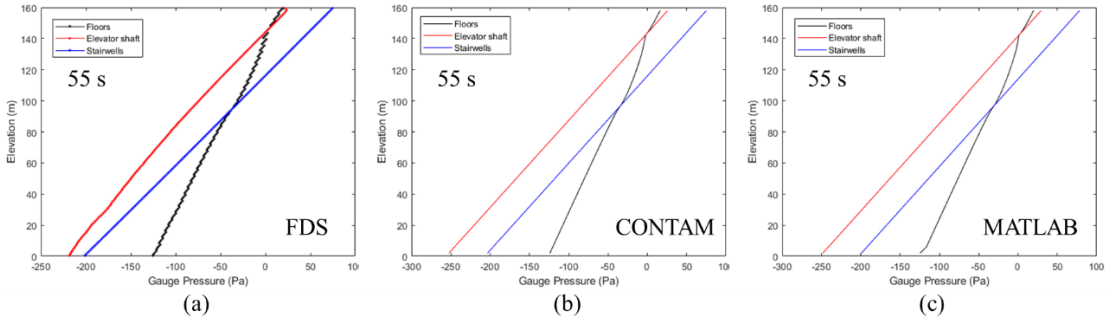

Figure 5.3: Elevation versus gauge pressure inside the high-rise building obtained by (a) FDS; (b) CONTAM; and (c) MATLAB for case 6 at 55 s.

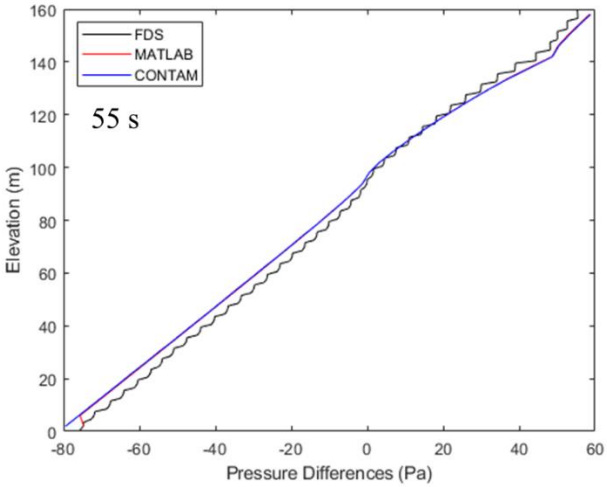

Figure 5.4: Elevation versus pressure differences between the stairwells and the floors obtained by FDS, CONTAM and MATLAB for case 6 at 55 s.

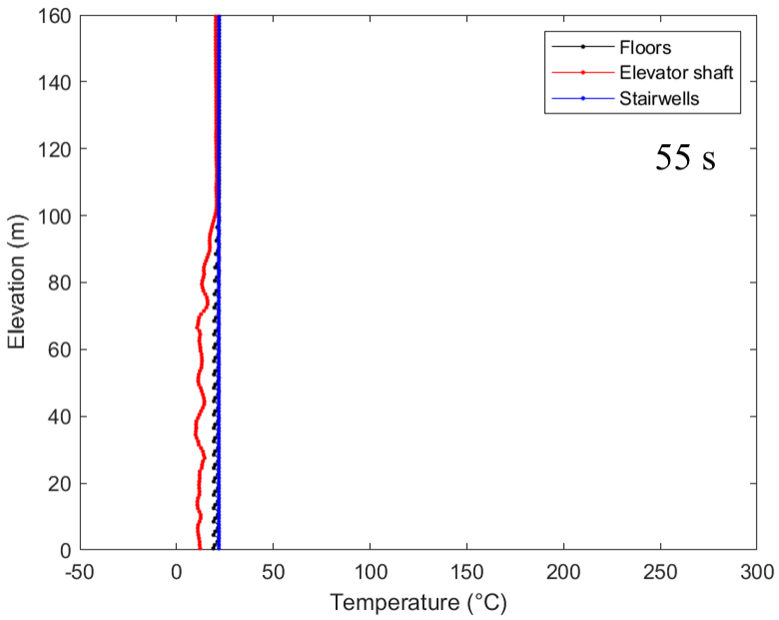

Figure 5.5: Elevation versus temperature inside the high-rise building obtained by FDS for case 6 at 55 s.

In Figure 5.3, the gauge pressures inside the high-rise building provided by FDS, CONTAM, and MATLAB at 55 s are plotted as a function of elevation. At the time, there is no fire. Therefore, the conditions inside the first floor are specified as 22 ℃ in CONTAM and MATLAB. (Note that, in CONTAM, the "shaft airflow model" is used for specifying both the elevator shaft and the stairwells, and the "orifice equation" with a pressure exponent equal to 0.5 is used for specifying all the leakages and openings. Additionally, the MATLAB program is based on the conservation of total mass at steady state in the high-rise building.) It is apparent that the outputs provided by CONTAM and MATLAB are very close. Also, the results obtained by FDS are nearly the same as those of CONTAM and MATLAB. The main discrepancy here is the elevator pressure curve which can be explained by the pressure distribution shown in

Figure 5.5. In this figure, the temperature inside the elevator shaft at the lower part of the building is less than 22 ℃ due to the leaking of cold air from the floors (see Appendix B), but the CONTAM model and the MATLAB program do not describe the heat transfer thus they keep the constant temperature (22 ℃). So, the colder temperature results in denser air inside the elevator shaft and leading to a curve that inclines more to the y-axis based on hydrostatic pressure equations (see Appendix C). Additionally, since we find similar floor and stairwell pressure curves in FDS, CONTAM, and MATLAB, the pressure differences across the escape stairwells are almost the same in Figure 5.4.

According to Figure 5.6, the gauge pressure inside the floors, the elevator shaft and the stairwells does not change much from 65 s to 600 s except for the fire floor. This is because that the temperature inside the floors, the stairwells and the elevator shaft has small change comparing with the dramatical increment of temperature inside the fire floor in accordance with Figure 5.8. Even though there is a relatively small change of the temperature, the temperature inside the stairwells at the bottom of the building is larger than 40 ℃ after 420 s which means that it will potentially hurt occupants. Moreover, Figure 4.7 compares the pressure differences between the stairwells and the floors at 11 different times. It is clear that the pressure differences across the escape stairwells remains nearly the same before (55 s) and after (65 s to 600 s) the ignition of the fire. And the pressure differences do not exceed 78 Pa throughout the simulation time meaning that no occupants would be blocked by overpressure across the escape stairwell doors.

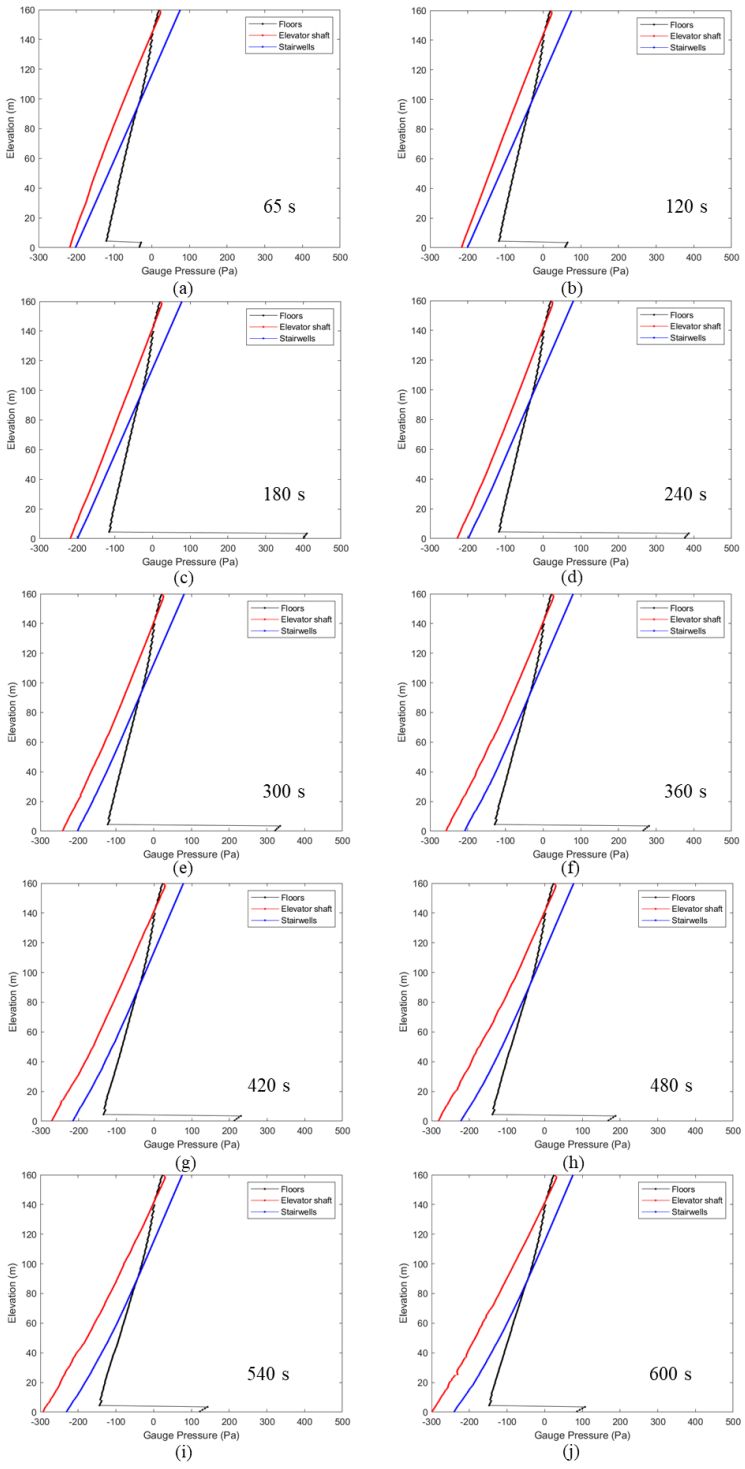

Figure 5.6: Elevation versus gauge pressure inside the building obtained by FDS at (a) 65 s; (b) 120 s; (c) 180 s; (d) 240 s; (e) 300 s; (f) 360 s; (g) 420 s; (h) 480 s; (i) 540 s; and (j) 600 s for case 6.

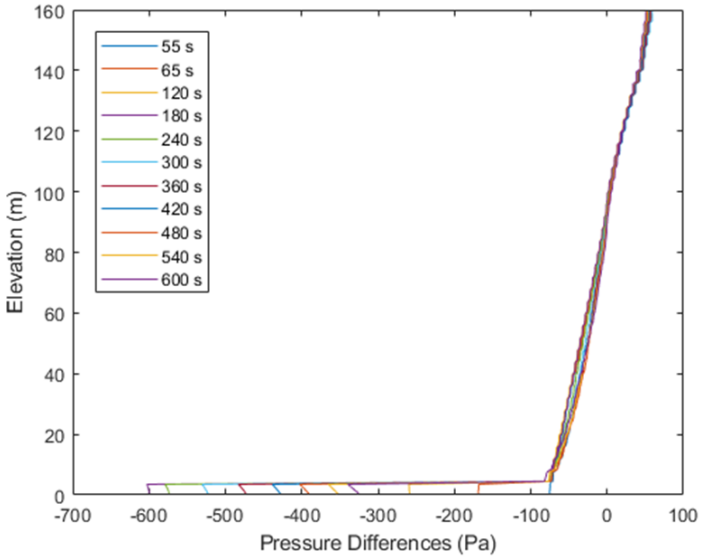

Figure 5.7: Elevation versus pressure differences between the stairwells and the floors obtained by FDS from 55 s to 600 s for case 6.

After the initiation of the fire (60 s), the fire conditions in CONTAM are prescribed as constant 700 ℃ for the temperature and 10 Pa for the gauge pressure inside the first floor. And the fire conditions in the MATLAB program are specified as constant 700 ℃ for the temperature and that the gauge pressure is not prescribed inside the fire floor. The outputs provided by CONTAM and MATLAB are constant (steady state) due to the absence of a representation of vertical thermal mixing inside the stairwells and elevator shaft, which means that each zone keep a constant temperature throughout the simulation.

The comparison of the results at 65 s among FDS, CONTAM and MATLAB is illustrated in Figure 5.9. The gauge pressure curves of the stairwells and the floors are practically the same except for the fire floor at 65 s. Therefore, Figure 5.10 shows that the pressure differences between the stairwells and the floors provided by three models

are very close. The difference in the elevator pressure curves is due to the lower temperature obtained by FDS presented in Figure 5.11.

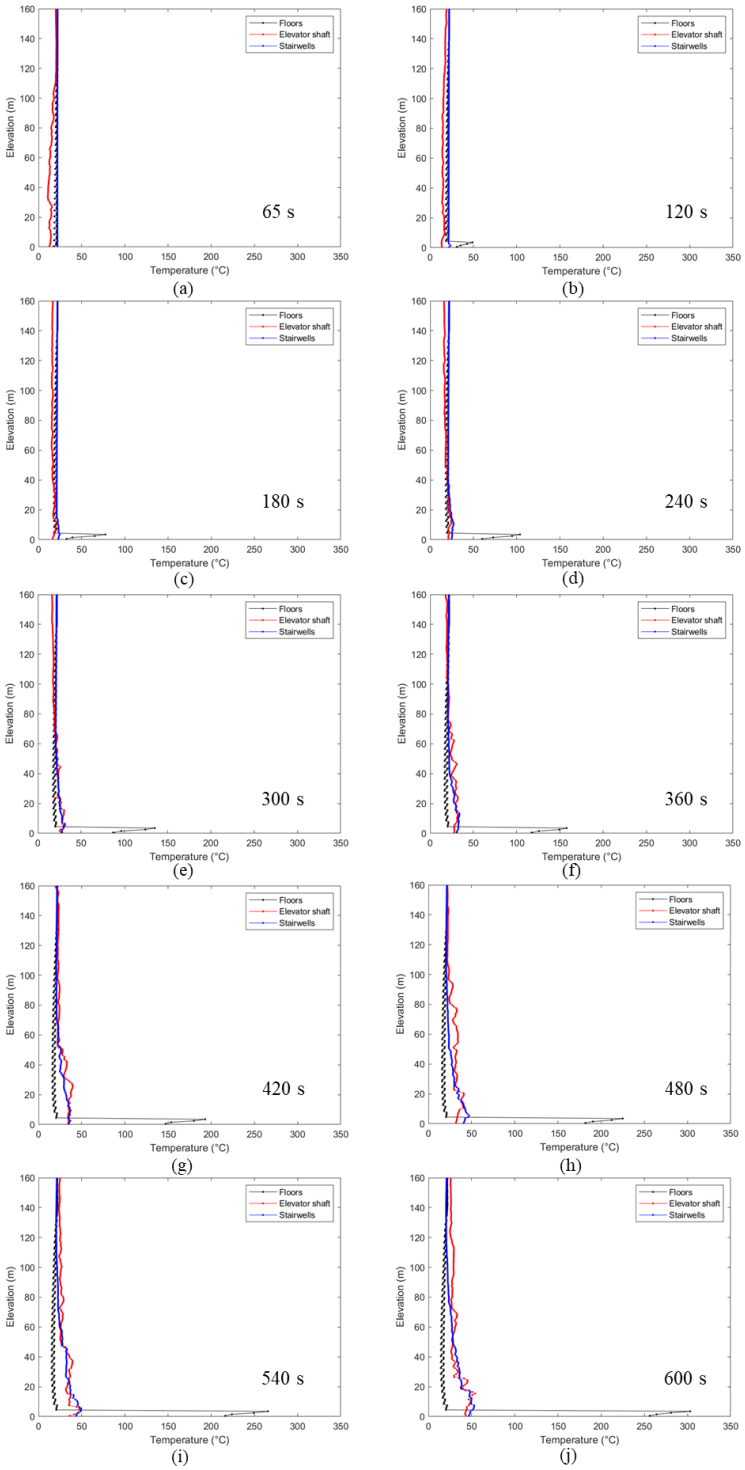

Figure 5.8: Elevation versus temperature inside the building obtained by FDS at (a) 65 s; (b) 120 s; (c) 180 s; (d) 240 s; (e) 300 s; (f) 360 s; (g) 420 s; (h) 480 s; (i) 540 s; and (j) 600 s for case 6.

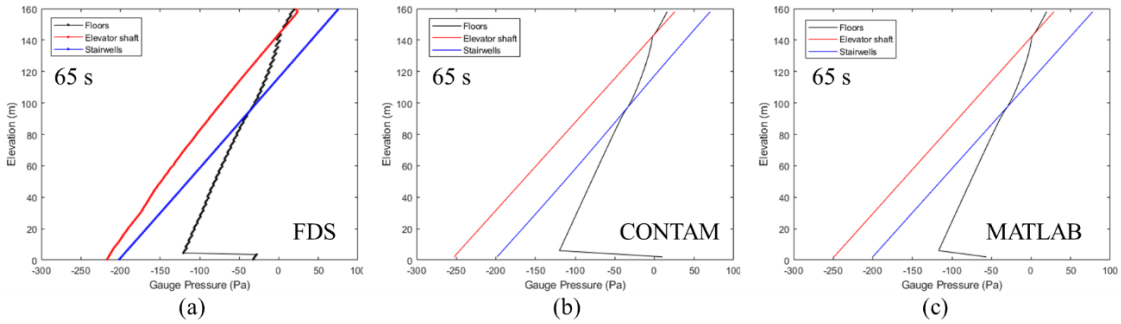

Figure 5.9: Elevation versus gauge pressure inside the high-rise building obtained by (a) FDS; (b) CONTAM; and (c) MATLAB for case 6 at 65 s.

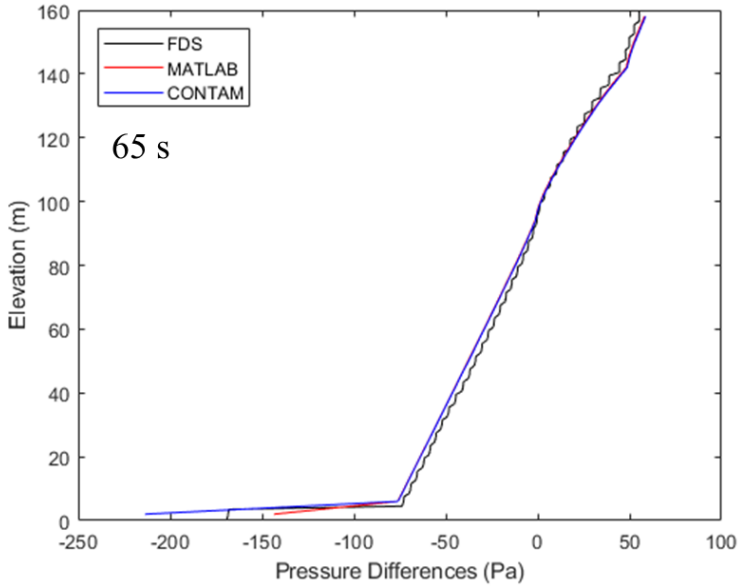

Figure 5.10: Elevation versus pressure differences between the stairwells and the floors obtained by FDS, CONTAM and MATLAB for case 6 at 65 s.

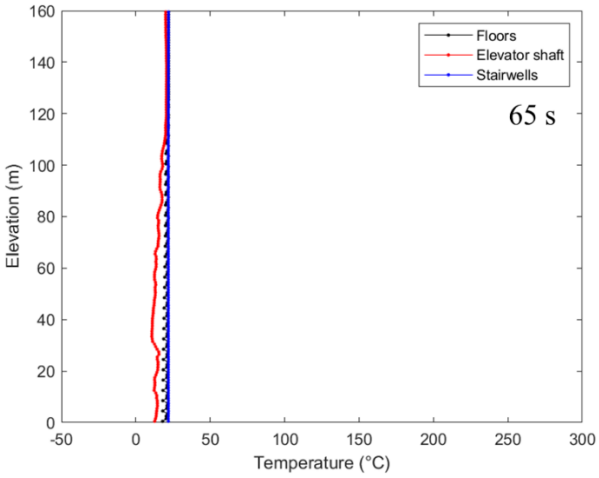

Figure 5.11: Elevation versus temperature inside the high-rise building obtained by FDS for case 6 at 65 s.

At 600 s, according to Figures 5.12 to 5.15, due to the increased temperature inside the elevator shaft and the stairwells resulting from the design fire, the gauge pressure curves of the elevator shaft and the stairwells lean more to the x-axis (less dense air) based on the hydrostatic pressure equation (see Appendix C), and the over-pressure inside the stairwells is slightly increased comparing with those of CONTAM and the MATLAB program and that of FDS at 65 s which means a stronger stack effect.

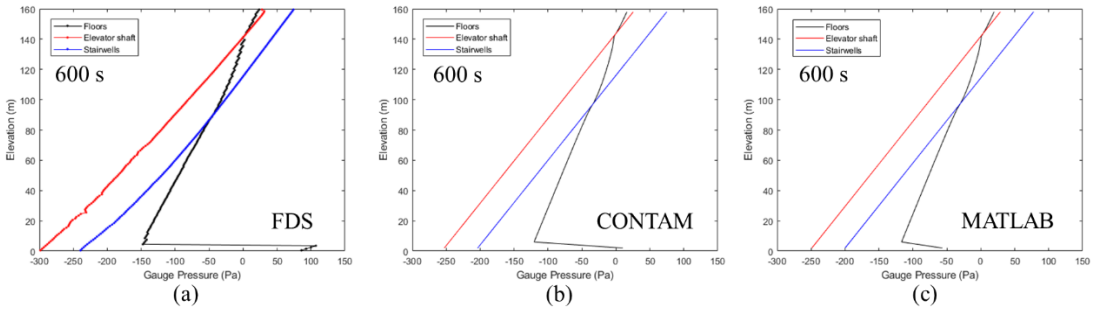

Figure 5.12: Elevation versus gauge pressure inside the high-rise building obtained by (a) FDS; (b) CONTAM; and (c) MATLAB for case 6 at 600 s.

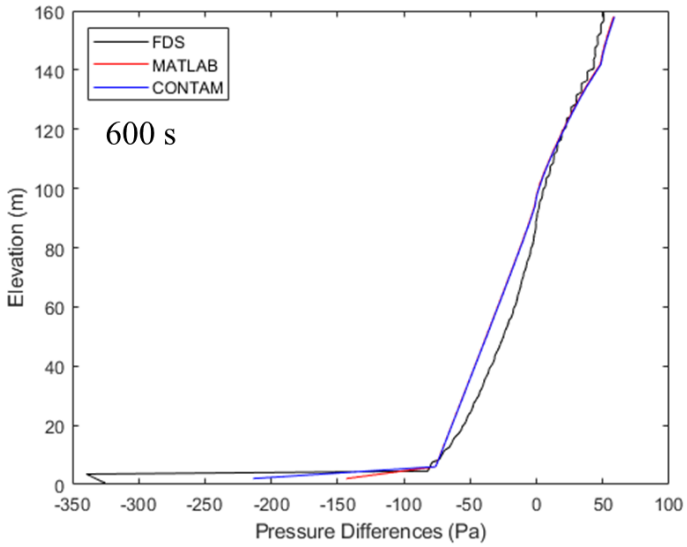

Figure 5.13: Elevation versus pressure differences between the stairwells and the floors obtained by FDS, CONTAM and MATLAB for case 6 at 600 s.

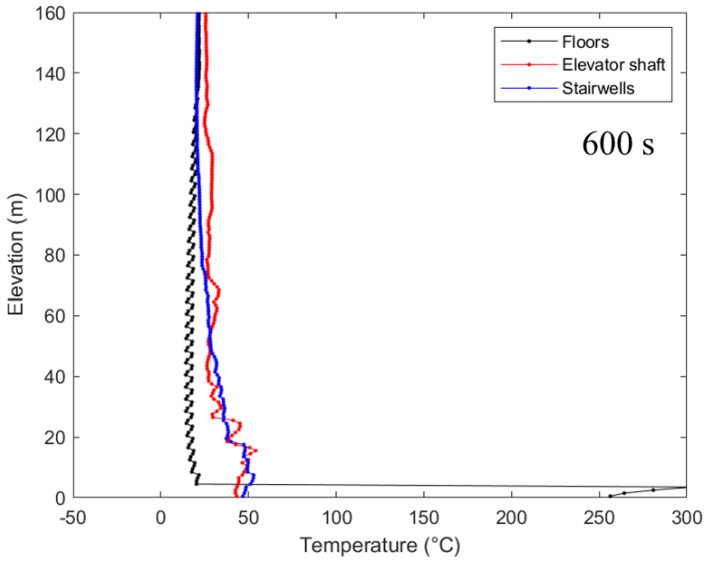

Figure 5.14: Elevation versus temperature inside the high-rise building obtained by FDS for case 6 at 600 s.

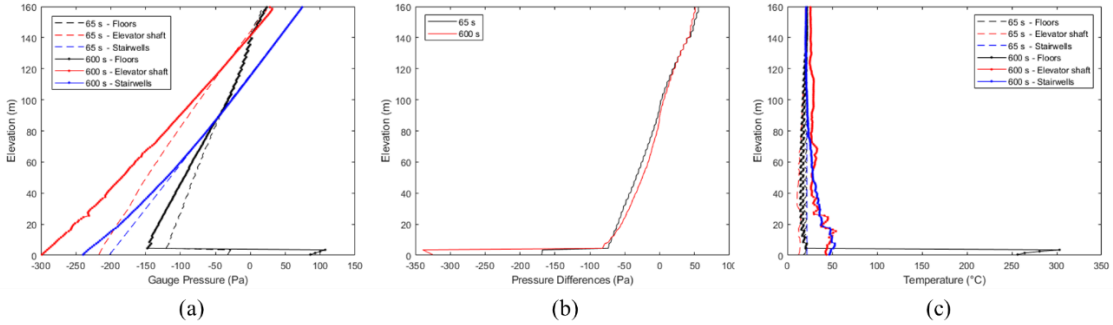

Figure 5.15: Elevation versus (a) gauge pressure; (b) pressure across the stairwell doors; and (c) temperature in the high-rise building obtained by FDS for case 6 at 65 s and 600 s.

In conclusion, FDS provides nearly the same results as those of CONTAM and MATLAB before and after the ignition of the design fire, the discrepancy is mainly owing to the vertical thermal mixing described by FDS but ignored in CONTAM and MATLAB.

5.2 Case 7: Open the stairwell ground doors to the outside

The only difference between case 7 and case 6 is that the ground doors (2 m by 2 m) between the stairwells and the outside are open along with the initiation of the fire right after 60 s of the simulation for this case. The configuration of the building and the boundary conditions are the same as before. Moreover, the configurations and conditions of the model in CONTAM and MATLAB are the same as that in FDS for this case. The total simulation time is also 600 s, and it takes less than 90 minutes to complete by Deepthought2.

In accordance with Figure 5.16, the ultra-fast 2.5 MW t-square fire starts at 60 s and reaches its fully developed stage at 175 s as prescribed (see case 6). Additionally, based on Figure 5.17, the gauge pressure and the temperature inside the stairwells at

the bottom of the building suddenly becomes around 0 Pa and – 17 ℃ respectively at 60 s. The oscillation of the gauge pressure inside the stairwells observed on the 21st and 40th floor right after 60 s can be attributed to the opening of the ground doors that creates the sudden change in the conditions inside the stairwells. The discussion for this section includes the results before and after the ignition of the fire and until the end of the simulation.

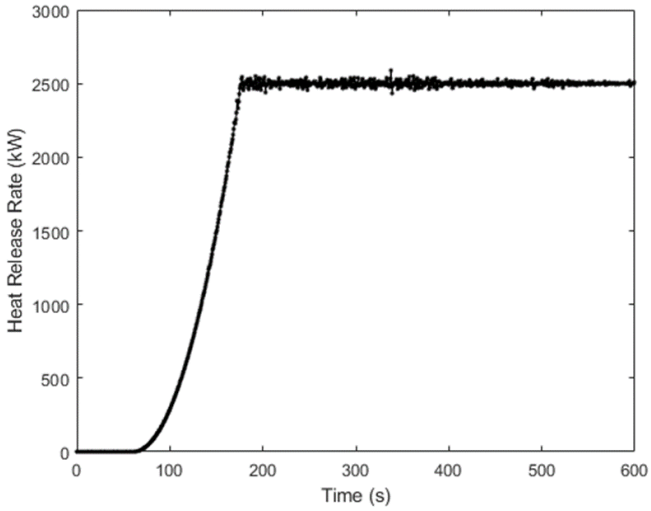

Figure 5.16: The time variations of the heat release rate for case 7.

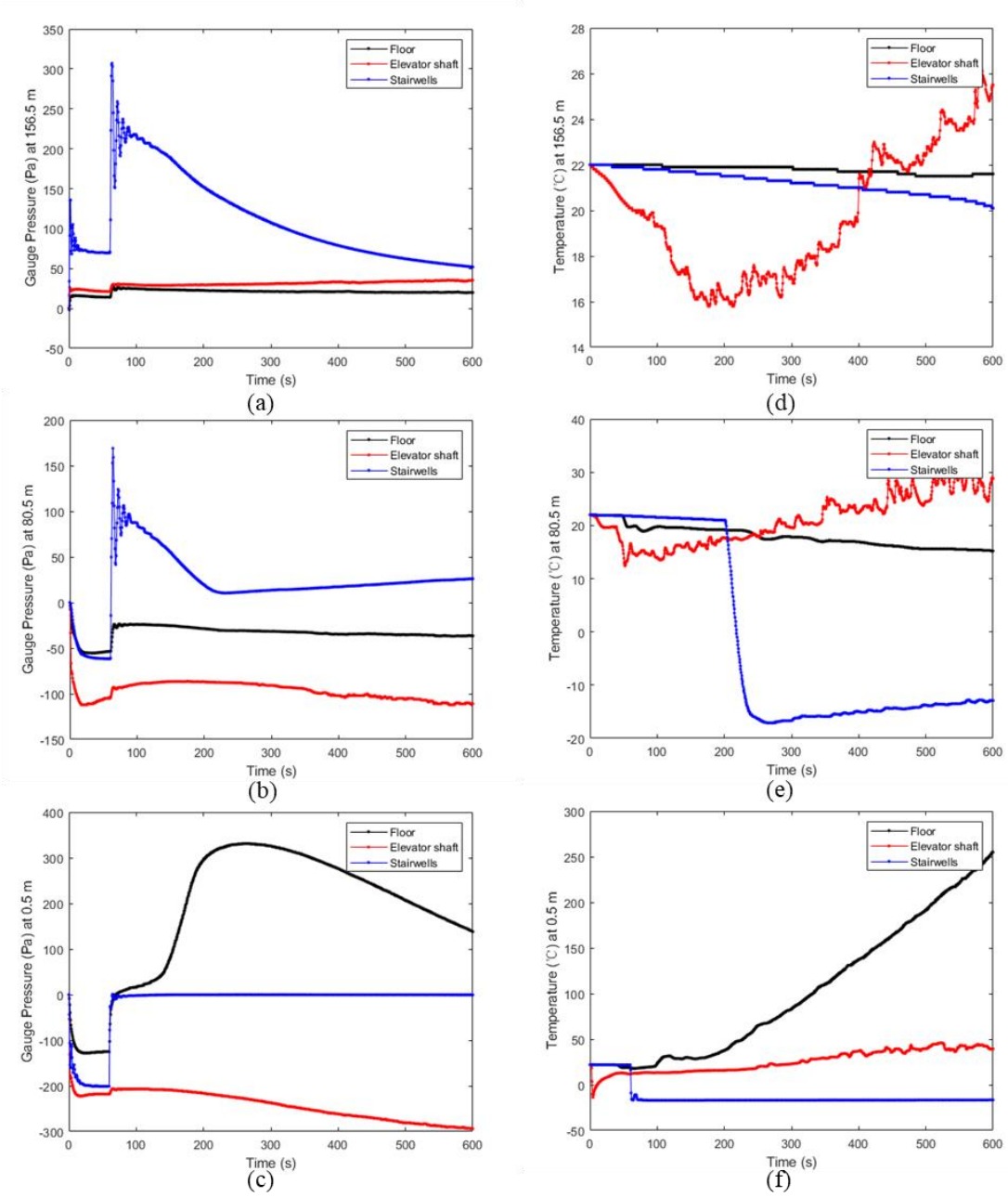

Figure 5.17: Time variations of the gauge pressure and temperature within the floors, the elevator shaft, and the stairwells at the heights of: (c)-(f) 0.5 m (1st floor); (b)-(e) 80.5 m (21st floor); and (a)-(d) 156.5m (40th floor) for case 7.

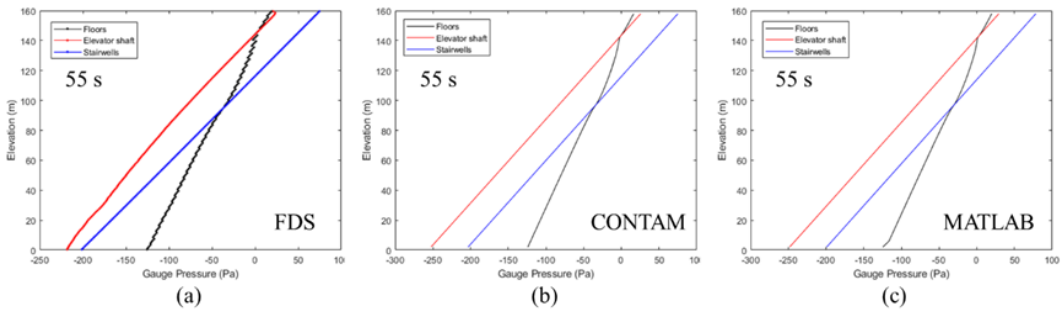

Figure 5.18: Elevation versus gauge pressure inside the high-rise building obtained by (a) FDS; (b) CONTAM; and (c) MATLAB for case 7 at 55 s.

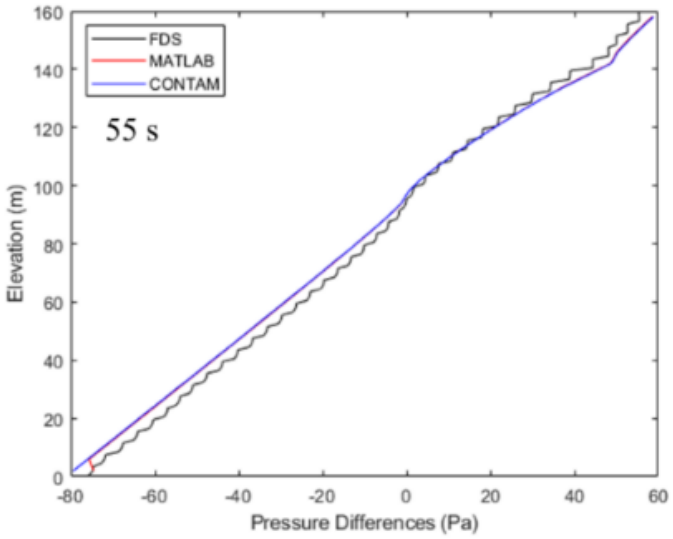

Figure 5.19: Elevation versus pressure differences between the stairwells and the floors obtained by FDS, CONTAM and MATLAB for case 7 at 55 s.

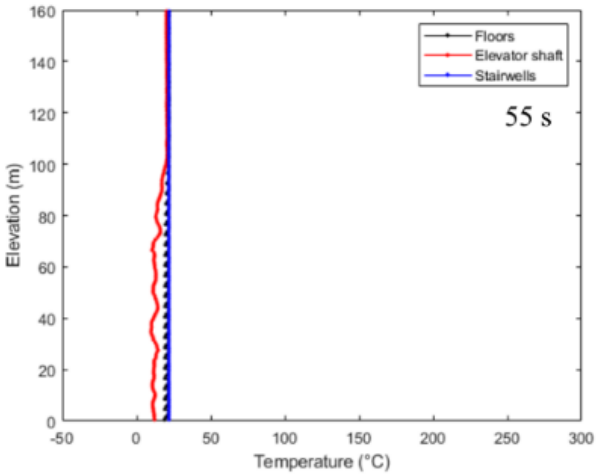

Figure 5.20: Elevation versus temperature inside the high-rise building obtained by FDS for case 7 at 55 s.

Because the same conditions for case 7 and case 6 before the fire starts, it is obvious that the results are the same at 55 s for both cases according to Figures 5.18 to 5.20 and Figures 5.3 to 5.5. As already discussed in Case 6, the lower temperature inside the elevator shaft leads to the discrepancy of the elevator pressure curves between FDS and COMTAN and MATLAB.

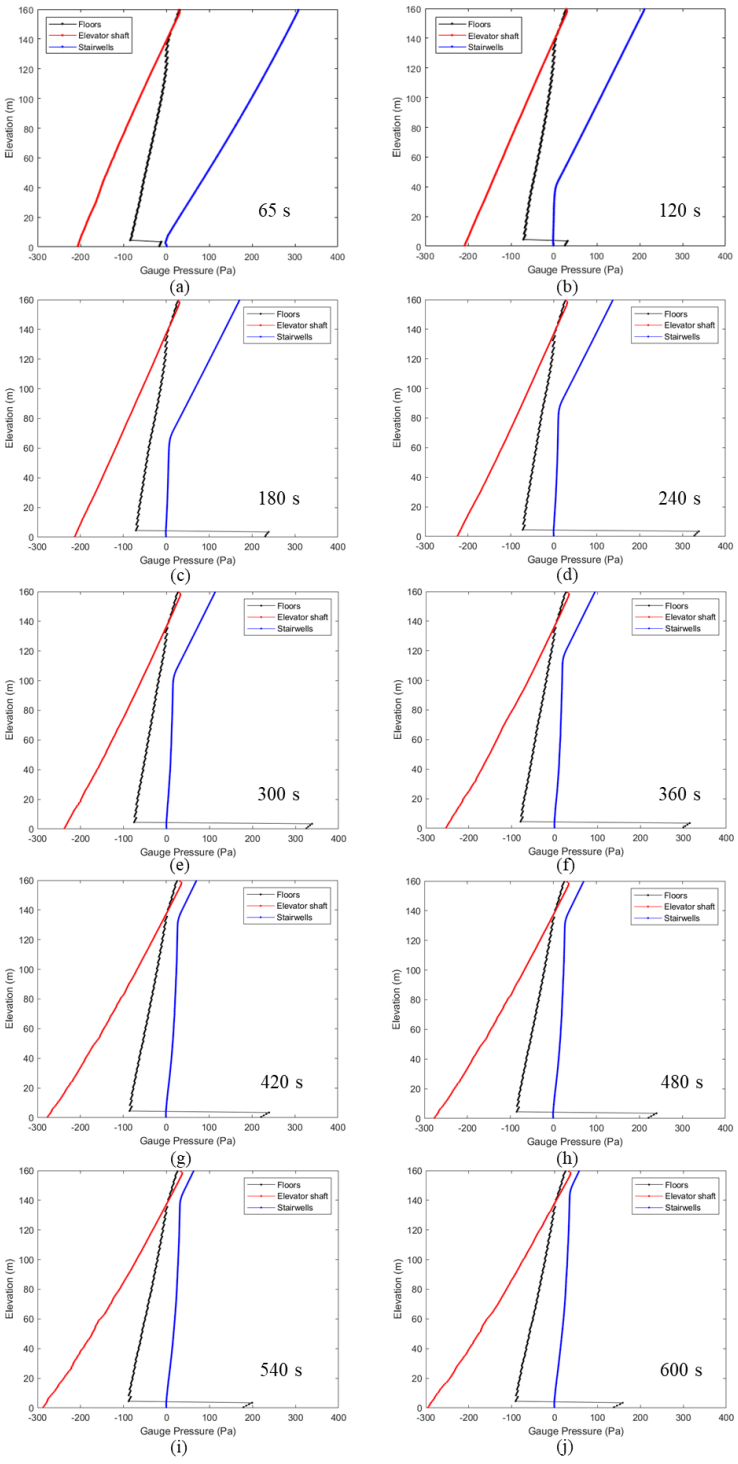

Figure 5.21: Elevation versus gauge pressure inside the building obtained by FDS at (a) 65 s; (b) 120 s; (c) 180 s; (d) 240 s; (e) 300 s; (f) 360 s; (g) 420 s; (h) 480 s; (i) 540 s; and (j) 600 s for case 7.

Figure 5.21 compares the gauge pressure inside the floors, the stairwells and the elevator shaft at 10 different times from 65 s to 600 s. The gauge pressure inside the floors has minor changes due to the fact that the temperature inside the floors remains almost the same during the time except for the fire floor in accordance with Figure 5.23. Additionally, Figure 5.23 shows that the temperature inside the elevator shaft becomes hotter during simulation which results in a stronger stack effect between the elevator shaft and the floors shown in Figure 5.21. Moreover, according to Figure 5.23, the temperature inside the stairwells at the bottom of the building is below 0 ℃ at 65 s owing to the inflow of cold air through the open doors. After 240 s, the temperature inside the lower half of the stairwells becomes negative. At 600 s, the temperature inside the stairwells below the 35th floor reaches negative values. Thus, Figure 5.21 illustrates that the gauge pressure is getting lower as the temperature is decreasing in the stairwells. Therefore, comparing with the small leakage paths, the open ground doors provide large openings that accelerate the thermal mixing process inside the stairwells in FDS.

The pressure across the escape stairwell doors as a function of elevation at 11 different times is illustrated in Figure 5.22. Before the ignition of the fire (at 55 s), the maximum pressure difference between the stairwells and the floors is only 56 Pa. Just after the fire starts (at 65 s), the minimum over-pressure inside the stairwells is 84 Pa (except for the fire floor) and the maximum over-pressure inside the stairwells is 277 Pa, so the occupants will have difficulties in opening the escape doors and evacuating. Moreover, after 360 s, 420 s 480 s, 540 s and 600 s, the over-pressure inside the stairwells in the lower part of the building is still more than 78 Pa, but the over-pressure

inside the stairwells in the upper part of the building becomes lower than 78 Pa. Consequently, the pressure change inside the high-rise building under a realistic fire is very dynamic.

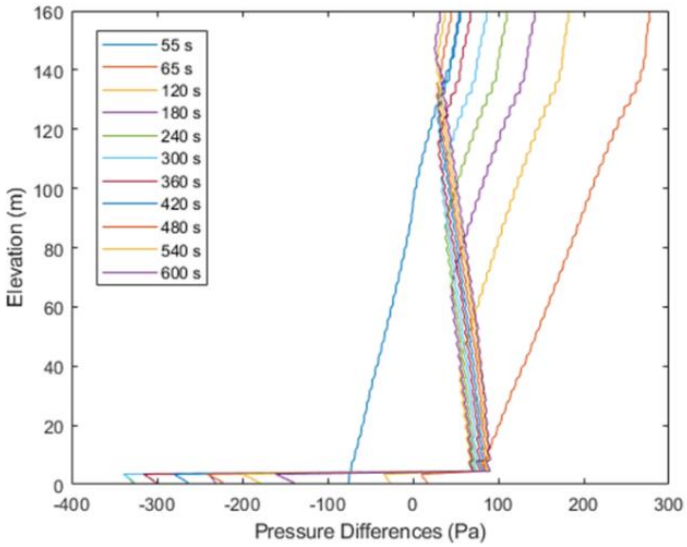

Figure 5.22: Elevation versus pressure differences between the stairwells and the floors obtained by FDS from 55 s to 600 s for case 7.

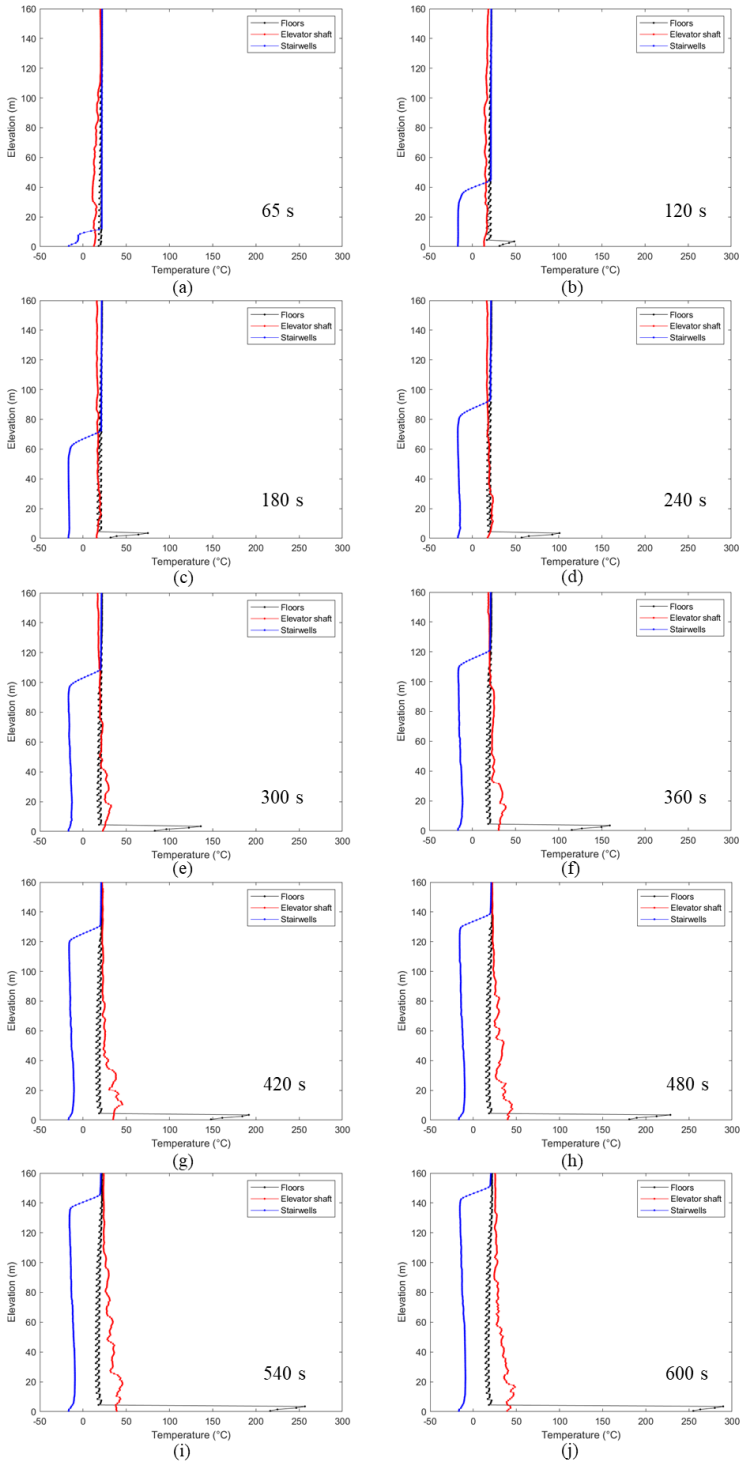

Figure 5.23: Elevation versus temperature inside the building obtained by FDS at (a) 65 s; (b) 120 s; (c) 180 s; (d) 240 s; (e) 300 s; (f) 360 s; (g) 420 s; (h) 480 s; (i) 540 s; and (j) 600 s for case 7.

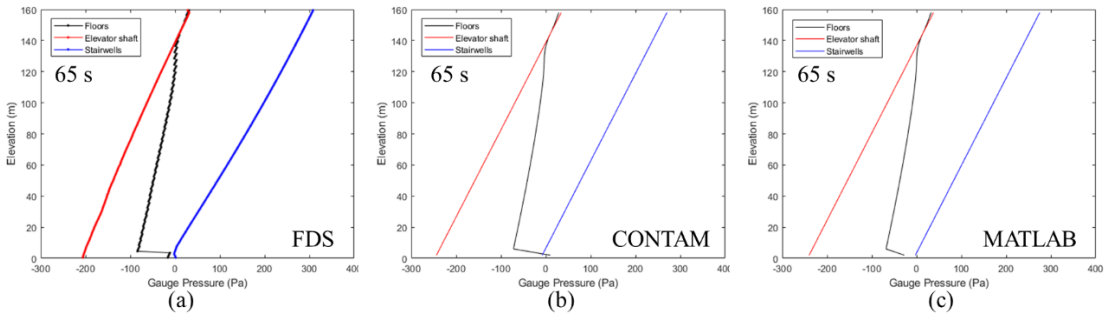

Figure 5.24: Elevation versus gauge pressure inside the high-rise building obtained by (a) FDS; (b) CONTAM; and (c) MATLAB for case 7 at 65 s.

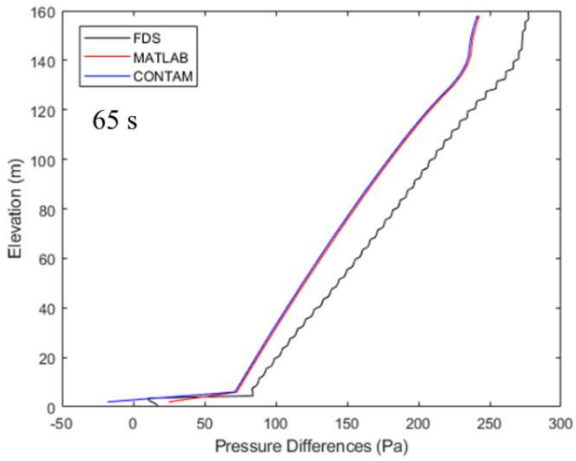

Figure 5.25: Elevation versus pressure differences between the stairwells and the floors obtained by FDS, CONTAM and MATLAB for case 7 at 65 s.

Figure 5.24 compares the gauge pressure inside the floors, the elevator shaft and the stairwells obtained from FDS, COMTAM and MATLAB at 65 s. The results provided by CONTAM and MATLAB are very close. (The fire conditions in CONTAM are prescribed as constant 700 ℃ for the temperature and 10 Pa for the gauge pressure inside the first floor. And the fire conditions in the MATLAB program are specified as constant 700 ℃ for the temperature and that the gauge pressure is not

prescribed inside the fire floor.) The gauge pressure curves for floors are nearly the same. The discrepancy of stairwell gauge pressure curves between FDS and CONTAM and MATLAB could be explained by the fact that CONTAM and MATLAB are under steady states (no thermal mixing), but FDS has pressure oscillations observed in Figures 5.17-(a) and 5.17-(b) right after the ignition of the fire. (At 65 s, according to Figure 5.17-(a) and 5.17-(b), the gauge pressures inside the stairwells at 80.5 m and 156.5 m is their respective peak value throughout the simulation.) Owing to the higher pressure reported by FDS, Figure 2.25 shows a larger pressure difference between the stairwells and the floors in FDS than CONTAM and MATLAB. And the difference in the elevator shaft gauge pressure curves is due to the lower temperature reported by FDS at 65 s shown in Figure 5.26. At this moment, the gauge pressure inside the high-rise building could be predicted by hand calculations (see Appendix C).

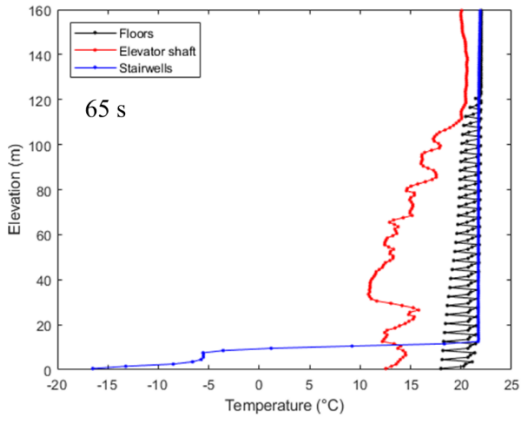

Figure 5.26: Elevation versus temperature inside the high-rise building obtained by FDS for case 7 at 65 s.

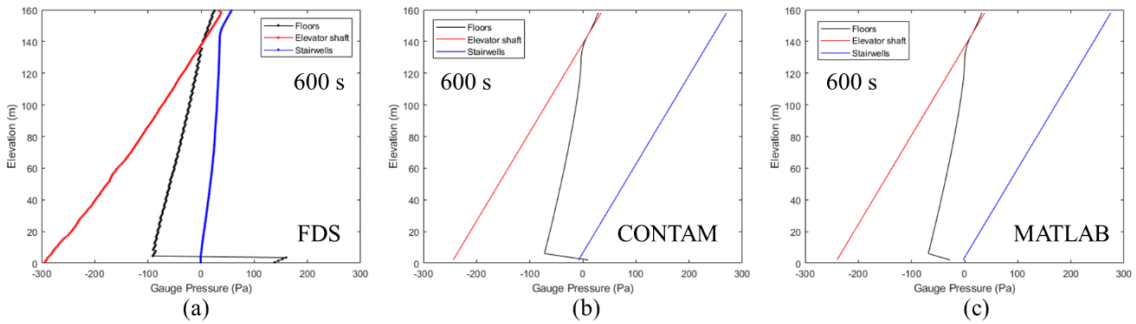

Figure 5.27: Elevation versus gauge pressure inside the high-rise building obtained by (a) FDS; (b) CONTAM; and (c) MATLAB for case 7 at 600 s.

The comparison of the gauge pressure inside the buildings among FDS, CONTAM and MATLAB at 600 s are demonstrated in Figure 5.27. Because the simulations performed by CONTAM and MATLAB assume steady state, Figure 5.27-(b) and Figure 5.24-(b) are the same, and Figure 5.27-(b) and 5.24-(c) are the same. According to Figures 5.27 to 5.30, it is notable that because of the decrease in temperature in the stairwells (due to vertical thermal mixing), the pressure difference across the escape stairwells doors is largely decreased and the stairwells become tenable from 4th floor to 40th floor at 600 s. However, the environment inside the stairwells is difficult for occupants to evacuate resulting from the large over-pressure across the escape stairwell doors at 65 s.

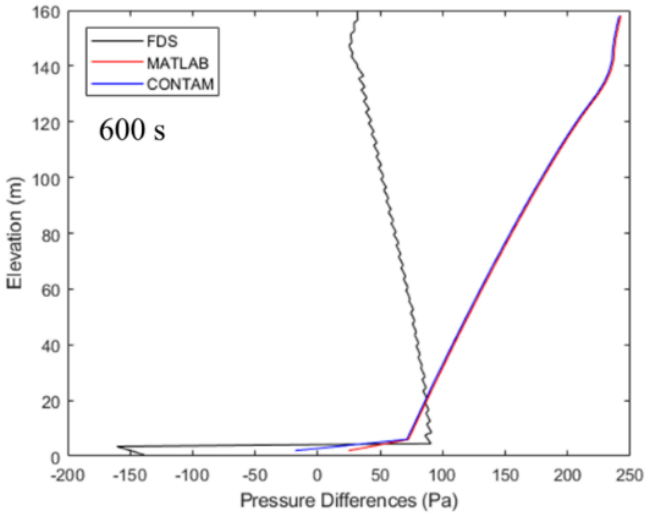

Figure 5.28: Elevation versus pressure differences between the stairwells and the floors obtained by FDS, CONTAM and MATLAB for case 7 at 600 s.

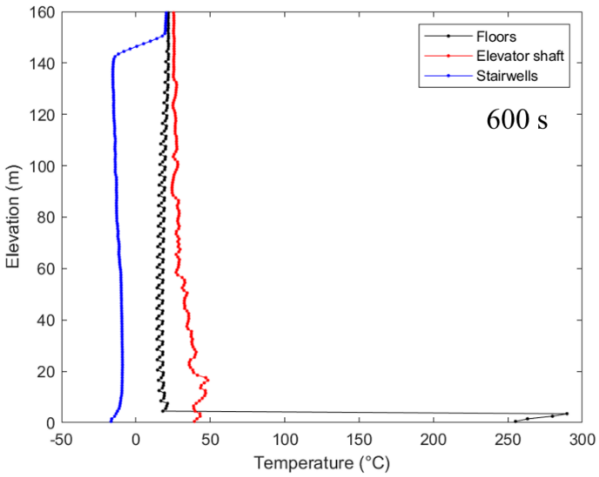

Figure 5.29: Elevation versus temperature inside the high-rise building obtained by FDS for case 7 at 600 s.

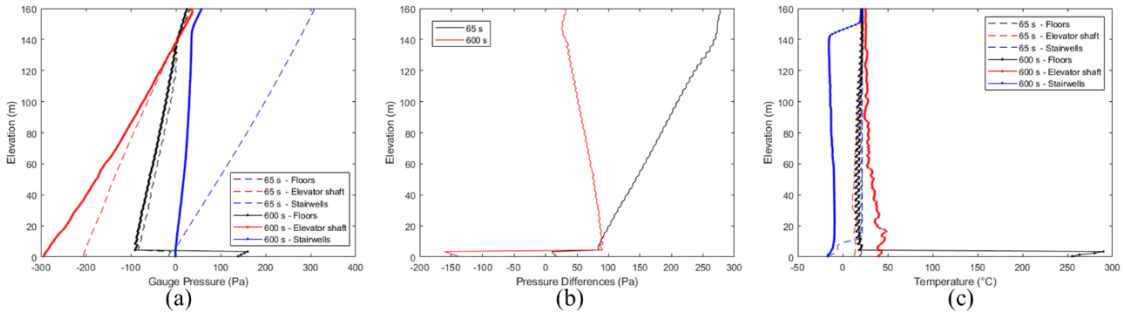

Figure 5.30: Elevation versus (a) gauge pressure; (b) pressure across the stairwell doors; and (c) temperature in the high-rise building obtained by FDS for case 7 at 65 s and 600 s.

In conclusion, the vertical thermal mixing process simulated in FDS leads to the fact that the pressure difference between the stairwells and the floor varies significantly with time for this case, an evolution that is not captured by CONTAM which lacks a heat transfer model.

Chapter 6: Conclusion

A total of seven FDS simulations are implemented and discussed in this study. It is concluded that FDS is not only capable of simulating the fire conditions throughout the entire high-rise building accurately by comparing with the results obtained by the network models COSMO, CONTAM and a MATLAB program, but also has a heat transfer model that captures the vertical thermal mixing process during simulations which is ignored in a commonly used HVAC software – CONTAM and thus it can help engineers to analyze fire smoke movement and management under different fire scenarios more comprehensively. Therefore, with the development of computer power, FDS has the potential to become an increasingly popular tool to simulate and study the smoke movement inside large-scale structures under fire conditions for fire protection engineers and HVAC engineers in the near future. (Regarding the subsequent research, more scenarios can be studied by using FDS. For instance, we could study the situation with the opening of the inside escape stairwells doors between the fire floor and the stairwells.)

Appendix A

The determination of flow rate and flow direction for HVAC duct in FDS by hand calculation

1. Objective

The goal of this section is to describe the method of determining the flow rate and flow direction in an HVAC duct in FDS by hand calculation. Correct equations and correct values that puts into the equations guarantee the accuracy of hand calculation.

2. Equations

The relationship between pressure and flow velocity in the HVAC network model used by FDS is based on the Bernoulli's principle and loss coefficient definition. According to Frank White, Fluid Mechanics, 5th edition, the loss coefficient (*K*) is usually given as a ratio of the head loss $\Delta P/(\rho g)$ through the device to the velocity head $V^2/(2g)$ of the associated pipe/duct system.

$$K = \frac{\frac{\Delta P}{\rho g}}{\frac{V^2}{2g}} = \frac{2\Delta P}{\rho v^2} \tag{1.1}$$

After rearranging the expression, we get:

$$\Delta P = \frac{1}{2} K \rho v^2 \tag{1.2}$$

ΔP – the pressure differences between two HVAC nodes

K – loss coefficient in the HVAC duct

ρ – mass density in the HVAC duct

v – flow velocity in the HVAC duct

Note that the loss coefficient should be specified in the FDS input file for the HVAC duct. The pressure reported by FDS at the HVAC nodes is the absolute static pressure. Hence, the pressure differences between two HVAC nodes should be:

$$\Delta P = |(P_1+\rho g h_1) - (P_2 + \rho g h_2)| \tag{1.3}$$

P_1 , P_2 $-$ pressure reported by FDS at node 1 and node 2

h_1 , h_2 $-$ the elevation of node 1 and node 2

v_1 , v_2 $-$ the velocity at node 1 and node 2

For a horizontal HVAC duct, the elevations of the two HVAC nodes are the same, so $h_1 = h_2$. In addition, the velocity in the HVAC duct is usually constant, so $v_1 = v_2$. Therefore, Equation (1.3) can be reorganized as:

$$\Delta P = |P_1 - P_2| = \frac{1}{2} K \rho v^2 \tag{1.4}$$

Here, if $P_1 > P_2$, the flow direction in the HVAC duct is from node 1 to node 2. However, if $P_1 < P_2$, the flow direction in the HVAC duct is from node 2 to node 1.

For a vertical HVAC duct, the elevations of the two HVAC nodes are not the same, but the velocity in the HVAC duct is still constant. Consequently, Equation (1.3) can be reorganized as:

$$\Delta P = |(P_1 + \rho g h_1) - (P_2 + \rho g h_2)| = \frac{1}{2} K \rho v^2 \tag{1.5}$$

$$\Delta P = |(P_1 + \rho g \Delta h) - P_2| = \frac{1}{2} K \rho v^2 \tag{1.6}$$

Here, P_1 is the pressure measured at the higher HVAC duct node and correspondingly $h_1 > h_2$. So, $\Delta h = h_1 - h_2 > 0$. If $(P_1 + \rho g \Delta h) > P_2$, the flow direction in the HVAC duct is from node 1 to node 2. If $(P_1 + \rho g \Delta h) < P_2$, the flow direction in the HVAC duct is from node 2 to node 1.

3. A Case Study

In a FDS simulation of a fire occurring in a 10-story building, there is a 1-m-long vertical HVAC duct with 0.1m2 cross-section area located at the top of each stairwells and that connects the stairwell to the outside atmosphere. The value of the loss coefficient specified in the input file is K = 1. The pressure at the HVAC outside node and the HVAC inside node reported by FDS are 100,749.62 Pa and 100,749.22 Pa, respectively. The mass flow rate inside the HVAC duct reported by FDS is 0.61 kg/s. In addition, the mass density in the outside atmosphere is 1.36 kg/m3, and the mass density in the stairwell is 1.15 kg/m3.

Here are the relevant lines of the FDS input file for this case:

```
&OBST ID='floor02', XB=0.0,52.0,0.0,42.0,40.0,41.0,
SURF_ID='ADIABATIC'/
&VENT ID='Vent63', SURF_ID='HVAC', XB=2.0,3.0,2.0,3.0,41.0,41.0/
&VENT ID='Vent64', SURF_ID='HVAC', XB=2.0,3.0,2.0,3.0,40.0,40.0/
&HVAC ID='Node63', TYPE_ID='NODE', DUCT_ID='Duct32',
VENT_ID='Vent63'/
&HVAC ID='Node64', TYPE_ID='NODE', DUCT_ID='Duct32',
VENT_ID='Vent64'/
&HVAC ID='Duct32', TYPE_ID='DUCT', AREA=0.1, PERIMETER=0.0,
LOSS=1.0,1.0, NODE_ID='Node63','Node64'/
&DEVC ID='P TOP STAIR OUT', QUANTITY='NODE PRESSURE',
NODE_ID='Node63'/
&DEVC ID='P TOP STAIR IN', QUANTITY='NODE PRESSURE',
NODE_ID='Node64'/
&DEVC ID='MFR TOP STAIR', QUANTITY='DUCT MASS FLOW',
DUCT_ID='Duct32'/
&DEVC ID='OUTSIDE D', QUANTITY='DENSITY', XYZ=2.5,2.5,41.5/
&DEVC ID='STAIR D', QUANTITY='DENSITY', XYZ=2.5,2.5,39.5/
```

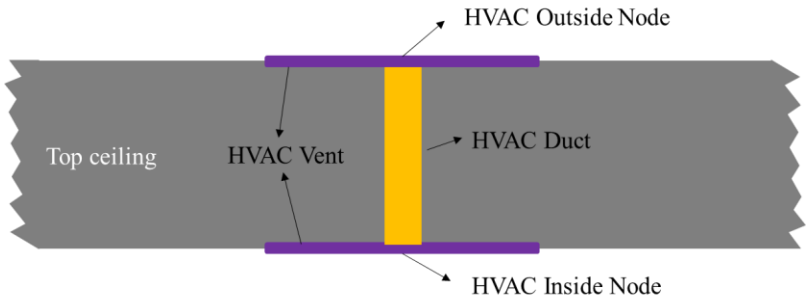

Figure A.1: The configuration of an HVAC flow passage located at the top of the building.

Node 1 designates the upper outside node; node 2 designates the lower inside node. Because $(P_1 + \rho g \Delta h) > P_2$, the discussion in the previous section suggests that the flow direction in the HVAC duct is from node 1 to node 2 (from outside to inside). The mass density to be used in Eq. (1.6) is the mass density of outside air, 1.36 kg/m3. Equation (1.6) gives the flow velocity and flow rate:

$$(100749.62 + 13.33) - 100749.22 = \frac{1}{2} \times 1 \times 1.36 \times v^2$$

$$v = 4.49\text{m/s}$$

$$\dot{m} = \rho v A = 1.36 \times 4.49 \times 0.1 = 0.61\text{kg/s}$$

We find that the hand calculation result is the same as the FDS result. This confirms that the flow direction is from the outside node to the inside node.

Note that one can also check results in Smokeview to determine the flow direction.

4. Conclusion

The flow rate and flow direction given by the HVAC network model used by FDS can be calculated by the equations introduced above. The key point here is to use the correct values for the pressure difference and mass density. Additionally, it is recommended that check the results in Smokeview to determine the flow direction.

Appendix B

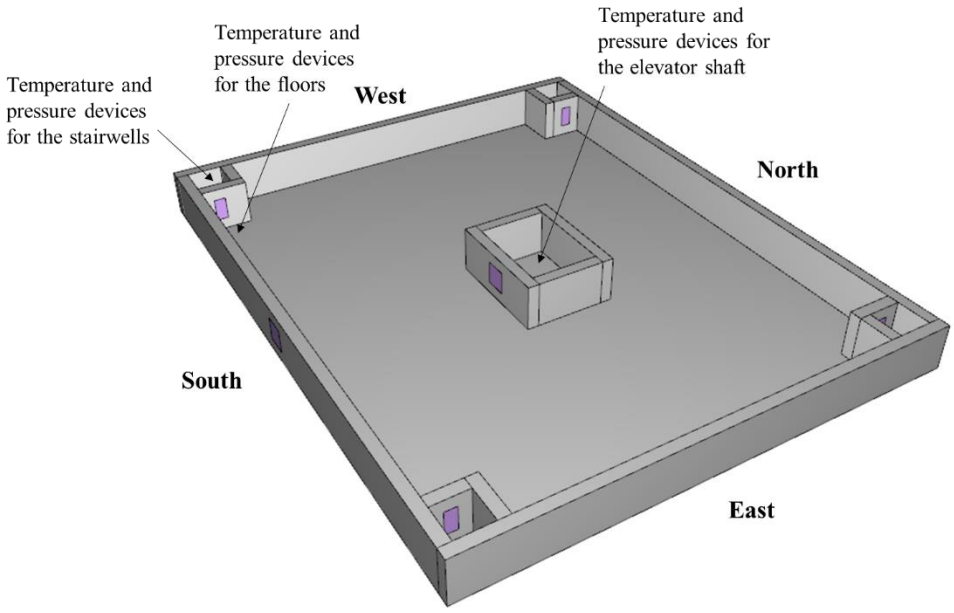

Figure B.1: The screenshot of the first-floor configuration of the high-rise building in PyroSim. All the other floors have the same configuration. The purple square is a part of HVAC system that shows the location of the leakage.

The configuration of the first floor of the building is shown in Figure B.1. It indicates that the leakage path of the floor and the leakage path of the elevator shaft are on their respective southern walls which means that it is easier for cold air from the atmosphere to spread into the elevator shaft through these two leaks. And it is possible that when the cold air is pushed into the elevator shaft, the cold air probably does not reach the point of the temperature device of the floor yet. Consequently, at certain moment, the temperature device of the elevator shaft probably reports that temperature inside the elevator shaft is decreasing while the temperature device of the floor reports that temperature inside the floor is keeping the constant.

Appendix C

Consider a scenario with the fire conditions: constant 700 ℃ for the temperature, 10 Pa for the gauge pressure inside the first floor. The indoor temperature is 22 ℃ and the outside temperature is – 17 ℃

According to hydrostatic pressure equation, we have:

$$p_{outside}(z) = p_{outside}(0) - \rho_{outside} g z$$

$$p_{floor}(z) = p_{floor}(0) - \rho_{inside} g z$$

$$p_{elevator}(z) = p_{elevator}(0) - \rho_{inside} g z$$

$$p_{stairwell}(z) = p_{stairwell}(0) - \rho_{inside} g z$$

When $T_{inside} = 22$ ℃, $\rho_{inside} = 1.2\ kg/m^3$;

When $T_{outside} = -17$ ℃, $\rho_{outside} = \frac{(273+22)}{(273-17)} \times 1.2 = 1.38\ kg/m^3$;

At the time when the ground doors between the stairwells and the outside is open, the gauge pressure at the bottom of the stairwells is close to 0 Pa. Assume that $\Delta p_{stairwells}(0) = 0\ Pa$. So:

$$\Delta p_{stairwells}(z) = p_{stairwell}(z) - p_{outside}(z)$$

$$\Delta p_{stairwells}(z) = (p_{stairwell}(0) - \rho_{inside} g z) - (p_{outside}(0) - \rho_{outside} g z)$$

$$\Delta p_{stairwells}(z) = \Delta p_{stairwells}(0) + (\rho_{outside} - \rho_{inside}) g z$$

$$\Delta p_{stairwells}(z) = 0 + (1.38 - 1.2) \times 9.8 \times z$$

$$\Delta p_{stairwells}(z) = 1.76z$$

Due to the large opening at the top of the elevator shaft, the gauge pressure at the top of the elevator shaft is also close to 0 Pa. Assume $\Delta p_{stairwells}(160) = 0\ Pa$. We have:

$$\Delta p_{elevator}(z) = \Delta p_{elevator}(0) + (\rho_{outside} - \rho_{inside}) g z$$

$$\Delta p_{elevator}(160) = \Delta p_{elevator}(0) + (1.38 - 1.2) \times 9.8 \times 160$$

$$\Delta p_{elevator}(0) = -281\ Pa$$

$$\Delta p_{elevator}(z) = -281 + 1.76z$$

Because the leakage area of the floors to the outside is approximately equal to the leakage area of the elevator to the floors ($A_{elevator} \approx A_{floor}$), we have:

$$\Delta p_{elevator} = \Delta p_{elevator-floor} + \Delta p_{floor}$$

$$\Delta p_{elevator} = \frac{1}{2} K \rho (\frac{\dot{m}}{\rho A_{elevator}})^2 + \frac{1}{2} K \rho (\frac{\dot{m}}{\rho A_{floor}})^2$$

$$\Delta p_{elevator} \approx 2 \times \frac{1}{2} K \rho (\frac{\dot{m}}{\rho A_{floor}})^2 = 2\Delta p_{floor}$$

So, when $4\ m < z < 160\ m$

$$\Delta p_{floor}(z) = -140.5 + 0.88z$$

And when $0\ m < z < 4\ m$, $\Delta p_{floor}(z) = 10\ Pa$.

By plotting $\Delta p_{stairwells}(z)$, $\Delta p_{elevator}(z)$, and $\Delta p_{floor}(z)$, we get:

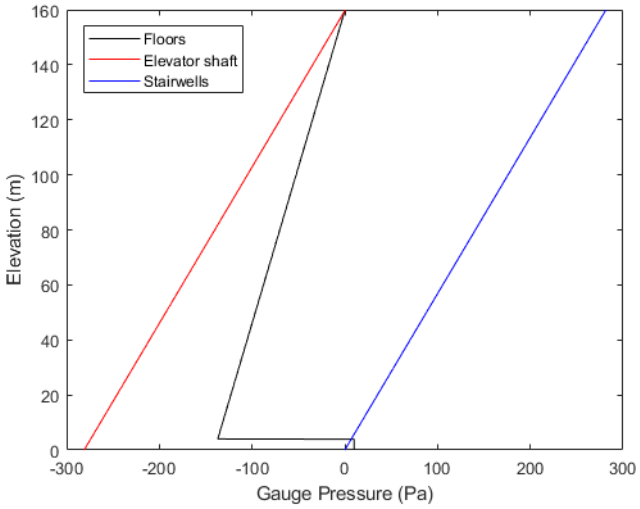

Figure C.1: The results of the hand calculation of the gauge pressure for the floors, the elevator shaft, and the stairwells (steady state, no thermal mixing).

Appendix D

According to Table 2.1 and the information from Dr. Black's paper (Table 1 in Ref. [4]), we know that:

The area of the floor is 40 m by 50 m, and the area ratio of openings in exterior surface of building is 3.5×10^{-4} m^2/m^2;

The size of the stairwells is 3 m by 3 m, and the area ratio of openings in stairwell walls is 3.5×10^{-4} m^2/m^2, and the height and width of each stairwell door are 2.13 m and 1.22 m, and average gap around stairwell doors is 1 mm;

The size of the elevator shaft is 6 m by 8 m, and the area ratio of openings in elevator walls is 3.5×10^{-4} m^2/m^2, and the height and width of each elevator door are 2.13 m and 1.52 m, and average gap around elevator doors is 3 mm.

Additionally, the elevator shaft and the stairwells connect to the atmosphere only at the top of the building which means that there is on leakage path between the stairwells and the outside, and no leakage path between the elevator shaft and the outside (This is the same assumption as Dr. Black did in his paper).

Now, we can calculate the leakage areas between each space.

The leakage area from the floor to the outside is:

$$A_{floor} = [(4\,m \times 50\,m \times 3.5 \times 10^{-4}\,m^2/m^2) + (4\,m \times 50\,m \times 3.5 \times 10^{-4}\,m^2/m^2)] \times 2 = 0.252\,m^2/floor$$

The gap around one stairwell door is:

$$10^{-3} m \times 2 \times (2.13\, m + 1.22\, m) = 0.0067\, m^2/door$$

Note that this value is low compared with the data in Table 3.5 in Handbook of Smoke Control Engineering (Ref. [10]) which gives a leak area in the range of 0.0089 m^2 to 0.0475 m^2 for one stairwell door.

The leakage area from each stairwell to the floor is:

$$A_{stairwells} = [(4\, m \times 3\, m \times 3.5 \times 10^{-4}\, m^2/m^2 \times 2) + 0.0067\, m^2/door]$$
$$= 0.0151\, m^2/floor$$

The gap around one elevator door is:

$$3 \times 10^{-3} m \times 2 \times (2.13\, m + 1.52\, m) = 0.0219\, m^2/door$$

Note that this value is low compared with the data in Table 3.8 in Handbook of Smoke Control Engineering (Ref. [10]) which gives a leak area in the range of 0.046 m^2 to 0.072 m^2 for one elevator door.

The leakage area from the elevator shaft to the floor is:

$$A_{elevator\ shaft} = [(4\, m \times 6\, m \times 2) + (4\, m \times 8\, m \times 2)] \times 3.5 \times 10^{-4}\, m^2/m^2$$
$$+ 0.0219\, m^2/door \times 8 = 0.2144\, m^2/floor$$

Bibliography

[1] McGrattan, K., Hostikka, S., McDermott, R., Floyd, J., Vanella, M., Fire Dynamics Simulator – User's Guide, NIST Special Publication 1019, Sixth Ed., National Institute of Standards and Technology, Gaithersburg, MD, USA, 2019.

[2] W.Z. Black, Floor pressurization as a means of controlling smoke during a high-rise fire, Engineered Systems (2009) 46–49.

[3] W. Stuart Dols, Brian J. Polidoro, CONTAM User Guide and Program Documentation, Version 3.4, NIST Technical Note 1887 Revision 1, National Institute of Standards and Technology, Gaithersburg, MD, USA, 2020.

[4] W.Z. Black, COSMO—Software for designing smoke control systems in high-rise buildings, Fire Safety Journal 45 (2010) 337 – 348.

[5] Helmut E. Feustel, COMIS—an international multizone air-flow and contaminant transport model, EnergyandBuildings30(1999)3–18.

[6] G.N. Walton, AIRNET—a computer program for building air flow network modeling, US Department of Commerce, National Institute of Standards and Technology, Gaithersburg, MD,1989

[7] W.Z. Black, Smoke movement in elevator shafts during a high-rise structural fire, Fire Safety Journal 44 (2) (2009) 168–182.

[8] W.Z. Black, Use of air handling equipment to manage smoke movement during a high-rise fire, ASHRAE Transactions 115 (1) (2009) 165–181.

[9] W.Z. Black, Pressurization of floors to improve life safety during a high-rise fire, ASHRAE Transactions 115 (2) (2009) 278–289.

[10] J.H. Klote, J.A. Milke, P.G. Turnbull, Handbook of smoke control engineering,

ISBN 978-1-936504-24-4, 2012

[11] Jung-yeon Yu, Kyoo-dong Song, and Dong-woo Cho, Resolving Stack Effect Problems in a High-Rise Office Building by Mechanical Pressurization, Sustainability 2017, 9, 1731.

[12] https://www.thunderheadeng.com/pyrosim/

[13] http://www.skyscrapercenter.com/

[14] Blockley, W.V., "Temperature Tolerance: Man. Part 1. Heat and Cold Tolerance With and Without Protective Clothing", in Biology Data Book, 2nd Ed, Volume II, p.781. Federation of American Societies for Experimental Biology. 1973.

[15] L. J. Marchetti, Fire Dynamics Series: Predicting Hot Gas Layer Temperature and Smoke Layer Height in a Room Fire with Natural and Forced Ventilation, PDHonline Course M314 (3 PDH), 2012

[16] Christine Pongratz, Methods to Increase velocity of makeup air for atium smoke control - a CFD Study, 2014

[17] Leif Staffansson, Selecting Design Fires, Department of Fire Safety Engineering and Systems Safety, Lund University, Lund 2010